U.S. Department of Energy
Scientific and Technical Information (STI) for Financial Assistance and Non-M&O/M&I

Final Technical Report

Award Number: DE-EE0005387

Project Title:

Thermoelectric Waste Heat Recovery Program for Passenger Vehicles

Principal Investigator: Vladimir Jovovic

Submission Date: April 29th, 2016
DUNS Number: 556879252
Project Grant Period: 10/01/2011 through 12/31/2015

Submitting Organization:
Gentherm LLC
1321 Mountain View Circle - Azusa, CA 91702

Subcontractors/sub-recipients:

Tenneco GmbH
Luitpoldstrasse 83
67480 Edenkoben, Germany

BMW AG
Research and Innovation Center
Knorrstraße 147
80788 Munich, Germany

Submitted By: GENTHERM

Disclaimer

Abstract

Gentherm began work in October 2011 to develop a Thermoelectric Waste Energy Recovery System for passenger vehicle applications. Partners in this program were BMW and Tenneco. Tenneco, in the role of TIER 1 supplier, developed the system-level packaging of the thermoelectric power generator. As the OEM, BMW Group demonstrated the TEG system in their vehicle in the final program phase. Gentherm demonstrated the performance of the TEG in medium duty and heavy duty vehicles. Technology developed and demonstrated in this program showed potential to reduce fuel consumption in medium and heavy duty vehicles. In light duty vehicles it showed more modest potential.

Executive Summary

In this project, a team consisting of Gentherm, BMW and Tenneco demonstrated the ability to produce, integrate and test a reliable thermoelectric power generation device for passenger vehicle applications. The goal of this program was to demonstrate the ability to reduce vehicle fuel consumption by 5% in the US06 cycle.

In addition, a team consisting of Gentherm and Tenneco worked on development of a heavy duty vehicle (HDV) waste heat recovery device under contract with the Department of Energy and the U.S. Army Tank Automotive Research Development and Engineering Center (TARDEC). The goal of this part of the project was to demonstrate the ability to produce between 1kW and 2kW of electric power from the energy recovered from exhaust of a Bradley Fighting Vehicle (BFV).

To reduce development time, both devices were designed using the same active power generation component. The basic building block used in both devices is a thermoelectric cartridge: a power conversion device developed by Gentherm and shown here in Figure 1. Gentherm has developed methods of manufacturing these devices, test methodologies, and performance models. A combination of 1D and 3D models was used to evaluate performance and structural stability of components.

Figure 1 lower left corner: thermoelectric power generation cartridge. Top: passenger vehicle thermoelectric power generation system.

The role of the Tier 1 exhaust supplier, Tenneco, was to design and build the complete thermoelectric power generation unit, applying technologies developed in packaging catalytic converters, particulate filters and other exhaust components. Tenneco used 1D and 3D modeling tools to predict system level performance and to design structural components of the TEG. As the TEG is a new component, structural integrity was verified following protocols similar to those used in development of active exhaust components such as catalytic converters.

BMW was the only OEM in this program. The role of BMW was to define packaging space and provide advice on system level requirements. In the final stage of this program, BMW performed vehicle level tests and evaluated the effect of integration of the TEG on fuel efficiency. Generators installed in the BMW X3 showed a neutral effect on fuel efficiency. Alternative installation of the TEG in a medium duty vehicle demonstrated the ability to generate over 1.1kW of electricity in a Ford F350 truck when tested with the US06 cycle. In this vehicle, the TEG installation resulted in fuel efficiency improvement of 1.2% and emission reduction of more than 9gCO_2/mile. The major difference between the two demonstration vehicles was the position of TEG. In the F350 medium duty vehicle, the TEG was installed closely coupled to the catalytic converter.

In a heavy duty vehicle application, Gentherm and Tenneco demonstrated the ability to generate 2kW of electricity from a moderately sized TEG system. This TEG system undersized for this application, it uses only ~20% of available heat. Larger system which would match engine size could potentially generate double amount of electricity.

In the development of the manufacturing process we focused on low-cost, high-yield technologies. Processing of thermoelectric materials requires fine control of ambient conditions and process parameters such as sintering temperatures. All thermoelectric materials are very sensitive to oxidation, contamination by impurities and phase separation. For this reason we have selected spark plasma sintering as our sintering process. As part of this project, we have developed a process to manufacture net-shaped thermoelectric elements using materials from the Skutterudite family. Both p- and n-type materials are produced with highly repeatable physical characteristics. The thermoelectric figure of merit, zT, is the best indication of material quality as it directly correlates to the efficiency with which thermoelectric materials convert heat to electricity. Based on in-process sampling of materials produced at Gentherm, we have peak zT values of 0.8 to 0.9 for p-type materials and 0.9 to 1.1 for n-type materials. The range shows our observed deviation in material properties in the past twelve months. Our manufacturing process is reliable, repeatable, and results in very low material loss. Yields are as high as 85%. Further improvements and automation of equipment could bring yields in the range of 92-95%. To demonstrate our ability to produce materials at a high rate, Gentherm has developed and installed automated equipment for handling of TE materials.

The major benefit of the scientific research and engineering development conducted in this program is in the systematic evaluation of cost drivers in manufacturing of thermoelectric elements and careful evaluation of performance of thermoelectric devices at the vehicle level. Analysis of conventionally accepted method of manufacturing thermoelectric elements - ingot manufacturing followed by dicing, polishing and metallization - shows inherently low yields and high costs of material handling. The approach developed in this program focuses on net shape manufacturing and yield increase. Reduction of processing steps and material waste is the only approach which will result in a commercially viable TEG system. At the device and vehicle level we have demonstrated the ability to generate significant power in heavy and medium duty vehicles. Appropriately integrated devices can reduce fuel consumption by up to 2%. Measured power outputs in the systems demonstrated here is 1-2kW of electricity. Fuel efficiency improvement in light duty vehicles is much harder. Vehicle level performance analysis – a methodology developed by BMW - takes into account all impacts of the TEG on vehicle performance. Considering the modest heat potential of high efficiency engines, a TEG installed in a mid-muffler position has neutral effect on fuel efficiency.

Table of Content

Comparison of the actual accomplishments with the goals and objectives of the project

A. Objectives

As defined in the award "statement of work", the objectives of this program are: *"… to establish commercialization readiness for the cylindrical thermoelectric generator (TEG) system for the conversion of exhaust waste heat to electric power in light-duty passenger vehicles with a demonstrated fuel economy improvement of at least 5% over the US06 drive cycle."*

In this program, the team has developed methodology for manufacturing thermoelectric materials and thermoelectric power generation devices and for packaging of those devices in exhaust systems and vehicles. Gentherm has installed capacity to produce several hundred kilograms of thermoelectric materials per year and Tenneco has developed a pilot manufacturing line for production of exhaust components for packaging of thermoelectric cartridges in vehicle-ready systems.

Vehicle level tests showed that the TEG can generate electricity and reduce fuel consumption by 1.2%. With increase in cost of components this value can be as high as 2%. In this aspect, the objective of demonstrating 5% fuel economy improvement over the US06 drive cycle was not achieved.

B. Scope of Work

a) *"This project includes the industrialization of TEG technology for passenger vehicle applications through scale up development of skutterudite (SKD) materials, proof-of-concept thermoelectric (TE) engines, and the processes and manufacturing techniques suitable for commercial practice."*

These tasks were fully completed. In this program, Gentherm developed methods for manufacturing of thermoelectric elements and installed automated and semi-automated equipment for manufacturing of materials. Gentherm developed assembly methods and tooling for manufacturing of cylindrical thermoelectric power generation devices – cartridges.

Tenneco developed tooling for mass production of exhaust components of TEG systems. Tenneco also developed a production prototype line in which seven fully functional and several partial TEG systems were built for this program.

b) "Key technical barriers to be addressed include sealing of TE materials at the die level to prevent atmospheric degradation and the scalability of TE engines to establish a building block for TEG systems that provide power at or near the buss voltage level and validation of TEG robustness compatible with automotive industry requirements. Work will include improvements in element-level encapsulation to prevent atmospheric corrosion, environmental testing of the TE engines, and integration of the TEG system into the underfloor exhaust system of a light-duty passenger vehicle including power management and control functionality."

Device level testing showed that encapsulation of TEG elements is not a feasible option for devices operating at temperatures reaching 550^{o}C internally and at 800^{o}C at the heat exchanger level. In this program Gentherm has developed methods of hermetically sealing devices which reliably performed in bench thermal cycle tests and vehicle level tests, thus preventing atmospheric degradation.

c) *"Confirmatory testing of the TEG subsystem to demonstrate TEG level efficiency and power output as a function of operation conditions as well as full vehicle level confirmation testing will be conducted. An assessment will be conducted to determine the economic feasibility of deploying the system in annual volumes commensurate with requirements of the automotive industry."*

This task was fully completed. Seven passenger vehicle TEG's were produced and tested. Independent testing at NREL, BMW and Gentherm confirmed the accuracy of vehicle level predictive models. A heavy duty vehicle TEG for TARDEC was produced and tested.

Summary of project activities

Thermoelectric power generation device – Cartridge

Device architecture

The goal of this program was to develop a thermoelectric power generation device which can be scaled to match the size of a wide range of vehicles and have power output from approximately 0.5 to 2 kW. The solution that was developed is the Thermoelectric Power Generation Cartridge (TEG cartridge) shown in Figure 2.This device consists of internal (cold side) and external (hot side) heat exchangers, closely integrated with functional TE materials shown schematically in Figure 3. The device is designed to operate with hot gas as a heat source and liquid coolant. The advanced design and manufacturing concepts that have been incorporated into this TEG make it a viable option for waste heat recovery applications.

Figure 2 Thermoelectric Power Generation Device - TEG Cartridge

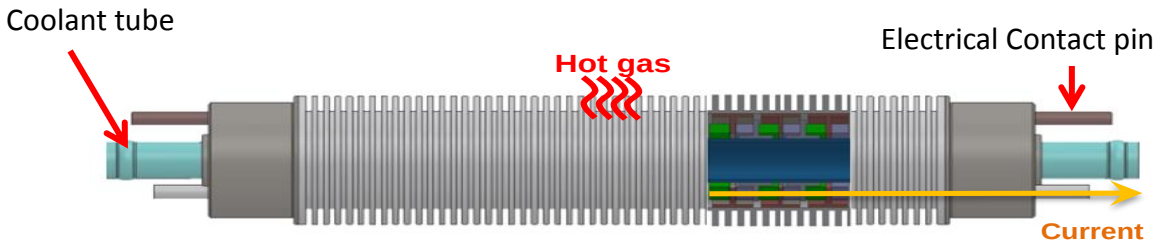

Figure 3 TEG Cartridge structure and principle of operation. Partial cross section shows stacked structure of TE elements in the interior of the cartridge. Outside and inside surfaces are finned tube hot and cold heat exchangers.

The TEG cartridge can generate power from any heat source such as hot gas or hot liquid. Hot fluid flows around the perimeter of the cartridge which works as a finned tube heat exchanger. Heat absorbed by the hot side heat exchanger is conducted through the device and thermoelectric materials to the cold side heat exchanger. The cold side heat exchanger is a tube with axially extended finned surfaces. The cold side heat exchanger can be cooled by gases or liquids. This particular cartridge configuration is developed for automotive applications and is optimized to operate with exhaust gas on the hot side and water-glycol mix on the cold side. The heat exchangers are optimized for use in exhaust gas with temperature range 400-650^{o}C and coolant (water-glycol) in the temperature range 40-100^{o}C.

The thermoelectric elements are p-type and n-type skutterudites and are hermetically enclosed in inert gas. The enclosure consists of a heat exchanger on the outside hot surface and a cooling tube on the inner cold surface of the cartridge. Dimensions of the cartridge and connection points are shown for reference in Figure 4. The materials used for the wetted components are shown in Table 1. The materials are selected to be compatible with exhaust gas on the hot side and 50/50 water/glycol mix on the coolant side

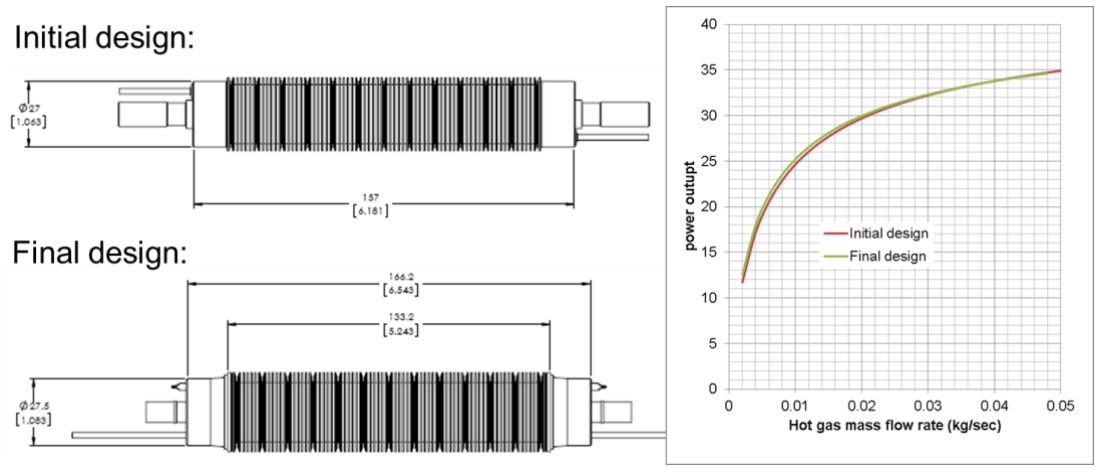

Figure 4 Cartridge- physical dimensions. Evolution of cartridge design (left). Bottom left: geometry of cartridge for final delivery. Right: performance curves for cartridges at 600C hot gas temperature and variable hot gas flow rate.

Table 1 Materials of construction.

External hot side HEX - fins	SS 304
End cap with liquid connections and electrical connections	SS 304
Liquid tube stems	SS 304
Coolant tube (internal)	Aluminum
Gas tube	SS 304
Electrical wire	Copper Cu101
Thermoelectric materials	Co-Fe-Sb based (Skutterudite)

Cartridge performance

An example of measured performance of cartridges is shown in Figure 5 and Table 2 for cartridges labeled SN-0007, SN-0008 and SN-0009. All three cartridges were tested for performance and for

repeatability and have shown excellent results. All other cartridges produced in this program show the same performance and the cartridge-to-cartridge variation is less than 10%. Figure 5shows the correlation between the predicted performance of the cartridge (dots) and the measured cartridge performance (lines). All tests were performed using hot air and water as a coolant. All tests were performed using 2l/min coolant flow and 20^{o}C coolant temperature.

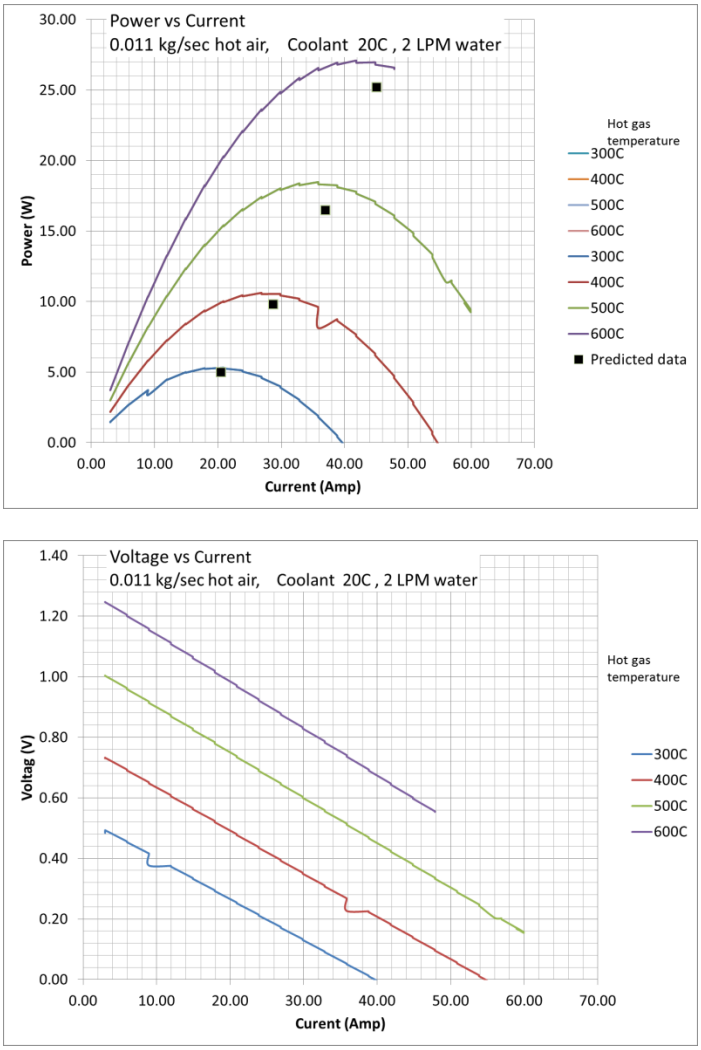

Figure 5 Performance testing: generated power vs. current and voltage vs. current of cartridge SN-0007.

As seen from the data in Table 2, all three cartridges, which were produced in the same batch, have similar performance. For example, when tested at a hot gas temperature of 600^{o}C and gas flow of 11g/sec, the cartridges produced 34.2, 37.9 and 35.7W of power. We consider this type of repeatable performance an indication of the stability of the material properties and good control of the manufacturing process.

Table 2 Performance testing results.

Cartridge # C-0007			**Cartridge # C-0008**			**Cartridge # C-0009**		
Gas temp °C / Flow (g/sec)	Open Circuit Voltage(V)	Power (W)	**Gas temp °C / Flow (g/sec)**	Open Circuit Voltage(V)	Power (W)	**Gas temp °C / Flow (g/sec)**	Open Circuit Voltage(V)	Power (W)
300/11	0.49	5.2	300/11	0.5	4.7	300/11	0.493	4.58
300/22	0.58	7.17	300/22	0.582	5.82	300/22	0.567	6
400/11	0.73	10.6	400/11	0.737	9.65	400/11	0.73	9.36
400/22	0.86	14.1	400/22	0.841	12.5	400/22	0.824	12.1
500/11	1.00	18.3	500/11	0.998	17	500/11	0.976	16.2
500/22			500/22			500/22	1.1	20.5
600/11	1.25	26.9	600/11			600/11		
600/22	1.47	34.2	600/22			600/22		
600/45	1.56	40.9	600/45			600/45		
300/22	0.566	5.97	300/22	0.586	6.4	300/22	0.571	5.86
400/22	0.827	12.1	400/22	0.852	12.75	400/22	0.832	11.9
500/22	1.12	20.75	500/22	1.14	21.8	500/22	1.11	20.4
600/22	1.4	31.5	600/22	1.44	33.2	600/22	1.41	31.4
			600/45	1.54	37.9	600/45	1.5	35.7

Durability testing of TEG cartridges was performed at 3 separate levels:

- Materials, including metallization
- The engine subassembly level, where all the interfaces from hot side heat exchanger to cold side heat exchanger and p/n couples are tested
- Cartridge level testing

Materials and metallization testing is continuing with standardized 150h tests. These tests consist of a 72h soak at a hot side temperature of 550°C and cold side temperature of 40°C, followed by a cycling test in which the hot side is rapidly heated and cooled in time intervals of 20 min. These tests are used to investigate materials and metallization stability.

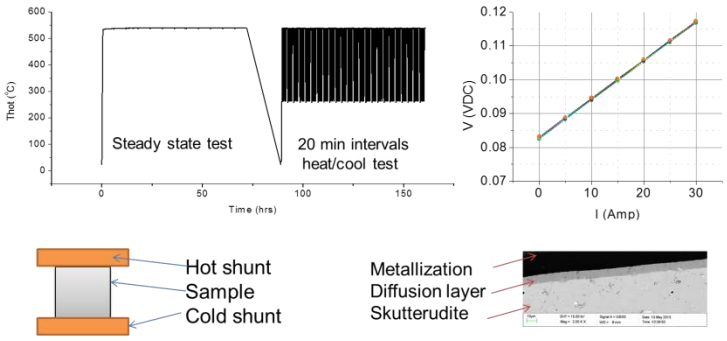

Figure 6 Illustration of materials level test. Top left: test temperature protocol. Top right: I-V curves collected during test process indicate material stability. Bottom left: TE material positioned in test fixture. Bottom right: diffusion barrier function.

Figure 7 shows performance of a cartridge during a 7 day trial. No measurable degradation in device performance is observed.

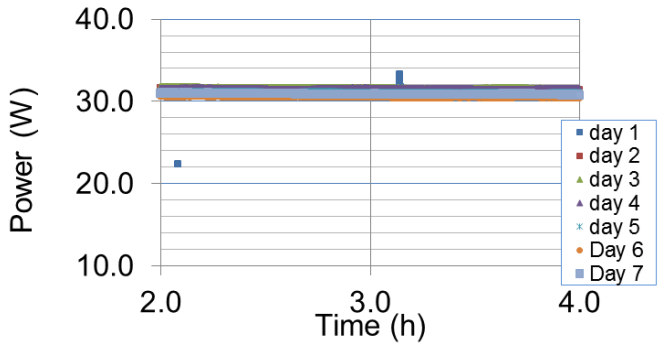

Figure 7 Illustration of TEG cartridge level performance during 7 day test. Each day included exposure to operating temperatures for a period of 2-6 hours.

Cartridge performance model

Fundamental model of cartridge is described in [CRN2011] and it is only adjusted here to capture performance of cartridge. Detailed discussion of modeling parameters is part of final report DE-FC26-04NT 42279. Here we show correlation between model predictions and test results. Good agreement is achieved throughout the measurement range as shown in Figure 5. This also translated in good agreement between device performance and models as shown in separate section discussing correlation between model and test results at NREL.

Cartridge model data is shared with exhaust component integrator in this program – Tenneco and used to design packaging of thermoelectric power generation system (TEG System). Cartridge performance map shown in Figure 8 illustrates predicted cartridge performance in the operating range of gas temperatures and mass flow rates. Peak performance per cartridge reaches nearly 50W.

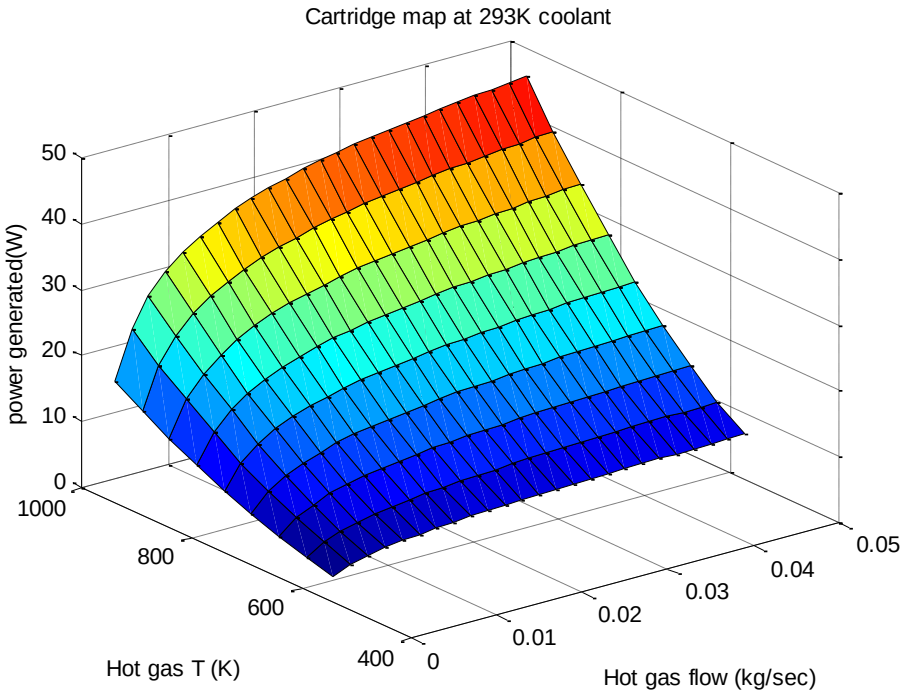

Figure 8 Sample map showing performance of TEG Cartridge as a function of exhaust gas temperature and mass flow rate. Performance shown here is representative of coolant temperature of 20°C and flow rate of 2l/min.

Table 3 Sample performance map table showing performance of TEG Cartridge as a function of hot gas inlet mass flow and temperature next to coolant inlet mass flow and temperature. Outputs include illustrated values and cartridge power output, open circuit voltage, resistance, peak point current, pressure drop on a gas side and liquid side, output hot gas and coolant temperatures, cartridge thermal resistance, heat absorbed by the coolant loop.

hot gas flow (kg/s)	hot gas inlet temp (K)	cold coolant flow (kg/s)	cold coolant inlet temp (K)	power (W)	load resistance (ohm)	Pressure drop exhaust gas: (mbar)	Pressure drop coolant: (mbar)
0.012	973	0.0165	333	32.61795395	0.013979183	4.987413868	10.58361063
0.014	973	0.0165	333	33.97525925	0.014011789	6.438768358	10.65639419
0.016	973	0.0165	333	35.10837137	0.014038483	8.036466754	10.71735106
0.018	973	0.0165	333	36.07305305	0.014060854	9.774504535	10.76941609
0.02	973	0.0165	333	36.9073075	0.014079951	11.64779102	10.8145845
0.022	973	0.0165	333	37.63807756	0.014096497	13.65192907	10.85426974
0.024	973	0.0165	333	38.28508365	0.01411101	15.78306382	10.88950662
0.026	973	0.0165	333	38.86314484	0.01412387	18.03777477	10.9210735
0.028	973	0.0165	333	39.38364621	0.014135368	20.4129962	10.94956914
0.03	973	0.0165	333	39.85550117	0.014145726	22.90595698	10.97546304
0.032	973	0.0165	333	40.28580264	0.014155118	25.51413406	10.99912946

Thermoelectric power generation system design and vehicle integration

Vehicle selection and preliminary testing

In the preparation to this program, Ford and BMW selected two vehicles for TEG testing and performance evaluation. The vehicle selected by Ford was the F150 with gasoline engine. In the final phase of this program this vehicle was replaced by Gentherm's F350 with 6.2L SOHC V8 flex fuel engine. The F350 was used as a demonstration of technology on larger size vehicle and this vehicle was not considered in design phase.

For passenger vehicle demonstration, BMW selected the X3 series SUV. The vehicle of type X3 xDrive28i has a four piston gasoline engine with 2.0 l capacity. To enable thermodynamic and thermoelectric sizing of the TEG-system vehicle level tests were completed by BMW and Tenneco. Detailed testing and modeling was performed only on configuration with the BMW vehicle. The purpose of these tests were to measure energy available in the exhaust gas flow, temperatures and mass flows of coolant in different branches of the cooling system. Furthermore, voltage and current of the battery and alternator were measured. This information was used to design the TEG system and evaluate interaction between the TEG system and the vehicle.

Test specified by terms of this award is US 06 cycle, all fuel efficiency improvements and CO_2 emission reductions are measured and calculated for this test cycle. In addition, fuel consumption and CO_2 emissions of passenger vehicles were measured in WLTP[1], NEDC[2] and US-Combined-Cycle[3]. NEDC is a relevant cycle in EU and it is expected that in 2017 it will be replaced by WLTP[4]. For this reason, the latter has been considered as the relevant EU-cycle and added as a test protocol in this project.

Analysis of exergy distribution in BMW X3

Figure 9 shows the exhaust gas temperature as a function of time (left graph) as measured at the underfloor position in WLTP cycle. This position in the exhaust system is also known as mid-muffler position. The temperature increases with higher velocities due to higher engine loads. In this test, a maximum 700 °C is reached during highway phase, while the average temperature is much lower at about 440 °C.

Plotting gas temperature against mass flow (Figure 9 right) indicates time vehicle spends at certain set of mass flow and temperature conditions. However concentrating on highly populated areas would be

[1] Worldwide harmonized Light vehicles Test Procedures
[2] New European Driving Cycle
[3] Combination of FTP-75 (Federal Test Procedure) and HWFET (Highway Fuel Economy Test)
[4] Worldwide harmonized Light vehicles Test Procedures

misleading since a high density in the mass flow/temperature map does not automatically correlate to high heat quantities or exergies. An exergy distribution was calculated by BMW to better visualize available energy. Exhaust data sampled at 1sec rate was clustered in mass flow/temperature groups (+/- 5 kg/h, +/-20 K) and used to calculate associated exergy. Exergy is, by definition, a measure of maximum potential energy in the system. Exergy maps for US-Combined and WLTP cycle are shown in **Figure 10**. Left figure shows the distribution of the exergy for the different mass flow/temperature combinations in the mass flow/temperature map in WLTP-cycle. The size of the bubbles correlates with the particular available amount of exergy. There is a concentration of high exergy around 100 kg/h / 600 °C as well as in the area of 175 kg/h / 650°C. Apart from that, exergy is distributed over a wide area. For US-Combined-cycle, the exergy overall is much more concentrated than in WLTP. In this cycle, area of high concentration of points can be found at around 60 kg/h / 550 °C.

The TEG can be thermodynamically dimensioned for certain (stationary) exhaust states (mass flow & temperature combinations). Using exergy analysis it is possible to identify range of flow conditions for which it would be reasonable to dimension TEG. Dimensioning of TEG for transient or dynamic states, such as those shown in Figure 9, is quite difficult and it would result in different optimal design for every drive condition. TEG system design in this program is dimensioned to have minimum cost and maximum performance at temperatures between 550 and 600C and flow rates 50-100kg/hr.

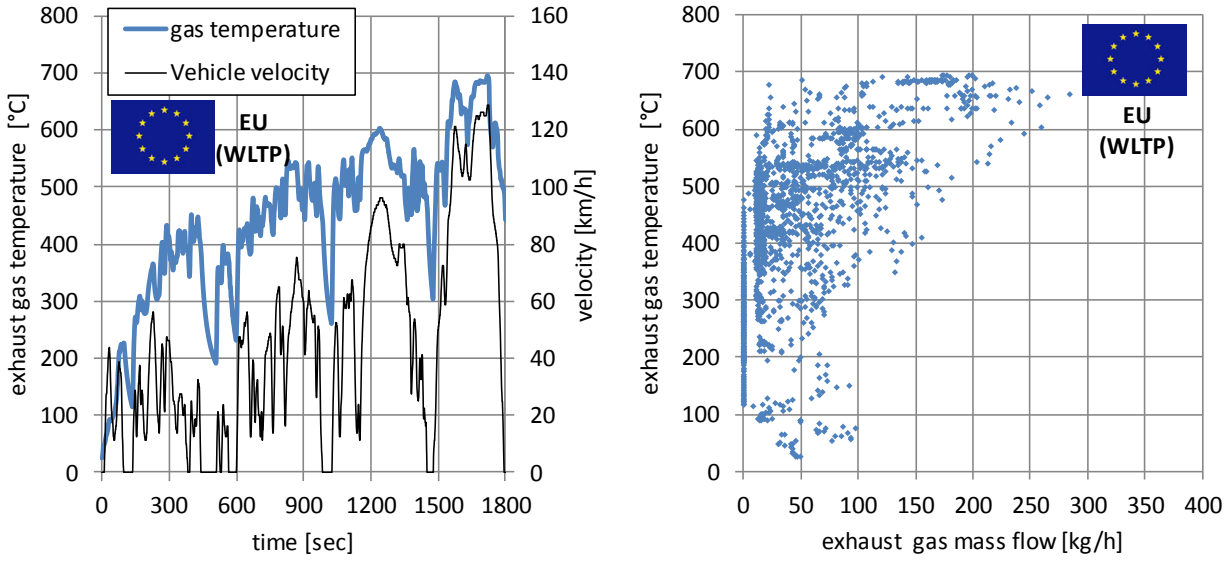

Figure 9 Left side: Exhaust gas temperature at under floor position and velocity of X3 xDrive28i over WLTP-cycle. Right side: Distribution of exhaust temperature over mass flow in secondary resolution in WLTP-cycle.

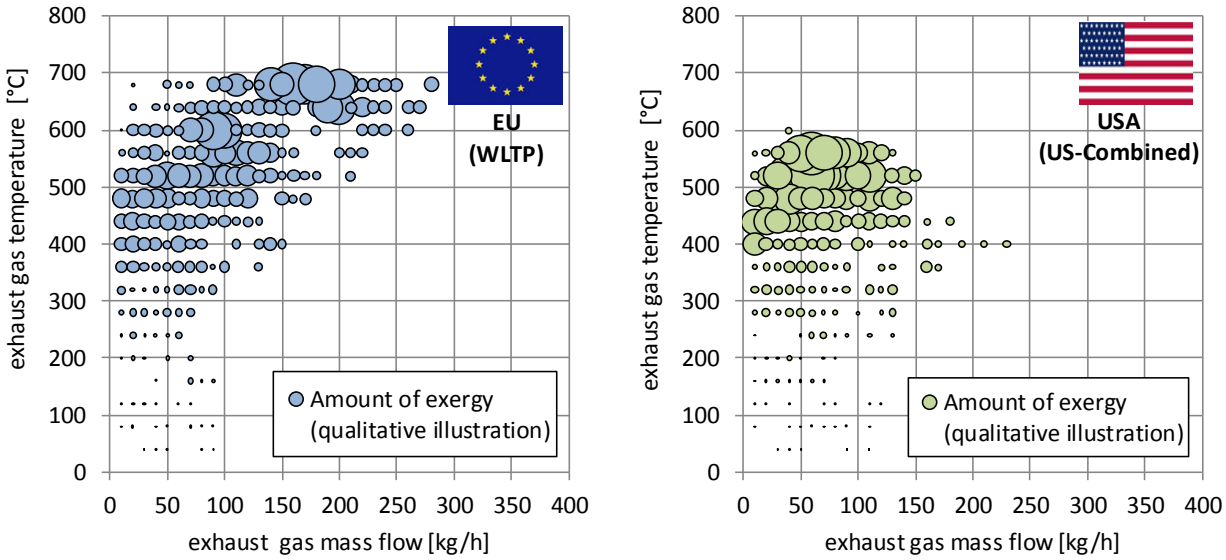

Figure 10 Illustration of qualitative amount and distribution of exhaust exergy clustered in mass flow/temperature groups (+/-5 kg/h, +/-20 K). The size of the bubbles correlates with the particular available amount of exergy. Left side: WLTP-cycle. Right side: US-Combined-cycle. Left side: WLTP-cycle.

Thermoelectric Generator – System level design and sizing of components

Device layout

Constraints in the system level design were geometric shape of TEG – Cartridge and available energy based on the analysis performed by BMW. For a given flow of gas and temperature, the TEG system can be designed by selecting an appropriate number of cartridges and their spatial layout. To maximize TEG system performances, it is necessary to consider a flow distribution of the exhaust gas on the cartridges. Cartridges will occupy only a portion of the system volume and will be distributed in such way that captures the maximum amount of available heat. Two extreme case designs of cartridge based TEG system are a configuration in which all cartridges are exposed to gas at the same temperature (parallel configuration) and a configuration in which all cartridges have 100% of gas flow (series configuration). Performance of TEG system and layout can be evaluated based on maximizing performance or minimizing number of cartridges used to generate certain power. The following discussion will try to explain the process used in selecting TEG system layout for this program.

The flat design shown in Figure 11 is one of potential layouts with relatively easy cartridge integration and connection of electrical and cooling circuit. This design uses twenty cartridges in two parallel flow lines and has integrated central bypass. We will use this design to illustrate design process.

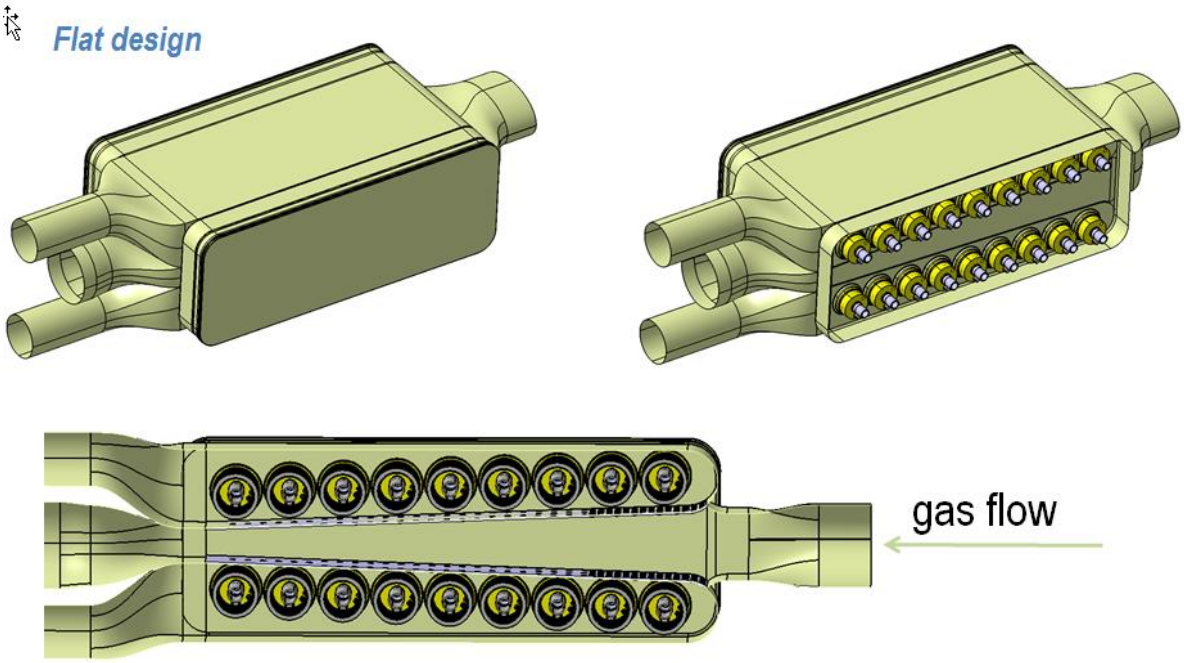

Figure 11 Flat design with integrated bypass.

Expected power output from this device can be easily calculated using performance maps for an individual cartridge. For example, at gas flow of 80kg/hr and temperature of 590^{o}C power output can be 210W. Individual contribution of every cartridge is shown in Figure 12. Largest power output and largest reduction in CO_2 emission with an increase in power can be achieved by simply adding more cartridges. In the limit case, about 1.8% of hot gas energy can be recovered and converted into electric power. Large number of cartridges increases the weight and cost of the overall system. To understand impact of device size to cost, we can calculate cost benefit ratio. Cost benefit is ratio of relative increase of cost and relative improvement in performance. We can limit increasing the size of device when cost benefit ratio reaches a certain value defined by OEMs for example. In this design phase we can limit cost benefit ratio to one (1) and determine that maximum feasible number of cartridges is approximately 10. In itself, this cost benefit optimization process is iterative as cost cannot be fully estimated until final device design is completed.

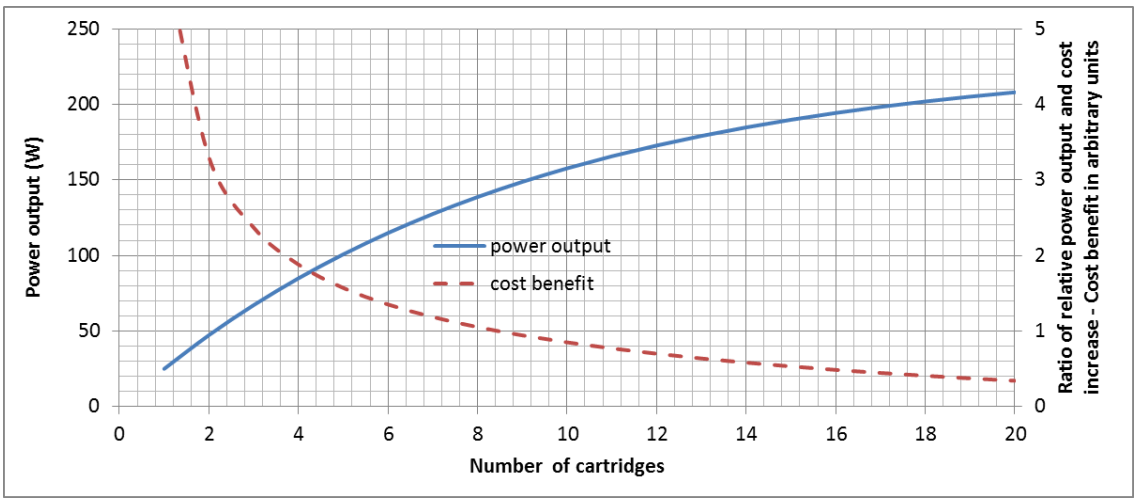

Figure 12 Individual contributions of cartridges to total power output shown in solid line. Dashed line is cost benefit ratio and defined as ratio of relative improvement in performance over relative increase in system cost.

TEG system performance modeling

Graph shown in Figure 12 is computed using simple one-dimensional physical model of TEG system. This model only captures cartridges and neglects heat transfer through other components of TEG system. Before entering the hardware design phase more comprehensive TEG model was developed. This model was used to compute TEG system performance. In addition to capturing physics of individual cartridges and associated TE materials and heat exchangers, system level model captures flow of gasses through TEG and through bypass line. GT-Power software is standard thermal modeling tool in automotive industry and it was used to perform these calculations. CAE department at Tenneco developed a complete TEG model cartridge performance maps. Using GT-Power model team evaluated performance of different cartridge and bypass layouts. Cartridges in TEG can be connected in series, parallel or combination of two. On the electrical side, they can also be connected in parallel and series. Coolant flow can be regulated separately as a parallel flow though individual cartridges or as a set of series connections. The number of possible configurations is very large and GT model was used to evaluate over 50 different combinations.

The Tenneco CAE team used its expertise on exhaust valve technology to develop a sophisticated model of exhaust gas bypass valve and included this model to simulate overheating control. Overheating

control refers to limiting heat removed by cooling system and preventing exposing cartridges to conditions under which the device could fail.

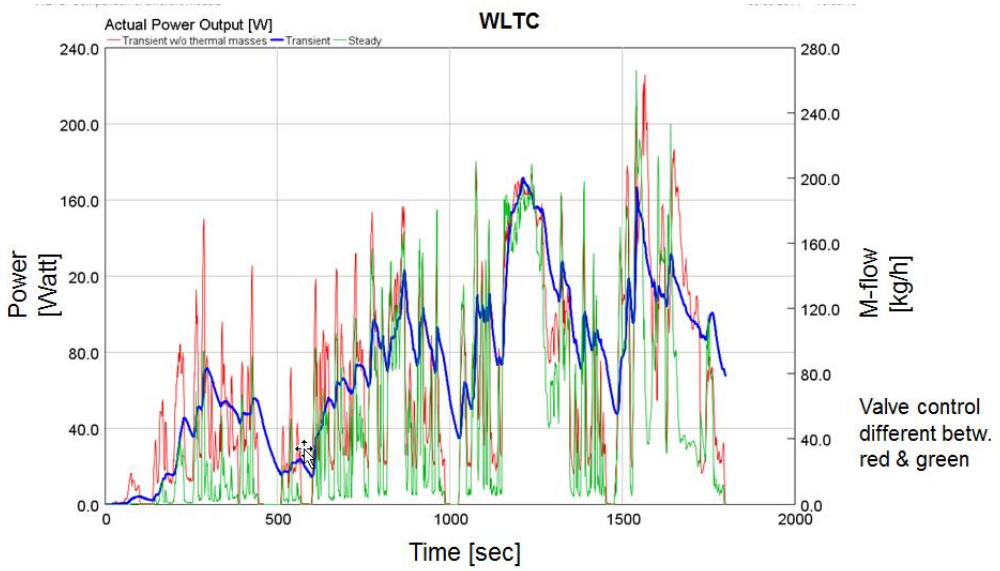

Figure 13 Steady state compared with transient valve model

Results shown in Figure 13 compare results of the transient GT-Model (red line) and steady state GT-Model. Steady state results show higher TEG System level performance. In steady state model change in gas temperature and flow will result in an instantaneous response in power output. Transient model includes thermal inertia of all components in the system. Masses of components are large compared to mass of active thermoelectric components; therefore, system is relatively slow to respond to fast changes. This was one of the challenges in designing valve control. Using instantaneous flow conditions to control bypass valve would significantly reduce the potential to generate power. Transient model had to be used to properly control valve.

End result of 1-D system level modeling study was selection of cartridge configuration with 2 cartridges connected thermally in parallel at the device leading edge and followed by 8 cartridges connected thermally in series; this configuration is illustrated by sketch in Figure 14. Second level of design optimization is related to configuring cooling and electrical connections. In the case of selected device layout we considered three different electrical configurations. All cartridges connected in series or combination of parallel and series connections. Results are illustrated in Figure 14. Optimizing electrical connections can result in 3-5% percent improvement in power output in this case.

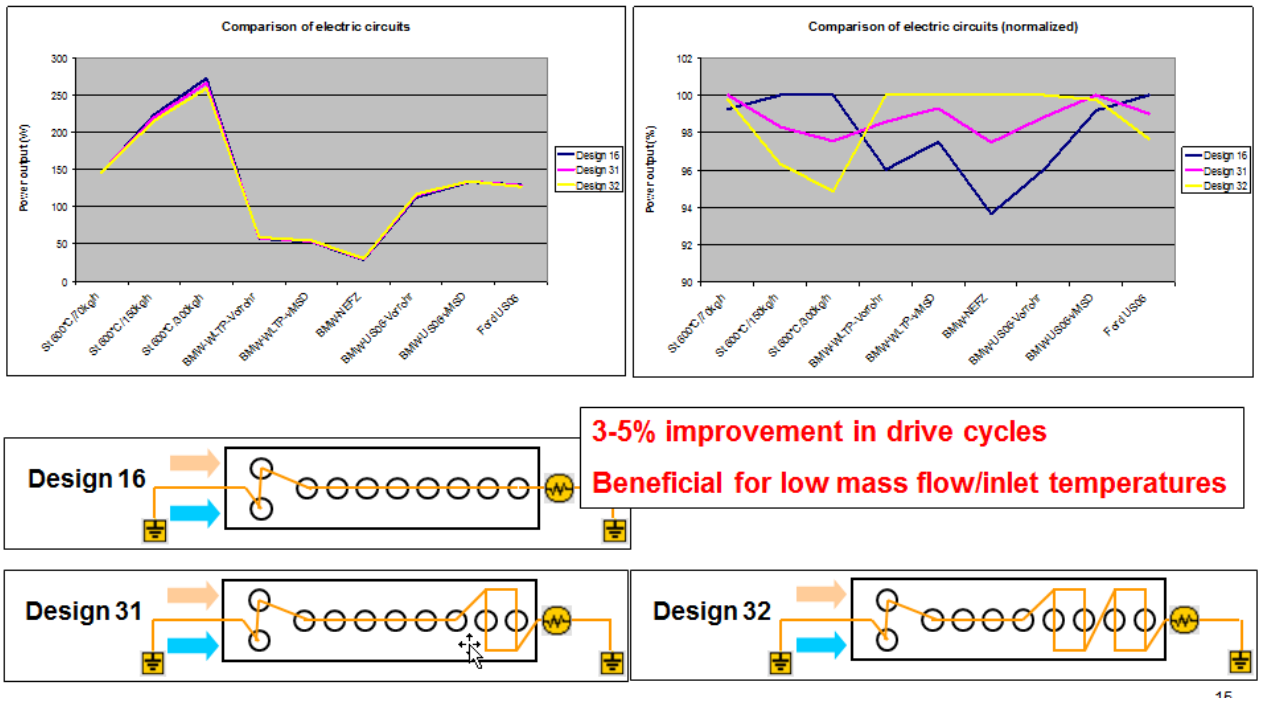

Figure 14 GT-Results with different cartridge configurations considering several electrical connection paths as indicated in the graphs showing configurations 16, 31 and 32.

Low mass-flow rates during drive cycles are common on big engines and small engines. As shown in analysis of US 06 cycle (Figure 10) majority of driving conditions correspond to flows < 50kg/hr and highest exergy is at flows above 250kg/hr. The TEG will be evaluated on common drive cycles like US06, NEDC or WLTC with low mass-flow rates. Based on that, the configuration “Design 16” was the chosen one. This is a combination of parallel and series connections between cartridges. In this configuration, two leading cartridges are connected in parallel and they are followed by eight cartridges connected in series. Expected maximum power output from this device in BMW X3 and in regulatory cycles is 172W with average of 70W. Difference in estimated power output as a function of cycle is small ranging from 163-172W.

CFD-Simulation

Preliminary flow modeling was necessary to understand to properties of flat design in consideration of a homogeneous hot gas flow distribution. A good illustration of the mass-flow distribution is shown in Figure 15.

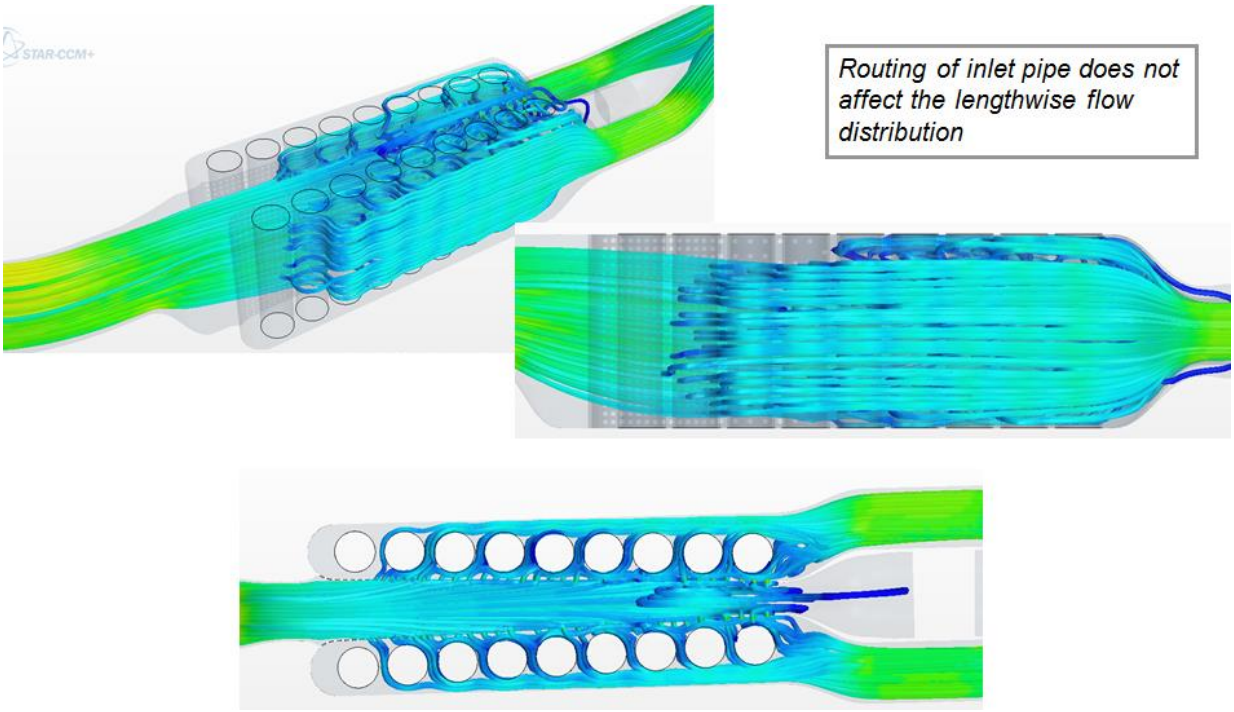

Figure 15 Mass-flow distribution shown with stream lines.

Observation from this modeling exercise are that the first two cartridges are without contact with flow of hot gas. This will reduce the TEG-Perfomance and invalidate GT model prediction which assumes uniform flow distribution. Combination between 3D modeling and 1D modeling lead us to conclude that full parallel flow would result in low power outputs form cartridges. This was the reason to evaluate larger number of possible configurations as shown in Figure 16. Different designs were checked regarding the veloctiy on the cartridge high temperature heat exchanger, the heat transfer coefficient values (HTC) and the system level pressure drop which was limited to 30mbar.

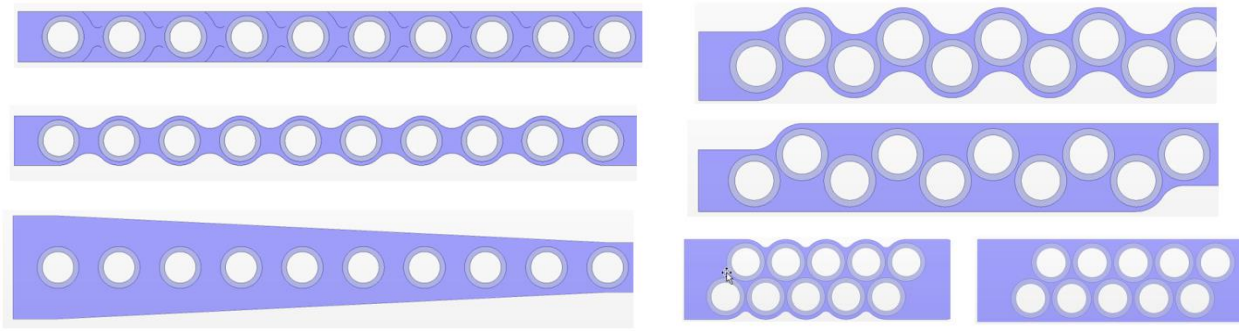

Figure 16 Cartridge configurations evaluated in 3D models. Table on the top shows "design set point" and model parameters.

Table 4 Summary of CFD results.

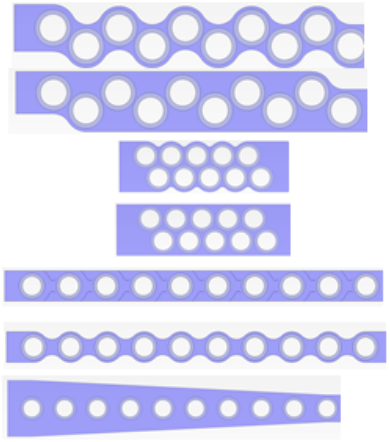

V_{ave} m/s	htc_{ave} W/m2K	Δp mbar
1,47	101,2	21,2
0,85	96,3	9,7
0,97	92,9	9,4
0,62	83,9	5,2
2,00	108,9	52,2
1,80	108,5	34,2
0,34	71,8	5,0

The green marked line in Table 4 is showing the design with the most potential. Although the blue marked design is showing a better perfomance in HTC-Value, the green marked design was elected because of a lower backpressure which has a big influence to the fuel consumption.

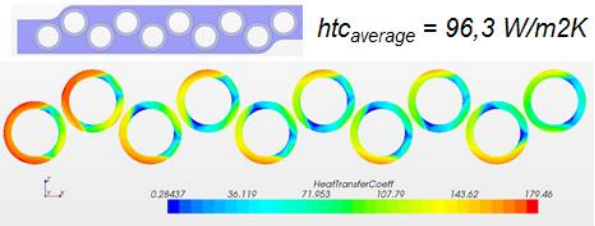

Figure 17 HTC-Value distribution (staggered configuration)

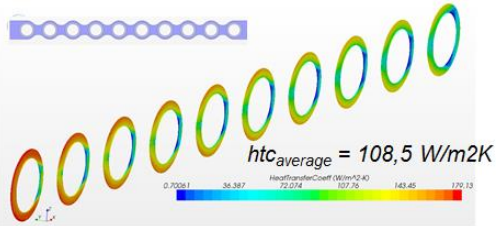

Figure 18 HTC-Value distribution (sequence configuration)

The figures above show the HTC-Values given by different colors. Red represents the maximum HTC-Value and blue lowest HTC-Value during simulation. The following figures show the velocity of the exhaust in the two best configurations.

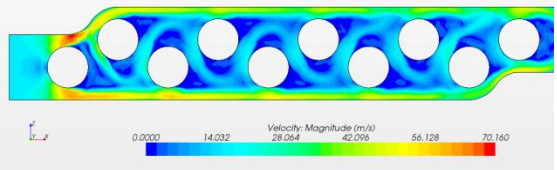

Figure 19 Staggered configuration (green marked)

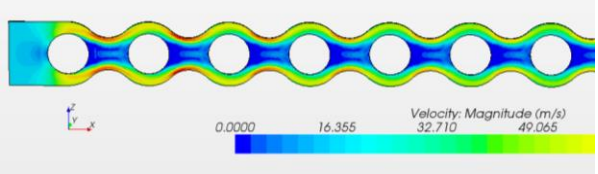

Figure 20 Sequence configuration (blue marked)

In essence, cartridges form cylindricall finned tube heat exchangerobserved flow paterns similar to those seen in laminar flow around the tube. Wake fields behind cartridges are large and for this reason pure series connection is not a good choice. In this case, shown in Figure 20, only the first cartridge is exposed to 100% flow and all others are in the wake region of their predecessor. Arranging cartridges in staggered configuration, as shown in Figure 19, reduces theoretical flow rate of gas arround the cartridge but it provides for better device performance. Comparing two designs, the staggered design has in average lower gas velocity and lower back pressure.

The staggered design is the configuration with the highest potential and this configuration is selected for final design.

A TEG was designed for a BMW X3 with a 2.0l turbo charged engine and Ford F150 with 3.6l turbo charged engine. The target was to use one design for both cars. Both cars were considered during the design process. This device is primarily designed to fit on the BMW X3 as available space was smaller in this vehicle. During the design phase, the F150 was considered and device was designed in such way that it fits in this vehicle. The device was also used in F350 with 6.2L V8 naturally aspirated engine but this vehicle was not taken in consideration during design phase.

Preliminary design shown in Figure 22 was created using design guidelines generated by simulation and modeling team, packaging constrains defined by OEMs. Device consists of bypass line with control valve and TEG System consisting of 10 cartridges. Cartridge configuration corresponds to “Design 16” shown in Figure 14 with cartridges in staggered configuration shown in Figure 17. Fit in BMW x3 underbody is shown in Figure 21.

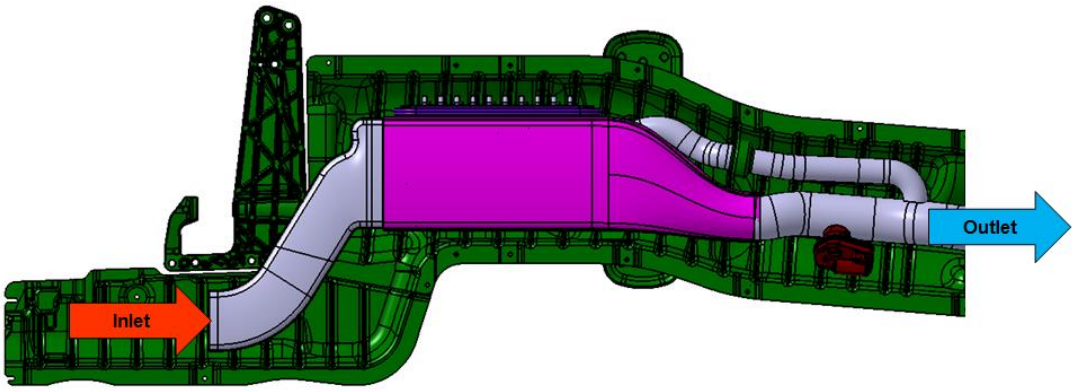

Figure 21 Preliminary design of flat TEG with single row of staggered cartridge. Image shows fit in BMW X3 allocated space.

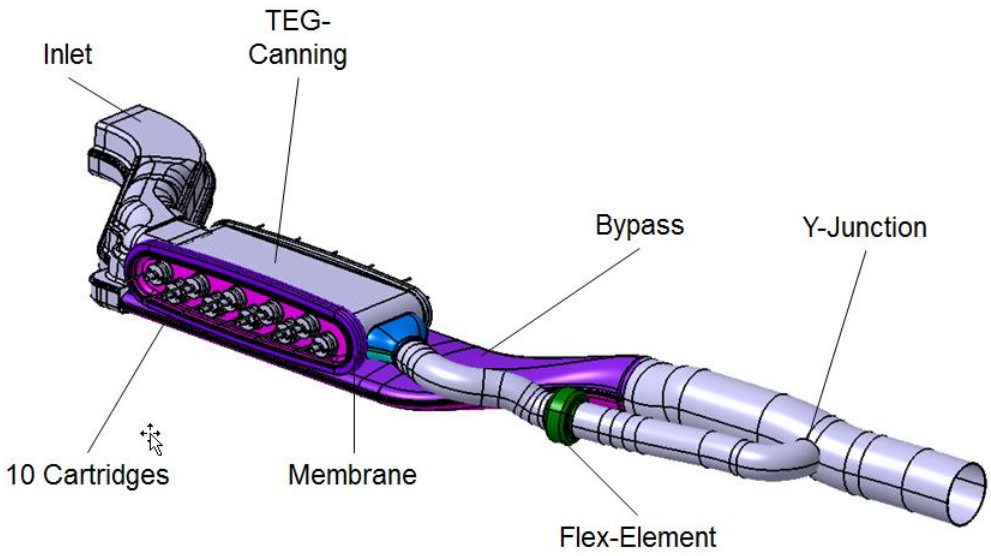

Figure 22 TEG system with active TEG section with 10 cartridges, bypass line and control valves.

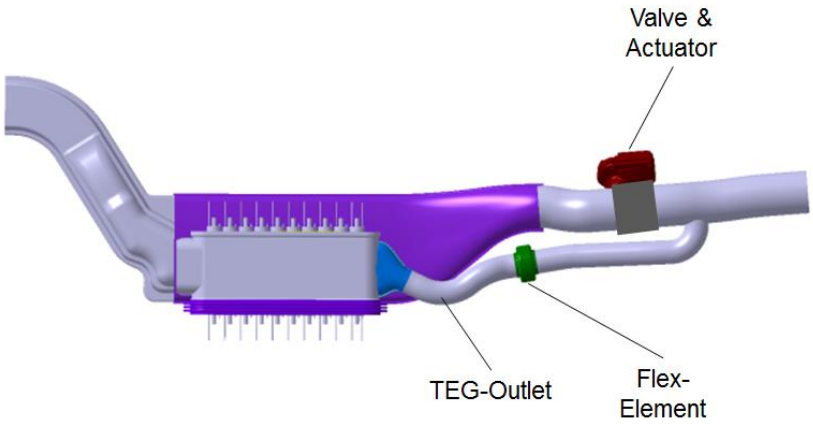

Figure 23 TEG system design detail shows control valve in the bypass line and flexible element used to compensate for the difference in thermal expansion between TEG and bypass.

Initial concept included only one valve as shown in Figure 21 through Figure 23. Function of this valve is to open bypass line when gas flow through TEG is too high and either reduce system level backpressure or reduce temperature of the cartridge. In fully open state, pressure drop in bypass line was approximately the same as in the main TEG line. This condition was not acceptable since it would result

in high heat load to vehicle cooling system under certain conditions. In order to reduce flow through TEG when bypass is open, designers added perforated inlet section to TEG line. If the bypass is open, the perforated plate should minimize heat transfer to TEG by providing flow constriction and diverting flow of gas to fully open bypass line. The flow paths are shown in Figure 24. CFD modeling is used to evaluate distribution of gas flow between TEG and bypass line, Figure 25. Model shows 21% of the mass flow of gass in TEG line vs 79% in bypass line. OEM defined requierment was that 99% of flow must be diverted to bypass under towing condition. For this reason, the second valve was added at the TEG inlet.

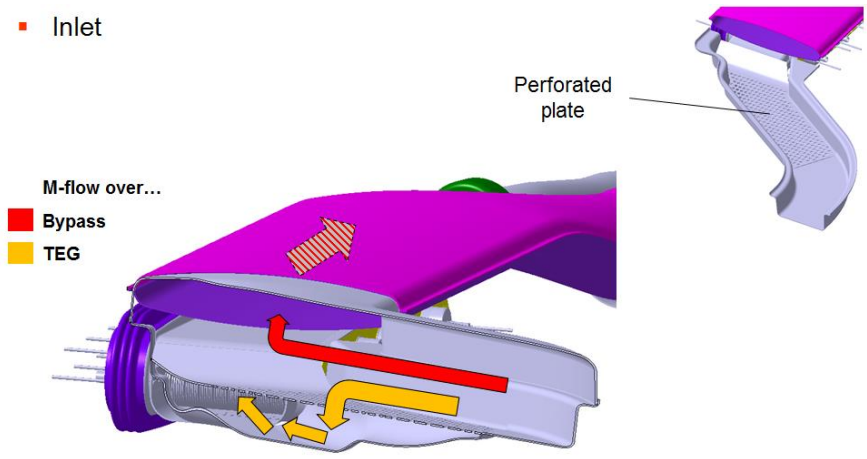

Figure 24 bypass path (red arrows) TEG flow path (yellow arrows).

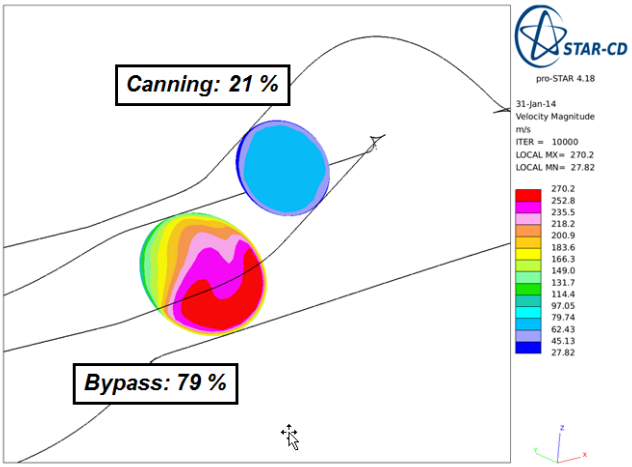

Figure 25 Mass flow distribution between TEG and bypass line with valve 100% open.

Considering flow analysis, final packaging was modified as shown in Figure 26. Final device design includes TEG and bypass line with flow control valves on both of these lines. Final device has ten cartridges arranged in a staggered configuration. First two cartridges are splitting flow of hot gas – parallel cartridge connection and additional eight cartridges are connected in series. This device meets geometric constraints and fits in allocated space in both the BMW X3 and Ford F150 as shown in Figure 27 and Figure 28.In order to minimize thermal stresses in the system, it was necessary to solve differential thermal expansion between the canning of the TEG and the active thermoelectric components - cartridges.

The thermal expansion of the canning is the function of the gas flow rate, temperature, and thermal expansion coefficient of the canning material. The cartridge is different. The thermal expansion of the cartridge is not dependent on the gas temperature; it is driven by the coolant temperature. This discrepancy had to be considered in the TEG canning designed and it was compensated by using component referred to as a “Membrane”. This structure is shown in Figure 29.

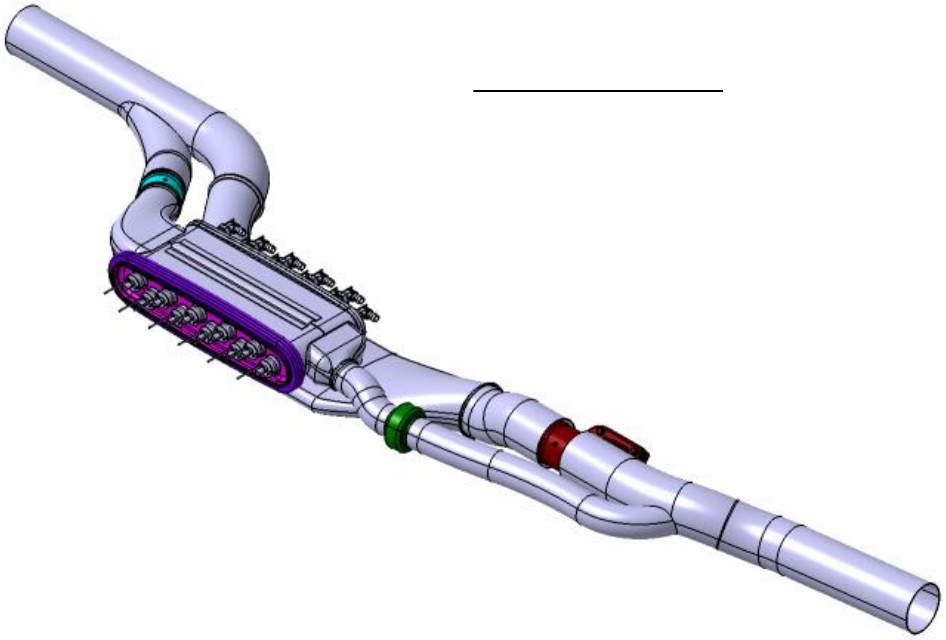

Figure 26 TEG-System with two control valves in TEG and bypass line.

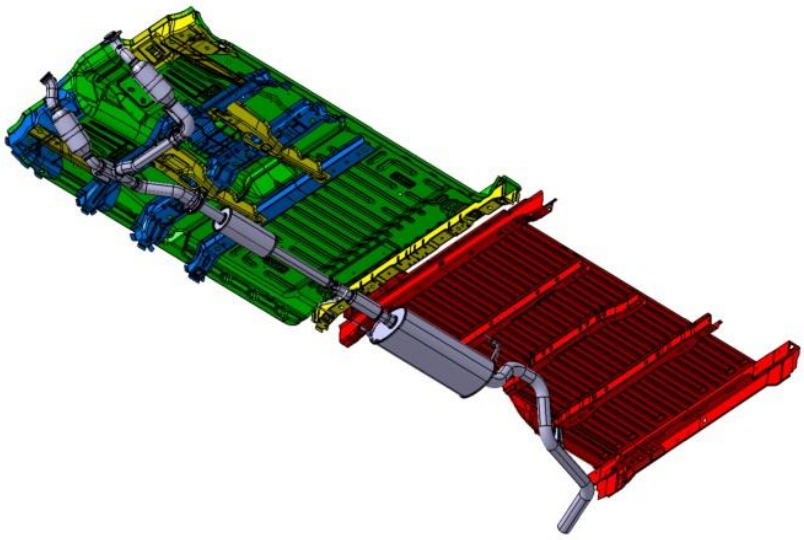

Figure 27 Fit of TEG system in F150 underbody structure.

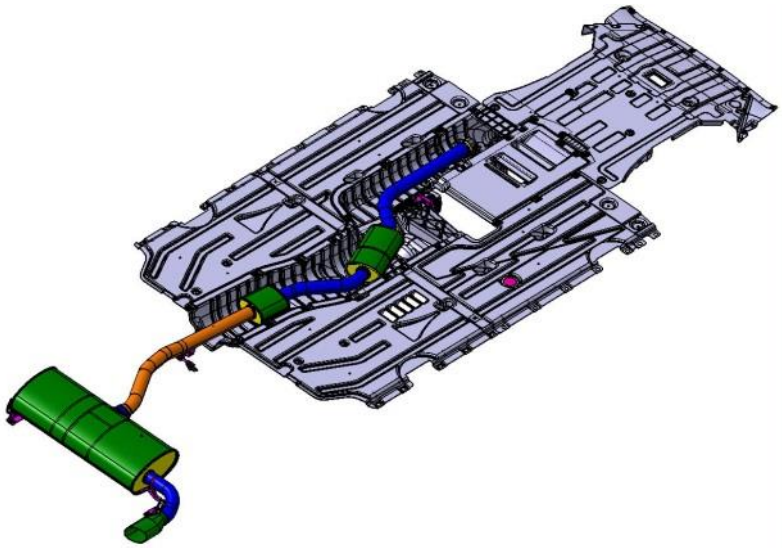

Figure 28 Fit of TEG system in BMW X3 underbody structure.

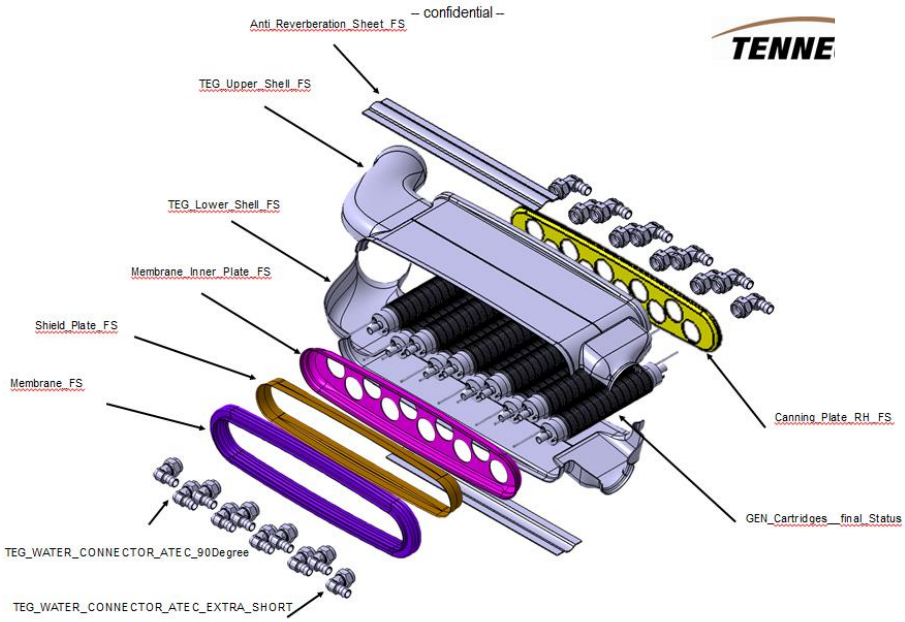

Figure 29 TEG-Canning. Elements of TEG are shown in the exploded view of TEG can.

The thermal expansions of the canning is the function of the gas temperature and the thermal expansion coefficient of the canning material. The thermal expansion of cartridge is the function of coolant temperature. The difference in thermal expansion was compensated by using the membrane. Extreme test conditions are: starting vehicle at -40°C in the winter and heating up the engine quickly, with a high engine load. The coolant will reach 50°C and the canning 650°C in the same time. At this condition, there is a thermal expansion discrepancy of 1.4mm which needs to be compensated on the canning side.

The solution was to use a flexible element, called membrane, between canning and cartridge like the following pictures show:

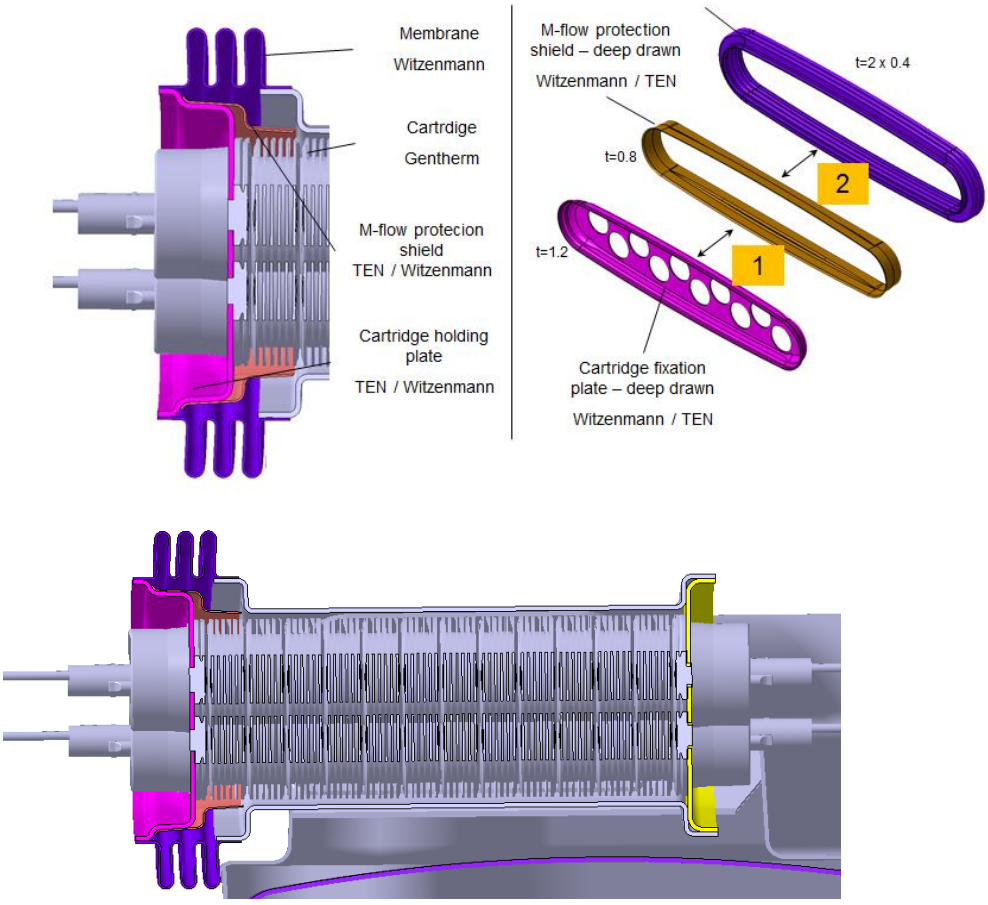

Figure 30 Cross section of TEG showing membrane.

Non linear FEM

After the membrane was designed and confirmed by the supplier regarding manufacturing feasibility, a nonlinear FEM-Simulation was necessary to check the membrane functionality.

Thermal analysis boundary conditions

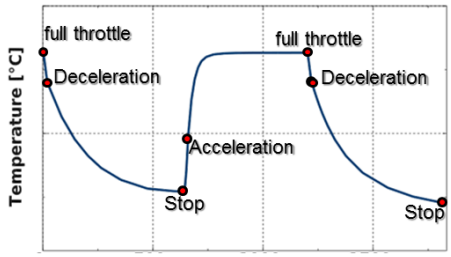

Thermo-shock cycle :	
Stop	635 s
Full throttle	565 s

Radiation	Emissivity
Inner	0.60
Outer	0.40

Convection (V02)	Mass Flow Rate	Tgas	htc -Watt/(m^2*K))
Internal Flow	240 Kg	710°C	CFD
External Flow	-	50°C	20

Figure 32 Boundary conditions of the thermal shock test for nonlinear FEM simulation

As mentioned before, the membrane was included in this design to reduce the difference in thermal expansion between the canning and the cartridge during heating and TEG operation.

Tenneco routinely uses round membranes in customers' exhaust systems – normally called flex elements. The membrane used in TEG is basically a flex element designed in an oval shape. As these are new and not standard components, simulation was used to evaluate ability of designed membrane to withstand loads and reduce stress on mismatched components. Figure 33 shows the deformation amplified by factor 10. At gas temperature of 700^{o}C, membranes take majority of deformation and reduce deformation of canning. In other words, FEA shows that membrane is functioning as envisioned.

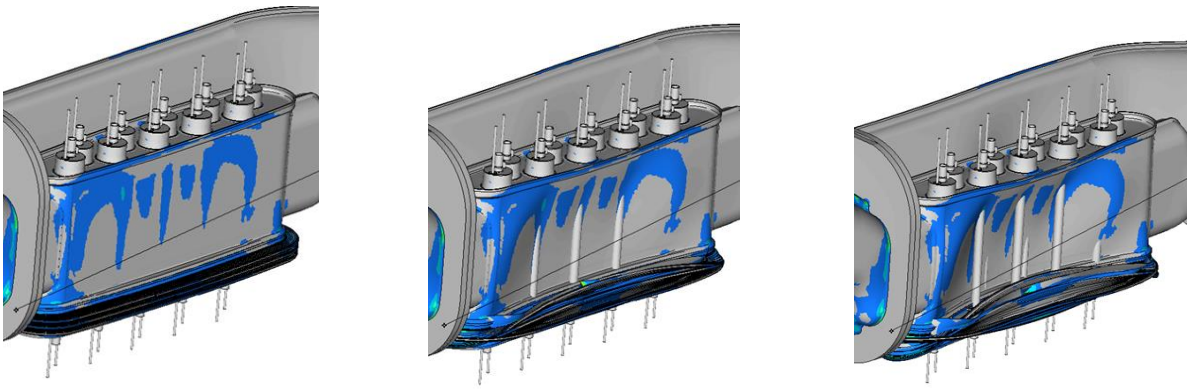

Figure 33 Left to right: Membrane at ambient, during heating up period and at 700°C.

Based on positive results of nonlinear FEM team has prepared first device for structural integrity testing. The system is identical to that shown in Figure 53. System was equipped with a membrane made from two layers of steel with 0.3mm thickness of each layer. Burner test bench was designed to perform thermal cycle tests. In these tests, the TEG is exposed to low temperature low mass flow gas immediately followed by high flow rate of gas at high temperature. The following table lists cycle times and flow/temperature conditions:

Stage	Duration (from…to)	Mass-flow [kg/h]	Temperature [°C]
1	0s	80	170
2	80	80	
3	120	400	660
4	220	400	660
5	220	80	660

All 5 stages define one cycle. These conditions are extreme and represent highest heating and cooling rates TEG and exhaust system would experience. For the purpose of this test, we repeated 700 cycles with satisfactory outcome.

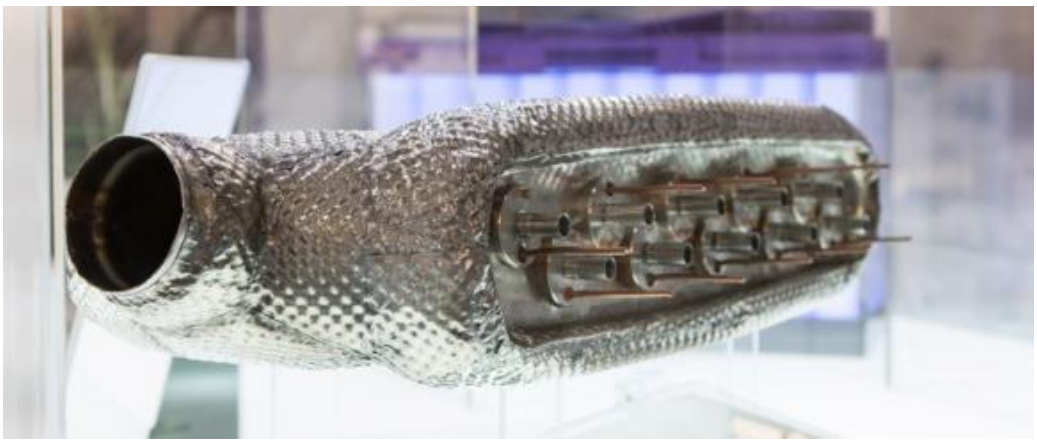

Figure 34 Assembled TEG section of TEG system (canning and cartridges without bypass.

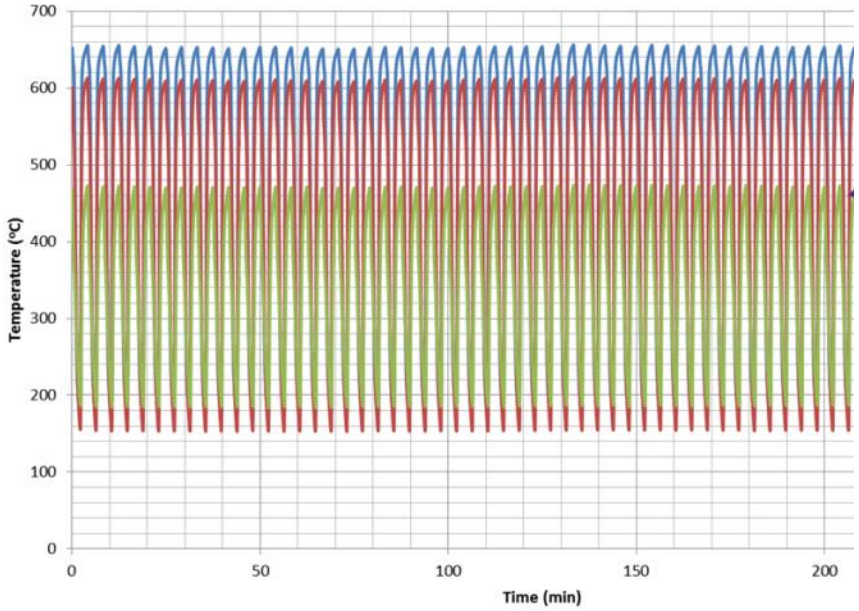

Figure 35 Exhaust temperature at different measurement points over time

Additional mass on the exhaust system exceeds 10kg so Tenneco had to validate hangers on the underbody of the vehicle. The simulation for static load shows, that the TEG-system has 8mm displacement under its own weight and under 1g load. This displacement is possible because of the flex-element (see Figure 36). Additional hangers are designed to compensate for this displacement. Separate FEM analysis was performed under 10g load and results are shown in Figure 37 through Figure 39.

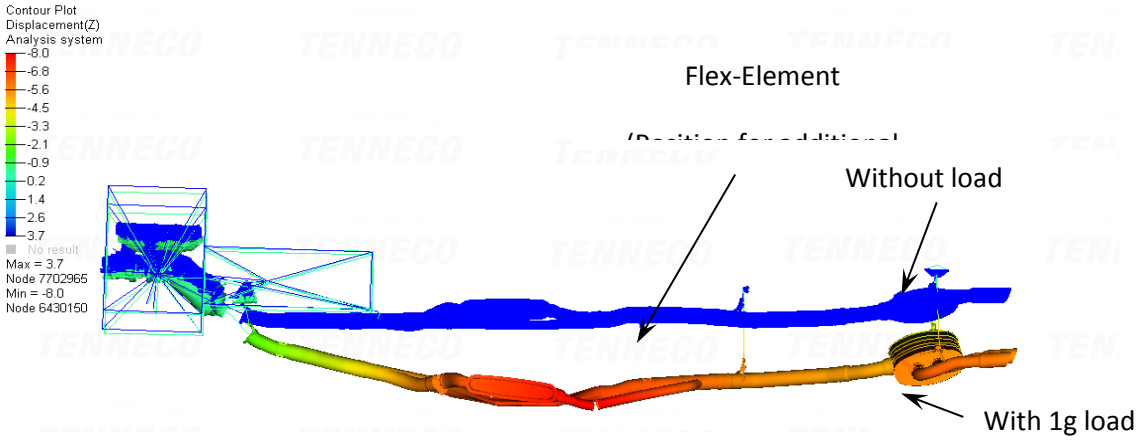

Figure 36 Displacement under assembly weight and without load

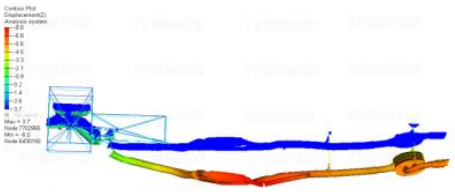

Figure 37 TEG-System with street load

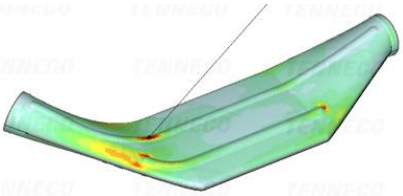

Figure 38 Critical position on Bypass shell

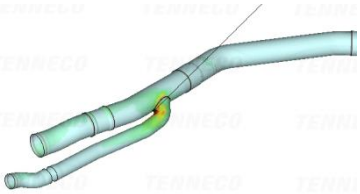

Figure 39 Critical position on Y-Junction

Analysis of the eigen frequency or resonant frequency was used to evaluate effects of dynamic loads. The following pictures show the ground position (green colour) and the displacement of the components under resonant loads (red colour).

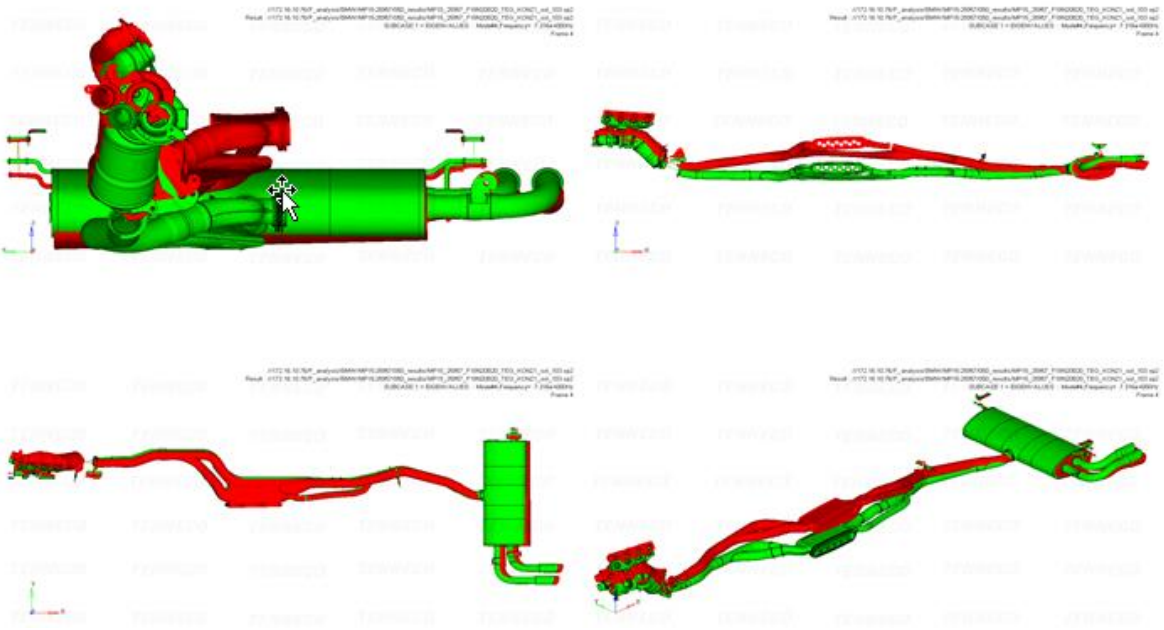

Figure 40 Displacements due to resonant frequencies

Based on all these simulation results, one additional hanger was needed and two hangers of the base design had to be reinforced. One example of a reinforced hanger is shown in Figure 42.

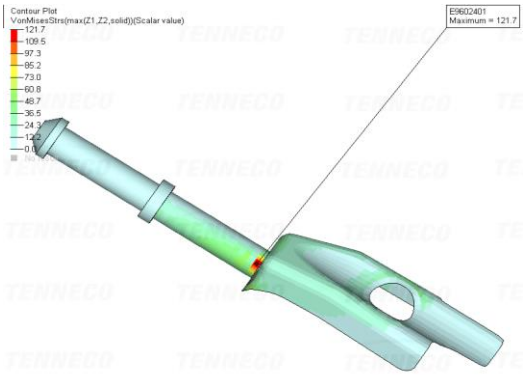

Figure 41 Area indicating critical stress.

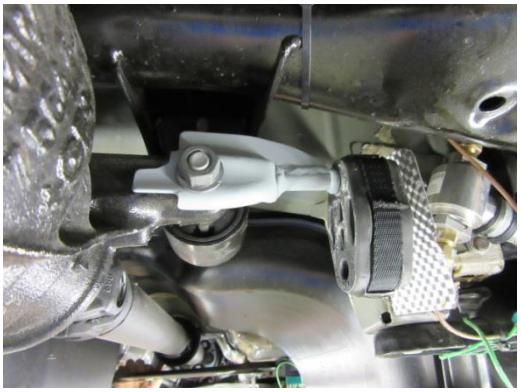

Figure 42 Reinforced hanger.

Performance testing of full scale TEG-System

Confirmatory performance testing of the TEG device was performed by the National Renewable Energy Laboratory using a bench testing facility consisting of a propane furnace, a coolant loop with radiator, and a direct current (DC) load bank. The National Renewable Energy Laboratory conformational testing of the TEG device measured the electrical power production and efficiency of the unit over a range of operational conditions. Several voltage levels were measured at each thermal test point, including the open circuit voltage and the voltage at which maximum power production occurs. This data provided a performance map that demonstrates how the system performs over a range of conditions typically expected during light-duty gasoline vehicle operation.

Test setup

To test the performance of the TEG device, it is necessary to provide a hot gas stream, a fluid cooling loop, and a DC load. A hot gas test furnace with variable airflow and temperature was employed to simulate the post catalytic converter conditions of an internal combustion engine exhaust stream. The air was drawn from the ambient building environment, heated via a propane flame, passed through the TEG device, and ejected via a building exhaust system. The hot gas test furnace employs two programmable PID controllers, one for the air flow rate and one for the outlet temperature. Hot gas temperatures are measured using K-type thermocouples, while air flow was measured with a laminar flow element, relative humidity sensor, and T-type thermocouple. The gas stream temperature is measured at the outlet of the test bench, at the inlet of the TEG module, and the outlet of the TEG exhaust assembly. An airside pressure drop measurement of the TEG exhaust assembly is taken using a differential pressure transducer plumbed to the inlet and outlet of the exhaust assembly.

To provide the cooling necessary for the TEG modules, a 50%water/ 50% ethylene glycol (WEG) cooling loop was constructed using an automotive radiator and 12 V DC electric fan assembly, a Coriolis mass flow meter, and an electric pump. WEG temperatures were measured with K-type thermocouples at the inlet and outlet of the TEG module, and the outlet of the radiator. The mass flow rate of the WEG system was measured with an inline Coriolis flow meter. The heat exchanger for the WEG loop is an aluminum automotive radiator with a pressure-regulating cap and external recovery tank. An electronic DC load bank applies the necessary loads to the TEG module by maintaining constant voltage set points, and it outputs data to the National Instruments data acquisition system. A schematic of the bench test system is shown in Figure 43, and images of the constructed system are shown in Figure 44.

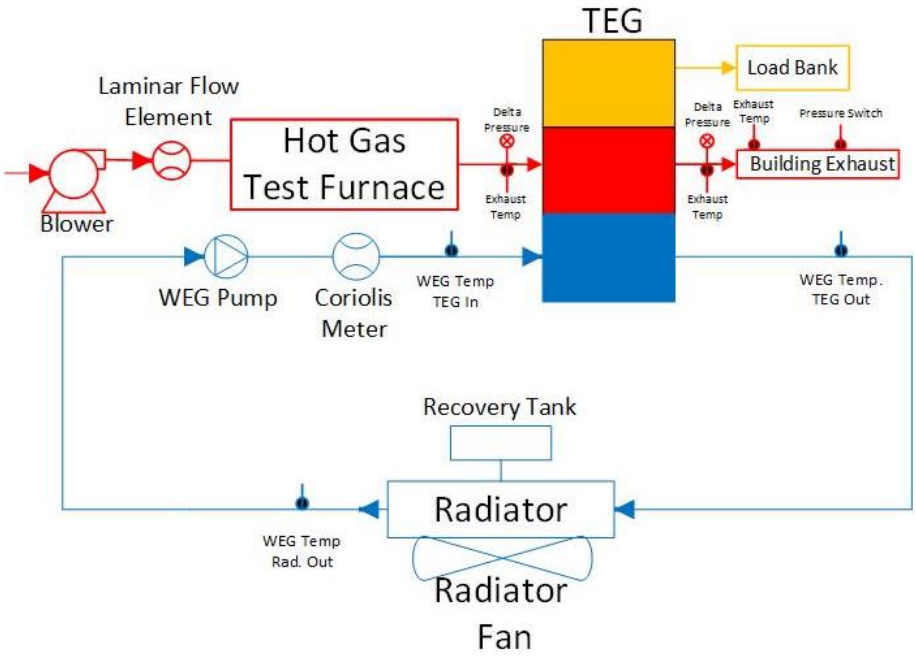

Figure 43: Schematic of test bench system with integrated TEG test article

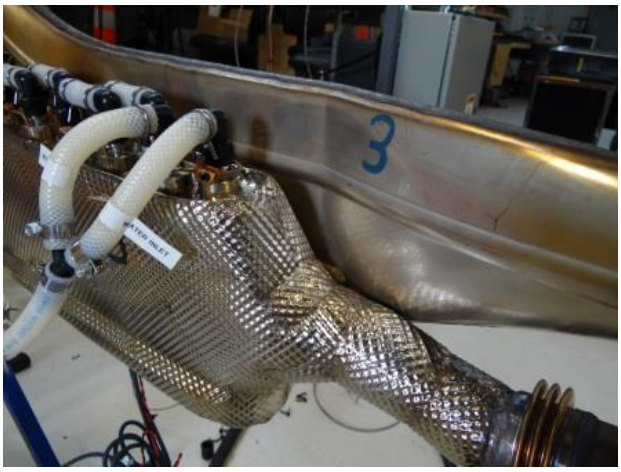

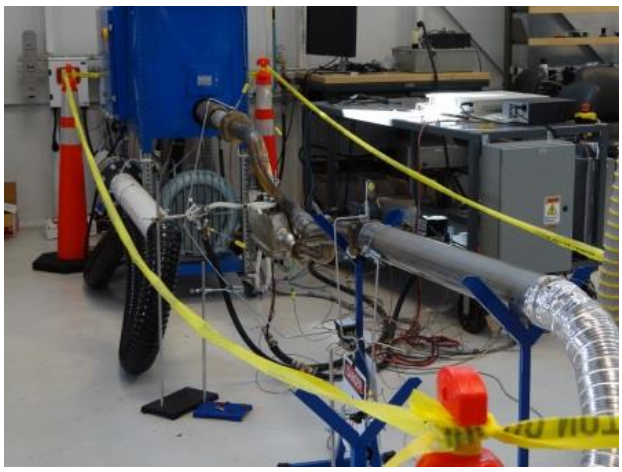

Figure 44: TEG exhaust system (top left); entire test bench system (top right); HG-500 Hot Gas Test Furnace (bottom)

Bench testing of the TEG device was performed to provide measurable and repeatable data for the purpose of confirming system performance as predicted by modeling, and to provide a two-variable data map that can be interpolated for the prediction of energy production during known vehicle drive cycles. The test matrix covers a range of nominally prescribed exhaust gas test section inlet temperatures and mass flow rates, as given in Table 5 and Figure 45. Exhaust gas mass flow rate values of 13.5, 20, 30, 50, and 75 grams per second (g/s) correspond to test bench inlet (ambient air) volumetric flow rate (VFR) values of approximately 29, 43, 65, 108, and 162 cubic feet per minute (cfm). The coolant mass flow rate was fixed, ranging from 158 to 163 g/s for all tests conducted, which is a volumetric flow rate of approximately 9.1 liters per minute. The coolant temperature into the TEG device ranged from 28°C to 40°C depending on the amount of heat absorbed from the TEG device (which determines the load on the coolant radiator).

Table 5: Test Matrix of Nominal Test Points for Exhaust Gas Inlet Conditions

Exhaust Gas Test Section Inlet Temperature [°C]	Exhaust Gas Flow [g/s]				
350	13.5	20		50	75
450	13.5	20		50	
550	13.5	20		50	
600	13.5	20		50	
620	13.5	20	30		
640	13.5	20			

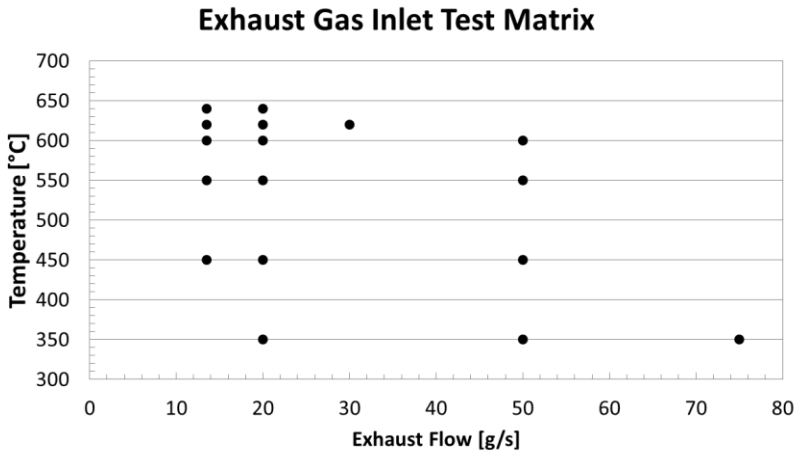

Figure 45: Plotted test matrix of nominal test points for exhaust gas inlet conditions

Systematic uncertainties for the sensors used for measurement of the TEG system performance are given in Table 6.

Table 6: Typical Measurement Systematic Uncertainties

Measurement Variable	Sensor Type	Systematic Uncertainty
Ambient humidity	Capacitive relative humidity	±1.0% RH
TEG exhaust pressure drop	Differential pressure	±0.012 psid
Atmospheric pressure	Atmospheric pressure	±0.26 kPa
Coolant mass flow rate	Coriolis flow meter	±0.25% rdg (max ≈ 0.41 g/s)
Volumetric air flow rate	Laminar flow element	±1.0% rdg (max ≈ 1.5 cfm)
Assorted temperatures	K-type thermocouple	±1.0 K
TEG voltage	Voltage (load bank)	±(0.02% rdg + 0.025% FS) (max ≈ 0.032 V)
TEG current	Current (load bank)	±(0.2% rdg + 0.15% FS) (max ≈ 0.27 A)

FS = full scale
rdg = reading

Test results

The testing was conducted for the test matrix given in Table 5. For each test point, four voltage levels were tested and recorded: the open circuit voltage without a current load, half of the open circuit voltage corresponding to the maximum power point, and a voltage level slightly above and below the maximum power point to capture TEG behavior. An example data set for an exhaust gas mass flow rate of 13.5 g/s is shown in Figure 46. It is apparent that the current varies linearly as a function of changing voltage level. Power is a function of the voltage times the current; therefore, the power is zero at the open circuit voltage (zero current), and maximum at half of the open circuit voltage.

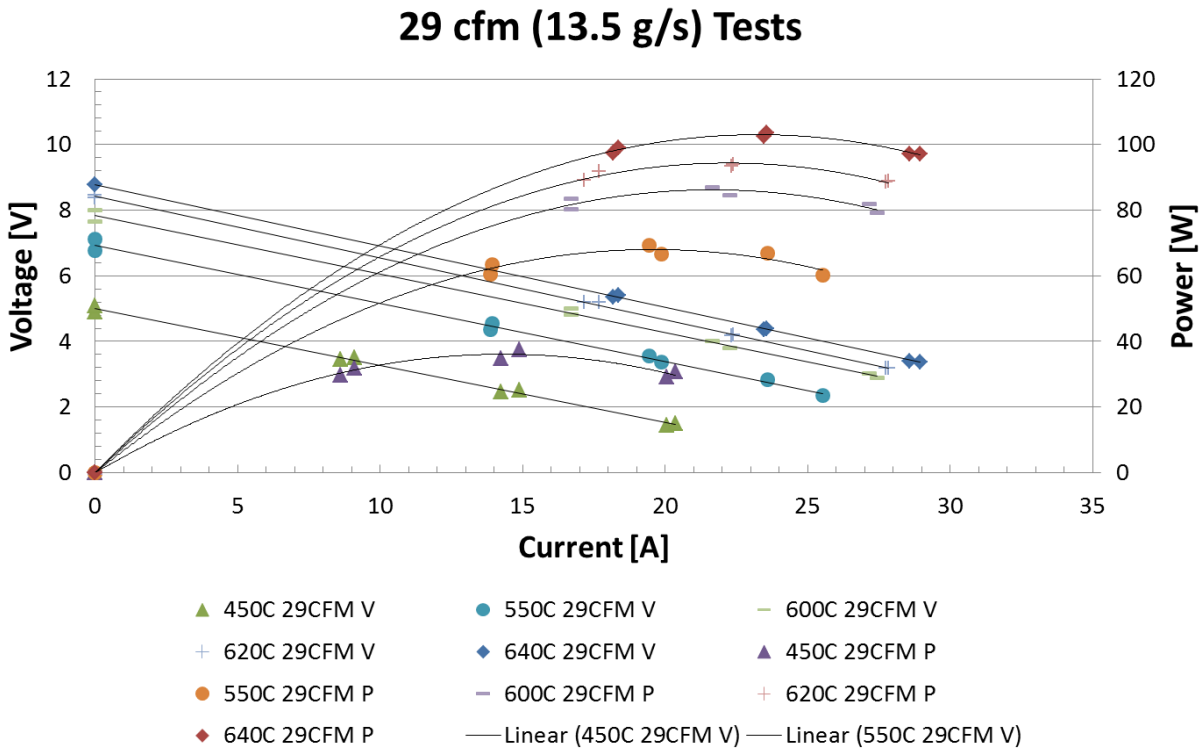

Figure 46: Voltage and power output of TEG device as a function of current for a variety of test section inlet temperatures and an exhaust gas flow rate of 13.5 g/s

Repeat runs of the majority of the test points were completed for demonstration of test repeatability. The exhaust gas mass flow rate through the TEG system was found to be very repeatable between tests. The exhaust gas inlet temperature just before the TEG elements varied slightly between tests even when the exhaust gas temperature at the inlet to the exhaust tubing test section was controlled to the same test value. However, it was found that the maximum power production as a function of exhaust gas inlet

temperature just before the TEG elements followed predictable trends and therefore validated the test results. Another way to state the differences between tests is that the power production variance between tests was proportional to the change in TEG exhaust inlet temperature. These trends are shown in Figure 47 as strong correlations in the relationship between the optimum electrical power production and the exhaust gas TEG inlet temperature for fixed exhaust gas flow rates.

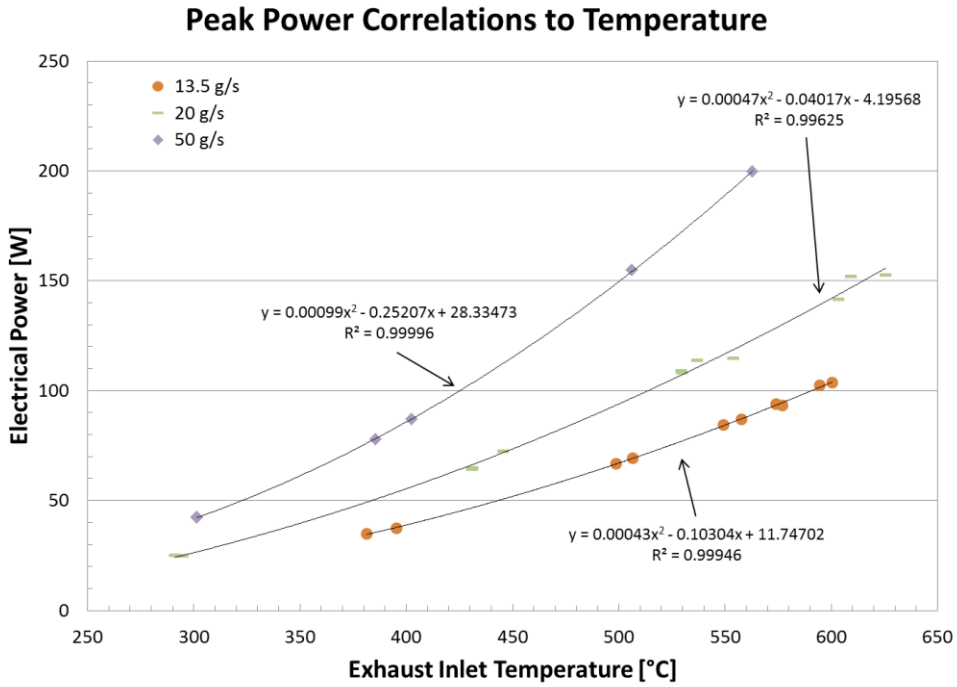

Figure 47: Peak power as a function of exhaust gas TEG inlet temperature for different exhaust gas mass flow rates

When considering TEG system performance, perhaps the most useful way to visualize the data is to look only at the optimal power test voltages for each exhaust condition test point as a function of exhaust gas flow rate and inlet temperature. The justification is that the TEG waste heat recovery device would be implemented in a vehicle with electronics that load the device at the optimal voltage for the given inlet conditions to produce the maximum benefit. If the maximum power points are plotted for all of the tests as a function of both exhaust gas flow rate and exhaust gas TEG inlet temperature, the resulting surface plot can be used to interpolate performance for any prescribed inlet condition, such as a particular drive condition in a given vehicle. The surface plot of maximum powers is given in Figure 48. The accuracy of the surface fit around the very edges of the plot is reduced due to slight extrapolation in some regions. A maximum power production of 199.6 watts was observed in the 550°C exhaust gas inlet temperature and 50 g/s exhaust flow rate case.

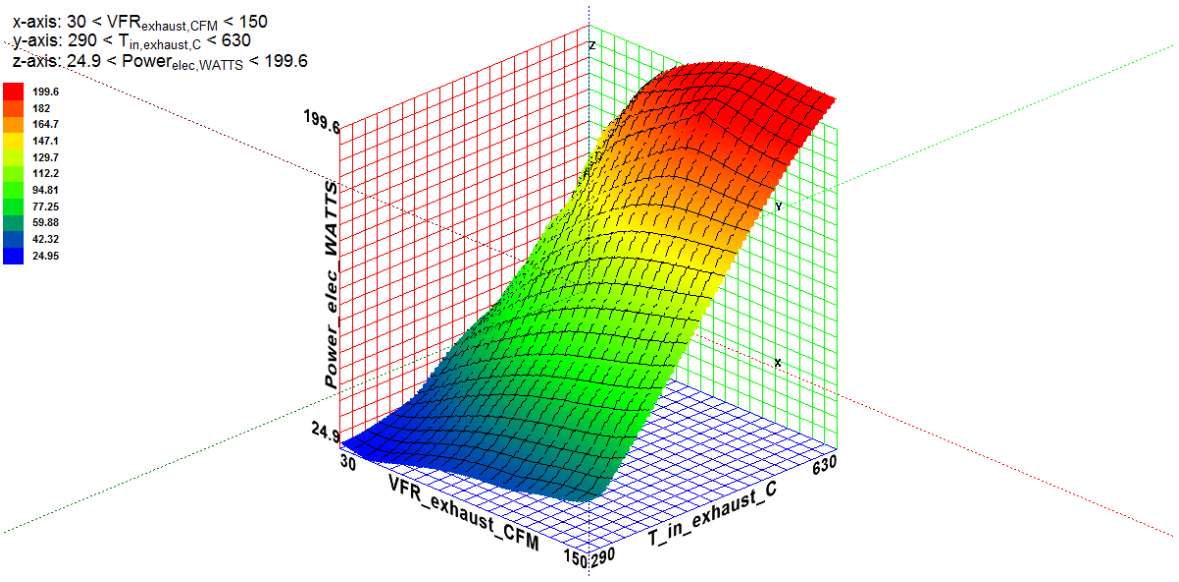

Figure 48: Electrical power generation as a function of exhaust gas TEG inlet temperature and exhaust gas flow rate

Examination of the surface plot of power production as a function of exhaust gas flow rate and exhaust gas TEG inlet temperature reveals two key findings. The first is that the electrical power production increases as the exhaust gas flow rate increases, but the rate of increase rapidly decreases after moderate flow rates are achieved, particularly at higher temperature levels. This trend can be seen in Figure 49. This is an intuitively correct result because the gas flow rate is strongly correlated to the air side heat transfer coefficient of the TEG cartridges. This means that at very low exhaust flow rates the heat transfer resistance on the airside is a limiting factor to the creation of a temperature differential across the TEG cartridge for a given coolant flow rate and coolant inlet temperature. When the exhaust flow rate is increased to moderate levels and beyond, the air side heat transfer coefficient is no longer a dominating factor and the temperature of the hot side of the TEG elements “saturates” (nears equalization with the exhaust gas inlet temperature).

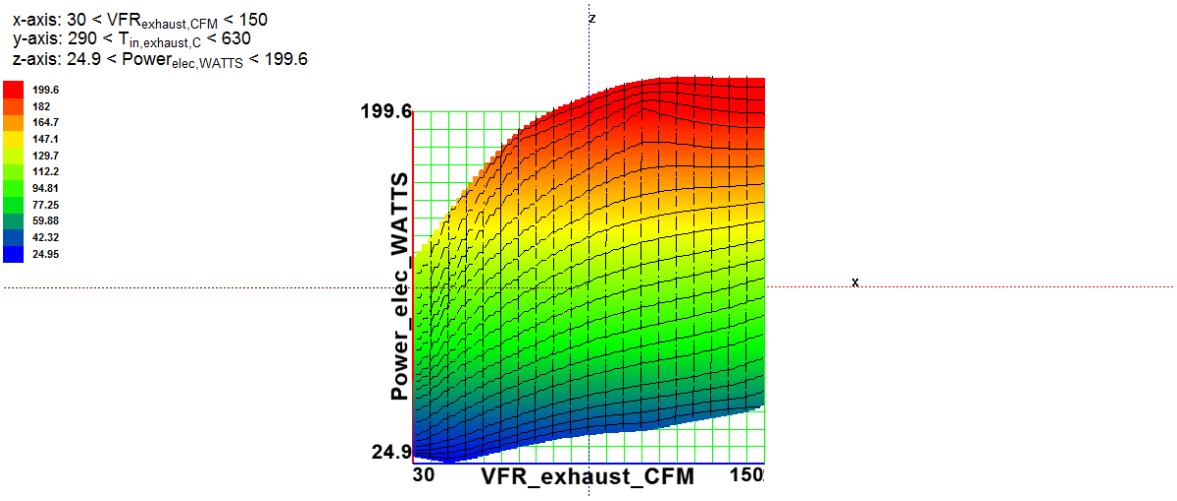

Figure 49: Electrical power produced as a function of exhaust gas flow rate

The second key finding is that the electrical power produced is strongly dependent on the exhaust gas TEG inlet temperature, as shown in Figure 50. In the case of increasing exhaust gas inlet temperature the power continues to strongly increase throughout the entire tested temperature range. The edges of the surface plot have reduced accuracy due to being at the limits of the available data, and therefore the change in trend at the very edges can be disregarded. The strong correlation between temperature and power production is an expected result because the power produced by the TEG elements is proportional to the temperature difference across them. The temperature difference across the elements increases linearly with increasing exhaust gas TEG inlet temperature when the coolant inlet temperature, coolant flow rate, and exhaust flow rate are held constant.

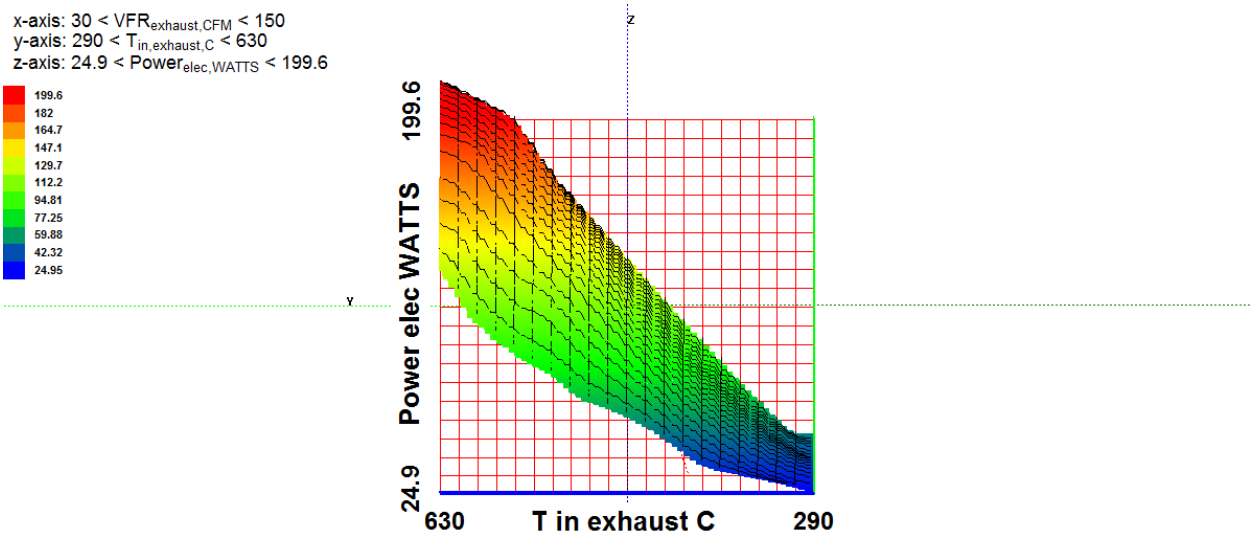

Figure 50: Electrical power produced as a function of exhaust gas TEG inlet temperature

The pressure drop across the TEG device on the exhaust (air) side is shown as a function of exhaust gas flow rate and exhaust gas TEG inlet temperature in Figure 51. As expected, the pressure drop is a strong function of exhaust flow rate, increasing as the square of flow velocity and therefore flow rate. The relationship to exhaust gas TEG inlet temperature is less strong, and the pressure drop increases only slightly as the temperature increases. This effect is predominately due to the decreasing air density at temperature increases, which increases flow velocity. It is important to recall that "VFR_exhaust_CFM" is the volumetric flow rate of the ambient air drawn into the system in cubic feet per minute and is therefore comparable to a measure of mass flow rate due to the near constant ambient conditions.

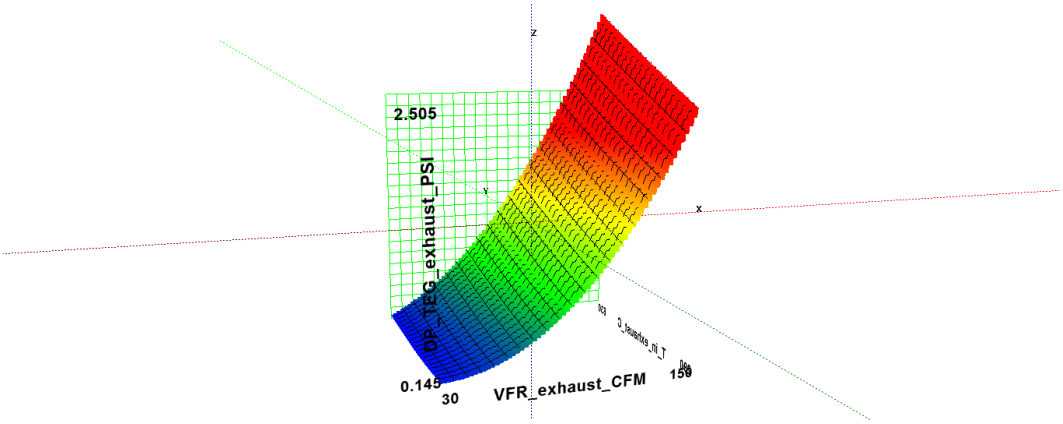

Figure 51: Pressure drop across exhaust side of TEG device as a function of exhaust gas TEG inlet temperature and exhaust gas flow rate

The findings related to exhaust temperature and flow rate are important because they demonstrate that at very high exhaust gas flow rates, the flow could be partially bypassed when necessary for engine pressure/flow reasons without significantly reducing the power output of the TEG device. This trade-off information can be used in the control algorithm design to optimize the overall efficiency of the entire vehicle.

Another metric of interest for power production performance is the efficiency of the thermal to electrical conversion process. The equation used for efficiency is:

$$Eff_{TEG} = \frac{Power_{elec,TEG}}{Q_{WEG,TEG}} = \frac{Electrical\ Power\ Produced\ by\ TEG}{Heat\ Absorbed\ by\ Coolant\ from\ TEG}$$

The efficiency of TEG power production as a function of exhaust gas flow rate and exhaust gas TEG inlet temperature is given in Figure 52. The notable characteristic of the efficiency plot is that the trends are nearly identical to the electrical power plot given in Figure 48, which shows that efficiency is dominated by electrical power production. The maximum recorded efficiency is 3.56% and it occurs at the maximum power case of 199.6 watts, 550°C exhaust gas inlet temperature, and 50 g/s exhaust flow rate.

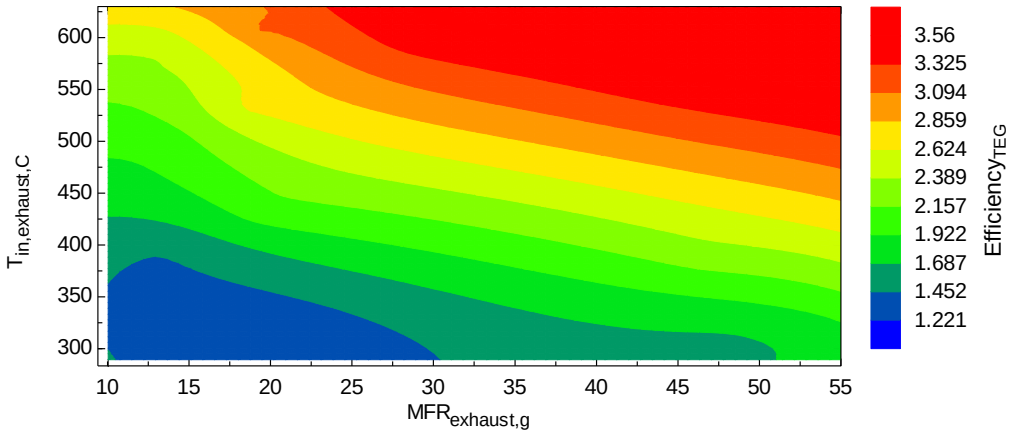

Figure 52: TEG efficiency as a function of exhaust gas TEG inlet temperature and exhaust gas flow rate
The peak power test results used to create the three dimensional plots are summarized in Table 7.

Table 7: Peak Power Data

Nominal Test Points	$T_{exh,in}$	VFR_{exh}	P_{TEG}	η_{TEG}	$\Delta P_{exh,TEG}$
13.5 g/s, 450°C	381.3	30.08	34.89	1.43	0.159
13.5 g/s, 450°C	395.3	30.08	37.4	1.47	0.145
13.5 g/s, 550°C	498.6	30.11	66.74	2.01	0.17
13.5 g/s, 550°C	506.7	30.04	69.18	2.04	0.161
13.5 g/s, 600°C	549.3	30.18	84.6	2.27	0.17
13.5 g/s, 600°C	557.8	30.31	86.88	2.29	0.163
13.5 g/s, 620°C	573.9	30.08	93.84	2.39	0.15
13.5 g/s, 620°C	576.8	30.14	93.36	2.37	0.167
13.5 g/s, 640°C	594.6	30.03	102.4	2.5	0.165
13.5 g/s, 640°C	600.6	30.04	103.6	2.51	0.171
20 g/s, 350°C	291.1	44.15	25.05	1.22	0.34
20 g/s, 350°C	294.7	44.21	24.9	1.22	0.201
20 g/s, 450°C	431.1	44.14	64.77	2.02	0.217
20 g/s, 450°C	445.6	46.06	72.48	2.14	0.246
20 g/s, 450°C	430.9	44.16	64.21	2.02	0.267
20 g/s, 550°C	529.7	44.07	108.3	2.64	0.248
20 g/s, 550°C	553.8	44.17	114.7	2.68	0.281
20 g/s, 600°C	529.3	44.16	109.2	2.65	0.402

20 g/s, 600°C	603.5	44.17	141.5	2.97	0.283
20 g/s, 620°C	536.8	44.21	113.8	2.71	0.411
20 g/s, 620°C	625.6	44.19	152.6	3.05	0.323
20 g/s, 640°C	609.1	44.15	152	3.13	0.269
30 g/s, 620°C	598.3	66.35	185.2	3.43	0.767
50 g/s, 350°C	301.5	109.5	42.5	1.63	1.181
50 g/s, 350°C	301.5	109.5	42.2	1.61	1.192
50 g/s, 450°C	402.6	109.5	86.88	2.36	1.409
50 g/s, 450°C	385.6	109.6	77.91	2.24	1.352
50 g/s, 550°C	506.1	109.5	154.8	3.16	1.497
50 g/s, 600°C	563.0	109.1	199.6	3.56	1.635
75 g/s, 350°C	309.5	148.8	52.32	1.78	2.505

NREL Bench testing summary and conclusions

Bench testing of the TEG exhaust waste heat recovery system at the National Renewable Energy Laboratory demonstrated that the TEG device performed as anticipated and was capable of producing useful electrical energy from what is typically wasted heat in a vehicle. Although the maximum efficiency for conversion of thermal energy to electrical energy was only 3.56% for the conditions tested, the abundant waste heat available in the exhaust stream of conventional vehicles means that the importance of thermal efficiency is minimal, with the main limitation being the increased radiator size for heat rejection. A more important metric is the absolute power produced, which was as high as 199.6 watts for the conditions tested. This is sufficient to reduce the load of the alternator/generator on a vehicle, which reduces the mechanical power load on the engine and therefore increases vehicle fuel economy. Vehicle operating conditions that exhibit high engine loads that produce high temperature exhaust conditions will benefit the most from this technology, as the TEG power production is most sensitive to exhaust gas inlet temperature.

An important design consideration for implementation into a vehicle will be the exhaust flow control between the TEG system and the exhaust bypass. A tradeoff between increasing the TEG power production and decreasing the back-pressure of the exhaust system on the engine will need to be considered. The observed pressure drop on the exhaust side of the TEG highlights the need for bypass capability and control at high engine load conditions in order to prevent excessive backpressure on the engine. The quick saturation of the effect of exhaust flow on TEG performance means that this tradeoff should be easy to achieve, as the TEG system will not benefit significantly from having 100% of the flow under high engine load conditions.

Vehicle level integration and tests

BMW X3

After all adjustments and improvements of the TEG-System, Tenneco installed the TEG-System in the BMW X3. BMW has performed cooling system integration and final testing. Following figures illustrate final vehicle integration.

Figure 53 TEG-System application in the BMW X3

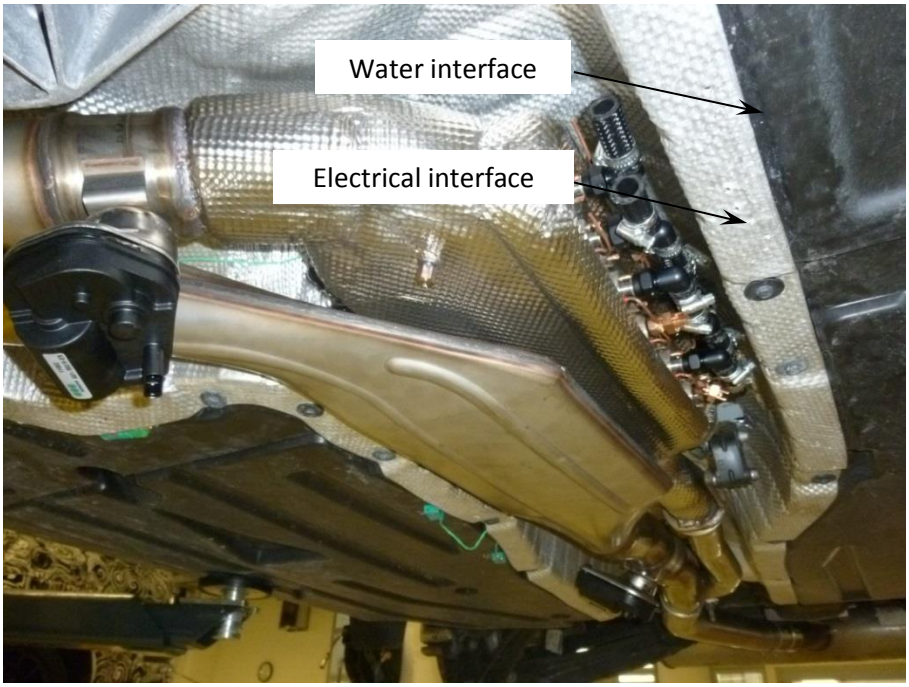

Figure 54 TEG-System interfaces for electric and coolant

Figure 55 Actuator of the TEG-Inlet

Figure 56 TEG integrated into the exhaust system of the BMW X3 xDrive28i.

Integration into coolant system

In order to find the best solution for the TEG-integration into the coolant system, 23 different concepts were created and evaluated. For the evaluation of these concepts several criteria were defined and weighted:

- Influence on engine warm-up
- Influence on engine cooling
- Influence on transmission warm-up
- Influence on transmission cooling
- Influence on TEG cooling
- Influence on warm-up of cabin heating
- Electric power consumption
- Weight

- Expected costs

Figure 57 shows the highest rated integration concept, which was subsequently realized in the test vehicle. The basic idea of this concept was to use the extracted exhaust heat for accelerate engine warm-up, without influencing the original warm-up strategy of the cooling system.

The exhaust heat extracted by the TEG is transferred to the engine oil by using the engine-oil/coolant heat exchanger. An additional small electric pump delivers the coolant and enables overrun (when main pump is off, but TEG still hot). A check valve ensures flow of coolant through the engine-oil/coolant heat exchanger.

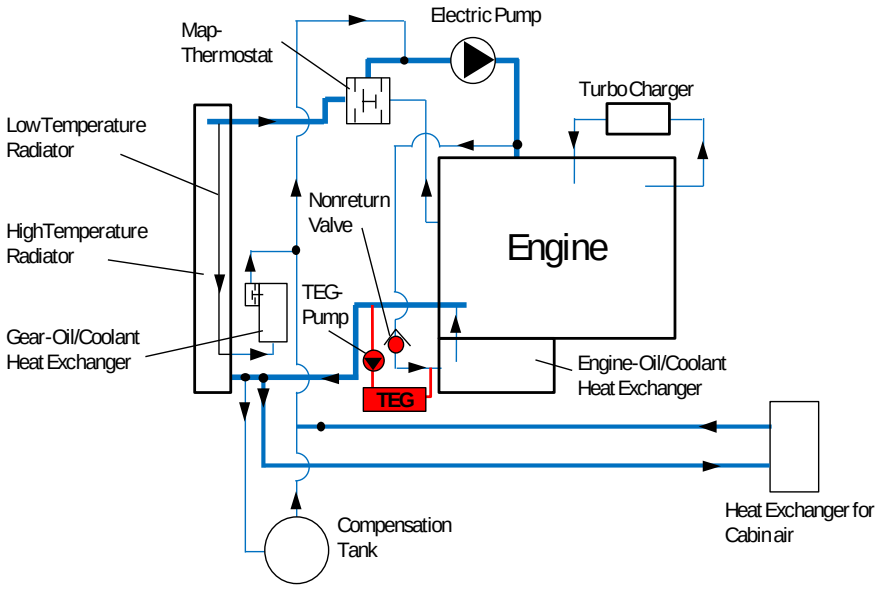

Figure 57 Coolant system of X3 xDrive28i with automatic transmission and selected concept for coolant integration.

Electrical connection of TEG

Electrical resistances were selected to provide electric load. Seven 1Ω load resistors were put into parallel and connected to the TEG. The measured overall resistance of the loads including electrical connectors amounted to 143.7 mΩ. The resistors were placed on an aluminum heat sink, which is cooled by two electric fans. This fixed load was used to substitute for DC/DC converter which would continually match internal impedance of TEG. Using fixed resistance load 3-5% of potential power generated by TEG was lost.

Instrumentation

The installed measurement equipment contains thermocouples for measurement and monitoring of exhaust gas and coolant, pressure sensors for the measuring of exhaust pressure drop over TEG, a flowmeter for TEG-coolant flow, as well as TEG-voltage measurement and a shunt to determine TEG-current. For enabling subsequent determination of total energy balance of the TEG-system, additional shunts were applied for measuring currents of exhaust flaps and coolant pump.

Control of TEG-system

In order to control the TEG-system, a Simulink-Model was programmed and dubbed to a MicroAutoBox[5].

The model controls the exhaust flaps (TEG path and bypass path), the coolant pump, the fans for resistor cooling, the open-circuit switch of the TEG as well as two warning lights. In standard operation mode PI-controllers prevent overheating of TEG by monitoring exhaust gas temperature, coolant flow and coolant temperature behind TEG.

[5] MicroAutoBox is a real-time system for performing fast function prototyping developed and marketed by *dSPACE*. It can operate without user intervention, just like an ECU [DSP2015].

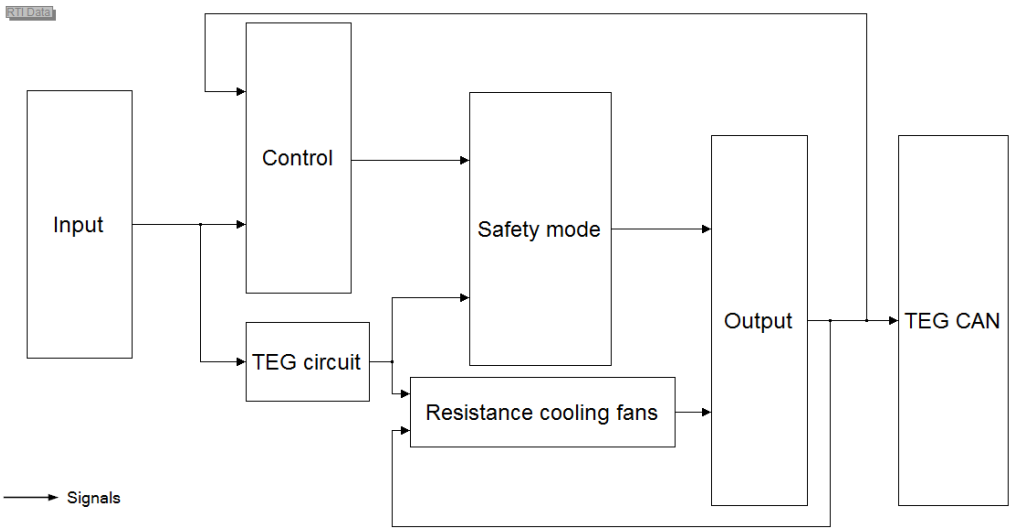

Figure 58 Detail of Simulink model, which has been set up to control the TEG-system.

BMW X3 vehicle test results

BMW X3 28i test vehicle was tested on BMW roller dynamometer by driving the relevant cycles in terms of CO_2-emissions (US-Combined-cycle in USA and from 2017 WLTP-cycle for Europe). Furthermore the cycles of US 5-Cycle-Testing were investigated.

TEG power output

Plotted in Figure 59, is the electrical power output of the TEG over WLTP-cycle[6] and power consumption of the auxiliaries (flaps, TEG-pump). Peak power from TEG is 120 W. The average power output of the TEG amounts to 30.2 W, the consumption of flaps and TEG-pump to 6.5 W. Plotted PWM-signals of the exhaust flaps show that bypass opens temporarily in the last phase of the cycle, where exhaust temperatures exceed 600 °C[7], whereas the TEG-flap is closed only two times very shortly in phases with high acceleration.

[6] Testing conditions: 23 °C, 40% r.h., 963,0 hPa

[7] Bypass- and TEG- flap: PWM-signal = 90% → flap closed; PWM-signal = 10% → flap opened;

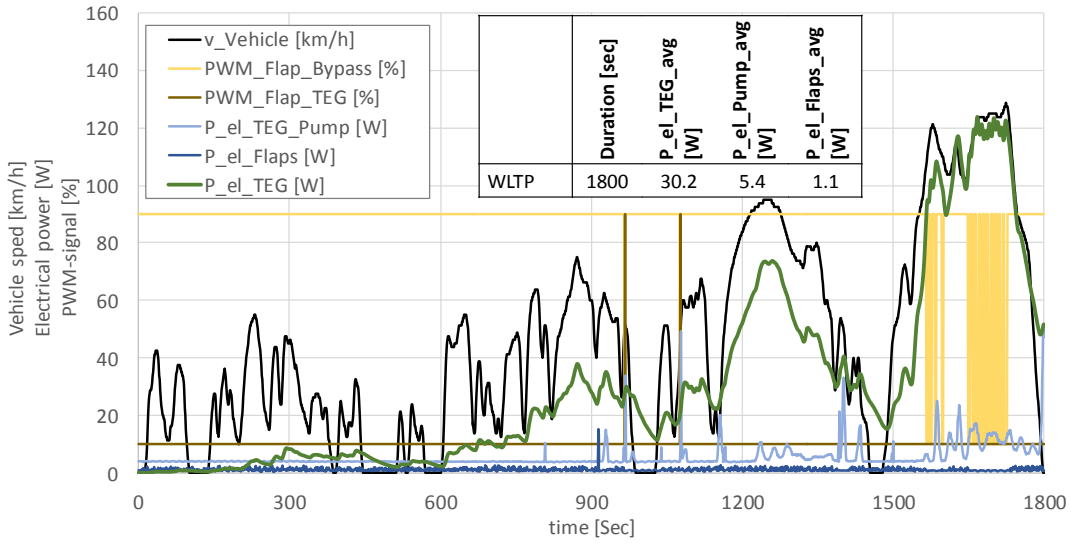

Figure 59 Vehicle velocity, TEG power output, power consumption of TEG-auxiliaries (flaps, pump) and PWM-signals of the exhaust flaps over WLTP-cycle

Figure 60 shows measurement results of the US-Combined[8] test procedure, which is composed of a cold started FTP-75 cycle and a hot started highway-cycle. In FTP-75 the average power output of the three phases lays between 10.2 and 12.6 W. Due to the higher engine load and exhaust enthalpy the power output is significantly higher in highway cycle (> 40 W in average). For subsequent CO_2-evaluation the power output in the different phases were weighted corresponding to their duration. This provides a weighted average of TEG power output of 19.8 W. The weighted average of power consumed by the auxiliaries (pump and flaps) lays at 5.7 W.

[8] Testing conditions: 24 °C, 40% r.h., 964,2 hPa

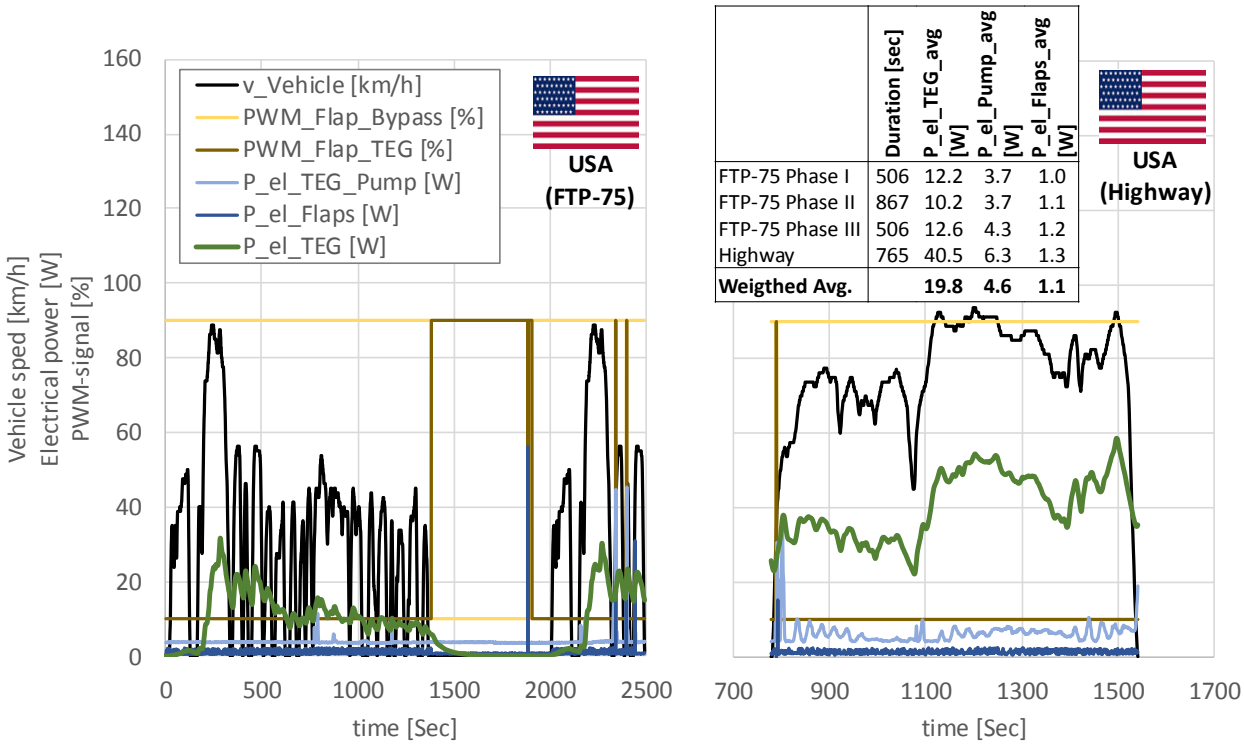

	Duration [sec]	P_el_TEG_avg [W]	P_el_Pump_avg [W]	P_el_Flaps_avg [W]
FTP-75 Phase I	506	12.2	3.7	1.0
FTP-75 Phase II	867	10.2	3.7	1.1
FTP-75 Phase III	506	12.6	4.3	1.2
Highway	765	40.5	6.3	1.3
Weigthed Avg.		**19.8**	**4.6**	**1.1**

Figure 60 Vehicle velocity, TEG power output, power consumption of TEG-auxiliaries (flaps, pump) and PWM signals of the exhaust flaps in FTP-75 and Highway-cycle of HWFET.

Corresponding to § 86.1869-12 of US "Code of Federal regulations"[9] US-agencies support technologies by off-cycle-credits if the benefit is not adequately captured by the federal test procedure and/or the highway fuel economy test. Beyond others a credit for "waste heat recovery"-technologies is granted, in which the electrical load reduction (ELR) in 5-cycle-testing is multiplied by factor 0.007 to get the allowed CO_2-credit in gCO_2/mi. 5-cycle-testing defines a combination of five different driving cycles: In addition to the two above mentioned cycles (FTP-75 and Highway-cycle) it also contains FTP-75 cold[10], SC03[11] and US06[12].

[9] § 86.1869-12 "CO_2 credits for off-cycle CO_2-reducing technologies" (Code of Federal Regulations CFR: Title 40, Chapter I, Subchapter C, Part 86, Subpart S, Section 86.1869-12) [GPO2015]

[10] Testing conditions: -7 °C, 40% r.h., 965,2 hPa

[11] Testing conditions: 35 °C, 40% r.h., 962,3 hPa

[12] Testing conditions: 24 °C, 40% r.h., 963,2 hPa

The table in Figure 61 shows TEG power outputs and auxiliary consumptions of FTP-75, highway-cycle, FTP-75 cold[13], SC03 and US06. For identifying the net power output of the TEG-system both arithmetic average of the single cycles as well as a weighted average can be determined. § 86.1869-12 claims that ELR is “calculated as an average over 5-cycle testing” and is therefore not explicit regarding the manner of average. Hence for the following CO_2-evaluation the higher arithmetic average (25 W) has been used, which results in 0.17 gCO_2/mi.

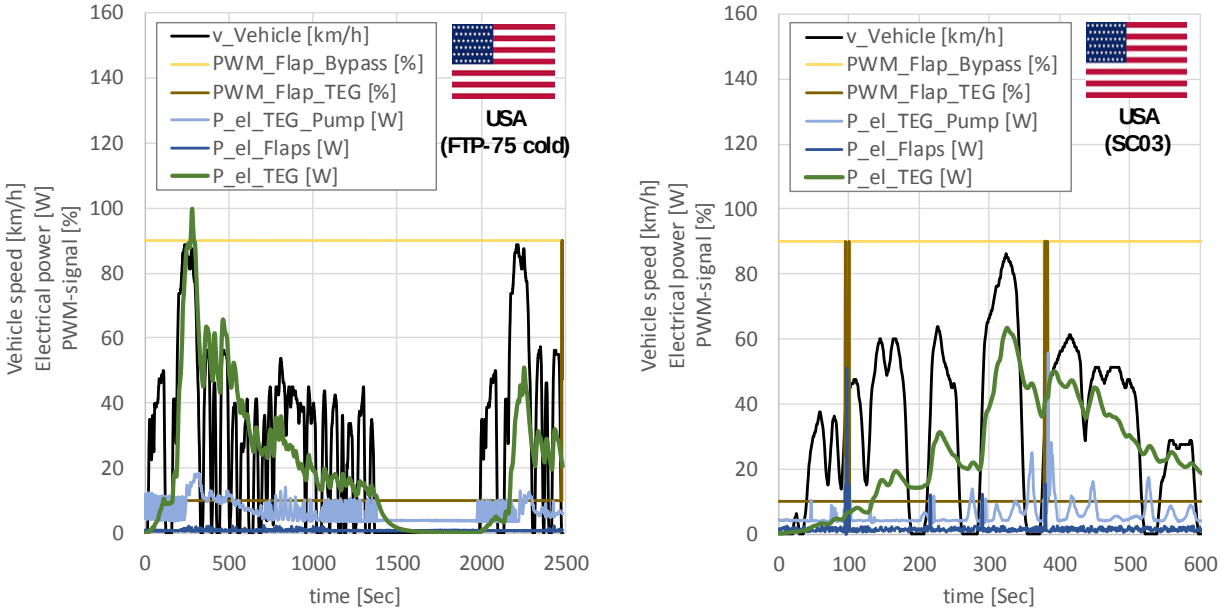

[13] Ambient test temeprature -7 °C

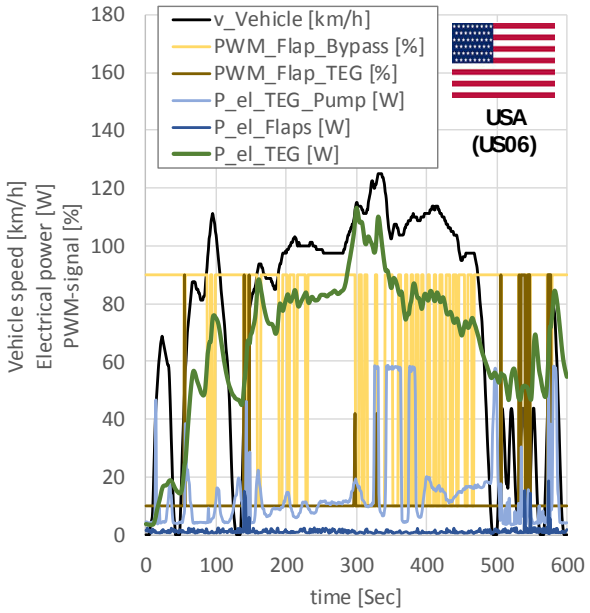

	Duration [sec]	P_el_TEG_avg [W]	P_el_Pump_avg [W]	P_el_Flaps_avg [W]	P_el_net [W]	CO2-Credit [gCO2/mi] (=ELR x 0.007
FTP-75	1879	11.4	3.9	1.1	6.4	
Highway	765	40.5	6.3	1.3	32.9	
FTP-75 cold	1879	21.1	6.4	0.8	13.8	
SC03	604	25.2	5.9	1.5	17.8	
US06	600	67.5	14.3	1.2	51.9	
Arithmetic Avgerage		33.1	7.4	1.2	**24.6**	**0.17**
Weigthed Average		25.8	6.3	1.1	**18.4**	**0.13**

Figure 61 Vehicle velocity, TEG power output, power consumption of TEG-auxiliaries (flaps, pump) and PWM-signals of the exhaust flaps over FTP-75 cold, SC03 and US06.

As mentioned above, the chosen concept for cooling system integration was intended to support warm-up of the engine-oil. However, tests did not prove a faster warm-up effect. Figure 62 shows the temperatures of the oil reflux into the engine (behind engine-oil cooler), thus behind the potential heat feed-in position of the TEG-heat, carried in the coolant. The oil temperature measured with installed TEG-system is during warm-up phase (T_{engine} < 90°C) consistently lower than without TEG-system. Analyzing the quantities of heat extracted from the exhaust on the one hand and delivered to the coolant on the other showed that there is a quite big gap between both values. In the warm-up phase of WLTP about 272 Wh are extracted from the exhaust but only 93 Wh enter the coolant. That means almost 2/3 of the extracted exhaust energy is used for warming up the TEG (Cartridges, Canning,…). Since there are further components in the coolant system (pump, tubes, connectors, additional coolant volume,…) which absorb heat there is no heat left which could be used for faster oil-warming. In conclusion: it is more efficient to use electrical coolant pump which is deactivated in engine start phase than to rely on TEG to provide oil preheating. In configuration with TEG electrical pump cannot be deactivated and engine warmup is slower.

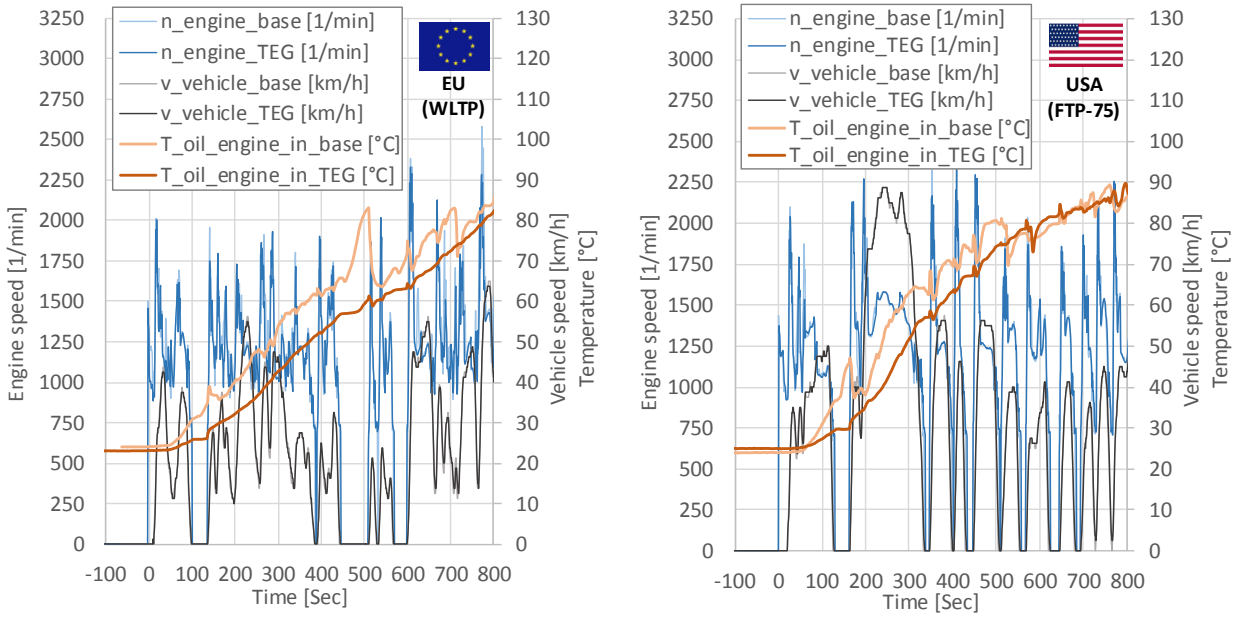

Figure 62 Temperature of oil reflux into the engine (behind engine-oil cooler) with (dark brown line) and without TEG-system (light brown line).

Evaluation of CO_2 emission reduction in BMW x3

Figure 63 shows CO_2-balancing of the single TEG-effects for WLTP (Europe) and US-Combined (USA) in gCO_2/km respectively gCO_2/mi. The associated assumptions are labeled in the caption.

Not considering any losses of DC/DC-converter or electrical wiring and without paying attention to eventual interactions with recuperation of braking energy, the pure electrical power output of the TEG leads to a CO_2-saving potential of 0.5 gCO_2/km in WLTP. Since no supporting warm-up effect could be verified, the correspondent CO_2-influence was zeroed. The (negative) CO_2-effect due to power consumption of the TEG-auxiliaries (plotted in Figure 63) amounts to 0.1 gCO_2/km for WLTP. The vehicle weight increases by 15 kg, in which it is supposed, that the TEG-system fulfills also the acoustic function of the original center mufflers which have been removed to clear space for the TEG-system. The pure additional weight leads to a CO_2-increase of 0.6 gCO_2/km in WLTP. Since there is no implementing

decision for waste heat recovery credits respectively eco-innovations in EU, the correspondent CO_2-influence is zeroed for WLTP. Since no accelerated warm-up effect has been approved, a warm-up credit can`t be taken into account. Balancing the above mentioned effects results in a slight increase of emissions by 0.2 gCO_2/km in WLTP.

The above explanation is qualitatively valid for US-Combined cycle, too. The only difference relates to the credit for the electrical load reduction. As mentioned above, this has been calculated to 0.17 gCO_2/mi. In total the CO_2-emissions for US-Combined increase by 0.2 gCO_2/mi with TEG-system.

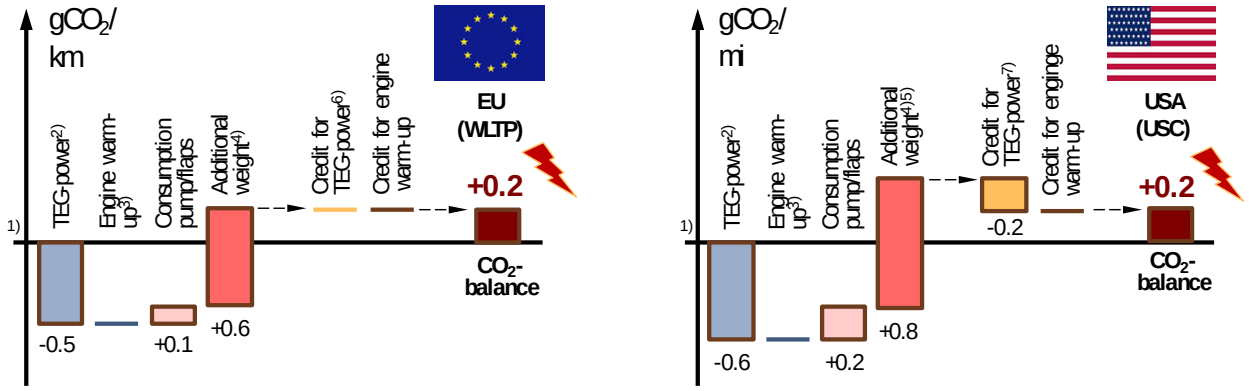

Figure 63 CO_2-evaluation of the developed TEG-system for WLTP (Europe) and US-Combined (USA). Assumptions: [1)] Evaluation basis: X3 xDrive28i. [2)] Interaction with recuperation of braking energy not considered. Losses of DC/DC-converter and electrical wiring not considered. [3)] Influence on engine warm-up not considered. [4)] 15kg; additional weight for center mufflers not considered. Assumption: TEG-System also fulfills function of center mufflers. [5)] Eventual jump in higher inertia class not considered. [6)] Up-to-date no implementing decision for waste heat recovery in EU. [7)] Credit for Off Cycle Technology „Waste-heat-recovery“ = 0.007 x Electric load reduction ELR, calculated as an average over 5-Cycle testing (see Code of Federal Regulations CFR § 86.1869-12 “CO_2 credits for off-cycle CO_2-reducing technologies”). Interpreting „average“ as arithmetic average of the five arithmetic net power averages. [8)] Influence on exhaust back pressure not considered.

Ford F350

Gentherm technology demonstration vehicle Ford F350 with 6.2L SOHC V8 flex fuel engine was selected for demonstration of TEG device performance in larger size vehicle. Installation of TEG, cooling system and final testing was performed by Gentherm. Tests were performed only in US06 cycle and vehicle was tested on a roller dyno in certified SEMA test facility.

Vehicle level integration is different than that in BMW x3. Major integration differences are:

- Cooling system architecture
- Position of TEG in the exhaust system.
- Number of TEG units used.

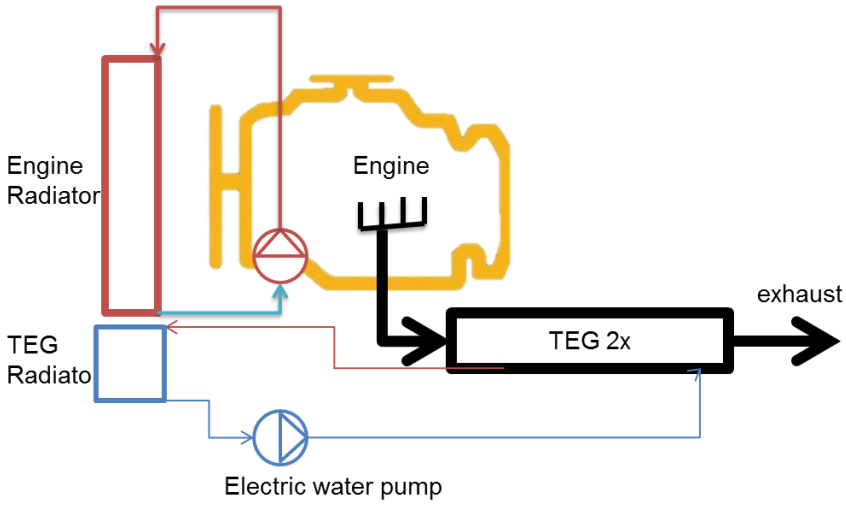

Figure 64 Integration of cooling system and TEG in F350 vehicle. TEG is cooled by the dedicated radiator installed on the bottom of the engine radiator.

Original radiator of F350 was replaced by new radiator with two split loops. Top radiator with same cooling capacity as original radiator and second radiator sized to provide adequate cooling to TEG system. Engine radiator remained on the OEM cooling loop with mechanical pump. TEG dedicated radiator operated on a separate loop with electrical coolant pump. Figure 64 shows diagram of this cooling system and TEG installation.

F350 has more than 3x larger engine volume. Ideal TEG for this vehicle would have 30 cartridges connected in 3x10 configuration. For demonstration purposes we have used only 20 cartridges and two

TEGs identical to those used in BMW X3, shown in Figure 34. Each of TEGs was connected to exhaust system immediately after catalytic converter. Distance between catalytic converter and TEG was approximately 500mm. Moving TEG to this position provided for much higher temperature exhaust gas as compared to TEG installed in mid-muffler position in BMW X3. As an end result: TEGs installed in this vehicle generated more than 1.1kw of electricity in US06 cycle compared to 120W generated by TEG installed in BMW X3. This result illustrates importance of location of TEG in the exhaust system. TEG is solid state energy conversion device. Efficiency with which TEG converts heat into electricity is proportional to temperature of hot gas – it is driven by Carnot efficiency.

Electrical loads used in this vehicle test are similar to those used in BMW X3 test. Total resistance was 280mΩ. Use of fixed electrical load resulted in effective loss of 3-5% of TEG power.

Figure 65 shows net power output from TEG's installed in F350. Gentherm has performed only tests in US06 cycle for this vehicle. Maximum power output in US06 cycle is 1,160W, average power is 440W with additional power generation after cycle is completed. As shown in Figure 65 TEGs continue to generate 200W of power at the end of the cycle. Since this energy is net gain to vehicle it can be included in average cycle generation and bring average power to 470W. Water pump consumption is constant for the duration of cycle and it is 25W. In this test we did not use control valve and no energy was consumed for this. Summary of power output and energy consumption is shown in Table 4.

Overall energy consumption in US06 cycle for F350 vehicle with nominal weight of 8.500lbs is 38.28MJ. Net energy generated by TEG system is 282kJ. Using average alternator efficiency of 60% contribution of TEG system to overall engine work reduction would be 0.47MJ. With this fuel efficiency improvement associated to TEG and to direct electricity generation is 1.2%. This is significant energy generation but it is below targeted 5% FEI.

Table 8 Summary of power generation and power consumption of TEG system in US06 drive cycle.

Test	Duration	P_el_TEG_avg [W]	P_el_Pump_avg	P_el_Flaps [W]	P_el_net [W]
US06	600	470	25	0	445

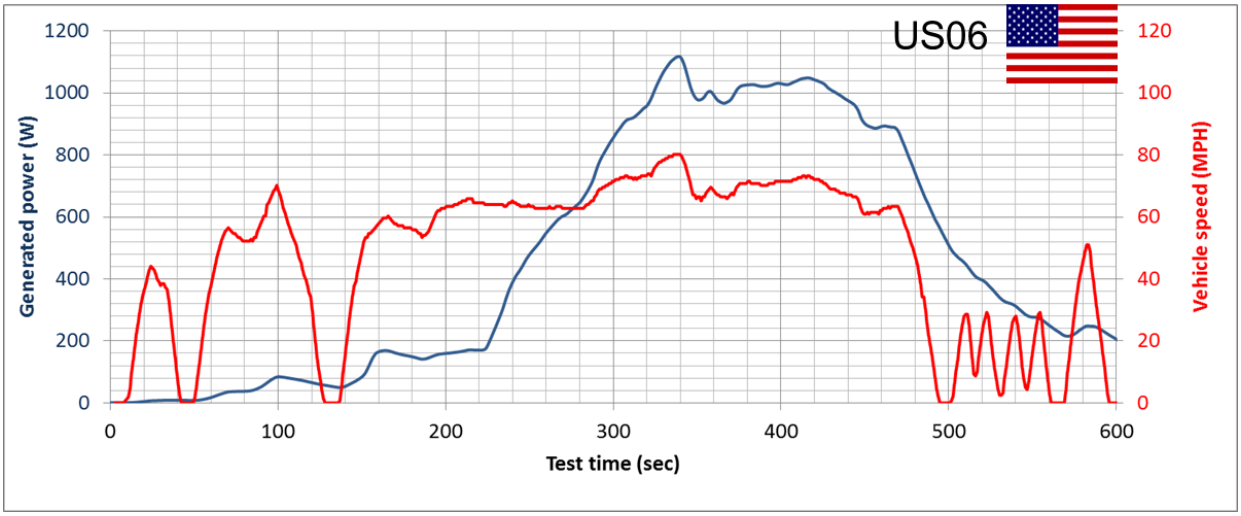

Figure 65 TEG power output and vehicle speed in US06 cycle. Peak power is 1160W and average power output is 470W.

Evaluation of CO_2 emission reduction in Ford F350 in US06 drive cycle

Figure 66 shows balancing of CO_2 emission due to effect of installation of TEG system in F350. Analysis is limited to available data and to US06 drive cycle. Not considering any losses of DC/DC-converter or electrical wiring and without paying attention to possible minimal changes in vehicle aerodynamics pure electrical power output of the TEG leads to a FEI of 1.2%. Fuel consumption of this vehicle in this test was 11.4 miles/gallon. Following US EPA guidelines [EPA2016] overall CO_2 emission can be estimated at 8,887 grams CO2/ gallon/11.4 miles/gallon or 779.4gCO_2/mile. Hence, 1.2% FEI can be converted to 9.3gCO_2/mile reduction. Negative CO_2 emission effect due to power consumption of the TEG-auxiliaries amounts to 0.5 gCO_2/mile. The vehicle weight increases by 22 kg and penalty on CO2 emission can be extrapolated from BMW emission calculations and estimated at 1.2 gCO_2/mile in US06 drive cycle. Credit for the electrical load reduction is 0.007 gCO_2/mi/Watt or total of 1.6gCO2/mile in US combined cycle. In total, the CO_2-emissions for US06 cycle decreases by 9.2 gCO_2/mile with TEG-system. In US06 cycle there are no additional benefits from heat delivered to engine by TEG as this is hot cycle.

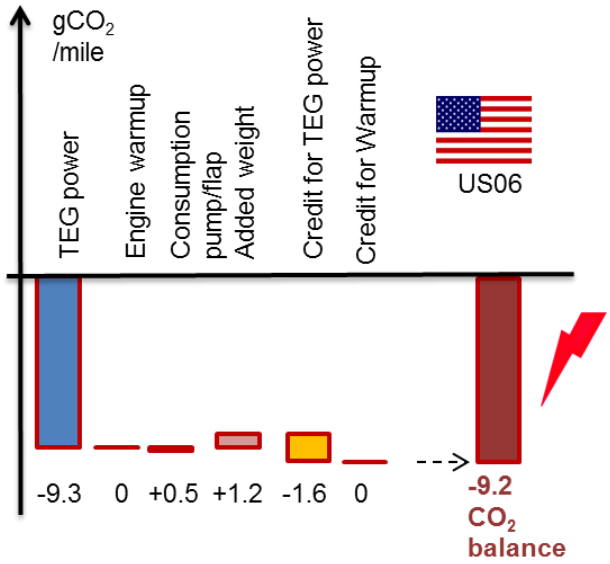

Figure 66 CO2-evaluation of the developed TEG-system tested in F350 US06 drive cycle. Actual emission reduction is 8% and it is offset by added energy use due to increased weight and added electricity consumption by water pump. With additional CO_2 emission credit total emission reduction is 8.6g/CO_2/mile.

Summary of CO2 emission reduction and FEI in this program

TEG designed in this program is shown in Figure 34. It consists of 10 thermoelectric power generation units – cartridges. Each cartridge has integrated hot side and cold side heat exchanger. Sandwiched between two heat exchangers are thermoelectric materials. In total of 40 gram of TE materials are used per cartridge. Maximum measured power output per cartridge is 56W. For the purpose of final validation of TEG performance two vehicles are outfitted with TEGs.

BMW X3 xDrive28i vehicle with 2.0L four piston turbocharge gasoline engine was outfitted with one TEG in mid muffler position. TEG is sharing cooling with engine and it uses same water cooling pump as oil cooler. In US06 drive cycle TEG generates maximum of 130W of electricity and net average of 52W. TEG is neutral or it has slightly negative effect on CO_2 emission or fuel efficiency.

Second demonstration vehicle is F350 with 6.2L SOHC V8 flex fuel engine. This vehicle was equipped with two TEGs connected immediately after catalytic converters. Due to selection of installation location TEG performs significantly better and produces maximum of 1,160 W of electricity or average of 470W of electricity. In US06 – cycle average fuel efficiency improvement is 1.2% and average net reduction of CO_2 emission is 9.2 gCO_2/mile. Percentage improvement of fuel efficiency is representative of potential of TEG systems in US-combined cycle as well. Range of fuel efficiency improvement derived from electricity generation is 1-2%.

Additional benefits can be derived from thermal conditioning of engine and accelerated engine warm-up. As reported by Faurecia [FAU2016] and consortium grouped around FIAT in EU sponsored program HeatReCar [HRC2014], additional 3-7% of fuel efficiency improvement can be achieved by effects of cold engine warmup. This effect was not observed in BMW vehicle due to different advanced coolant temperature management strategy. In F350 this effect was not measured as we only performed tests in hot US-06 cycle. However, considering coolant circulation strategy in F350 it can be expected that accelerated coolant warmup would have effect on fuel efficiency improvement.

Measured 1.2% FEI and corresponding 9.2 gCO2/mile emission reduction is below targeted 5% but it is significant number. Total sales of trucks in 2015 reached 9.7M in 2015. With 8 gCO_2/mile emission saving per truck, total reduction in CO_2 emission would be 77.6 tonCO_2/mile. Per Federal Highway Administration [FHWA2016] average annual mileage in 2015 was 13,476 miles.

Electricity generated by TEG, without addition of emission reduction due to accelerated engine warmup, would result in reduction of $C0_2$ emission of over 1,000,000 ton of CO_2.

TEG for heavy duty vehicles (HDV) TARDEC system

The heavy duty vehicle TEG system designed per TARDEC specifications was completed and tested in this program. The system shown in Figure 67 consists of: TEG canning designed for fifty-six cartridges (4x14 units), radiators, fans, water pump and manifolds. This is a self-contained system with integrated cooling designed to fit in the 2x2x4ft space

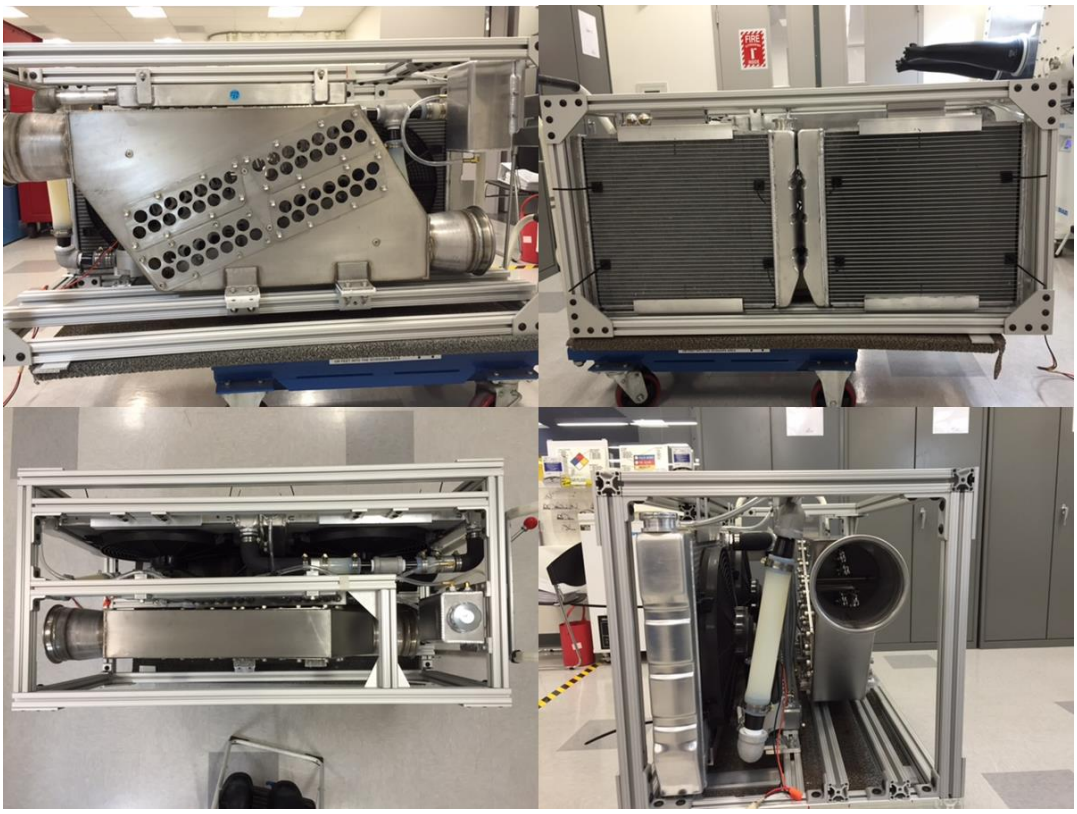

Figure 67 TARDEC test TEG device in a frame.

Cartridge installation is shown in Figure 68. The TEG can is a simple welded box with inlet and outlet cones. The cones are used to direct hot exhaust gas to and from the cartridges. The design is selected for its simplicity as the allocated space was much larger than was needed for this TEG design. Here, we show the assembly sequence. The can is designed with larger openings which are used to hold “quick install” side plates. These side plates position cartridges and allow for compression of thermal insulation between the inner walls of the TEG, the cartridge end caps, and the side plates themselves. This simple solution compensates for the difference in thermal expansion between the cartridges and canning. The completed system has 4 individual sections which can be easily removed for service and cleaning. The entire TEG is insulated using high temperature insulation and shielded using stainless steel thin wall sheet metal.

Figure 69 shows the water connection diagram. The cooling system is designed to provide 1.5-2l/min of coolant to every cartridge. Cartridge cold side heat exchangers are connected in 14 parallel flow lines with 4 connections in series. As shown in Figure 69, the direction of coolant flow is from bottom to top and coolant is supplied using a 12V electric water pump (JEGS 555-5509). Flow is monitored using a volume flow meter.

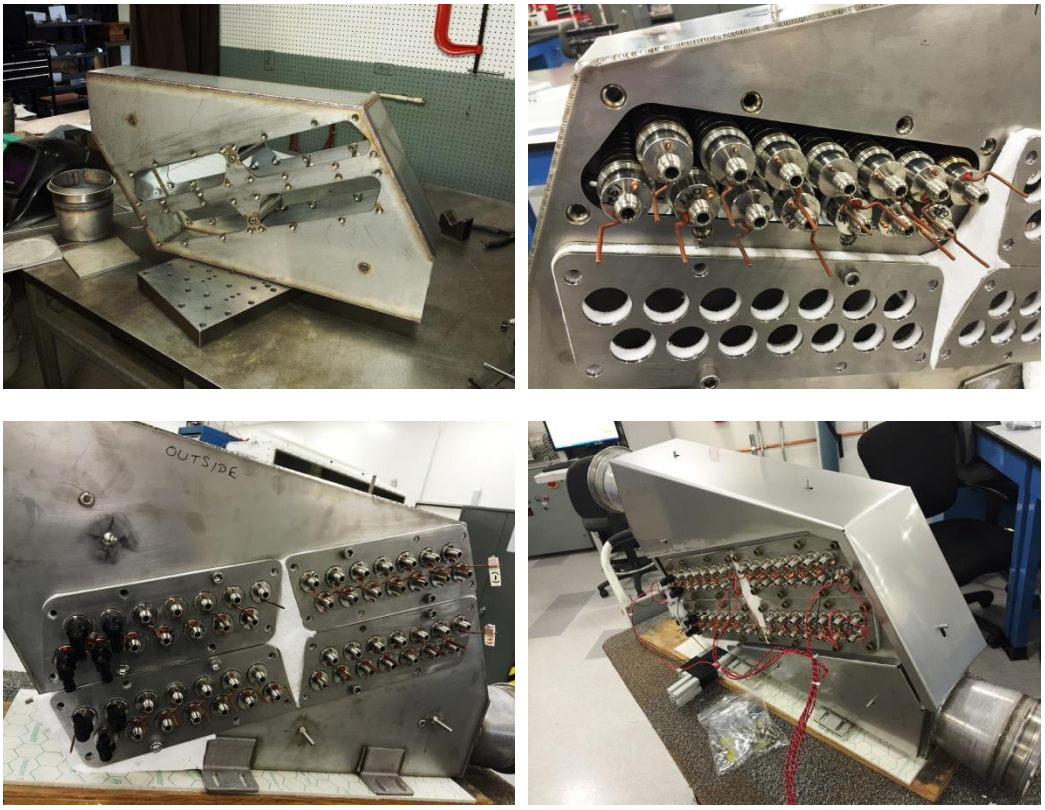

Figure 68 Top left: TEG can with inlet and outlet cone and space allocated for installation of cartridges. Top right: cartridge installation using "quick install" plates. Bottom left: complete layout of cartridges in the TEG. Bottom right: completed TEG with 56 cartridges and added thermal insulation.

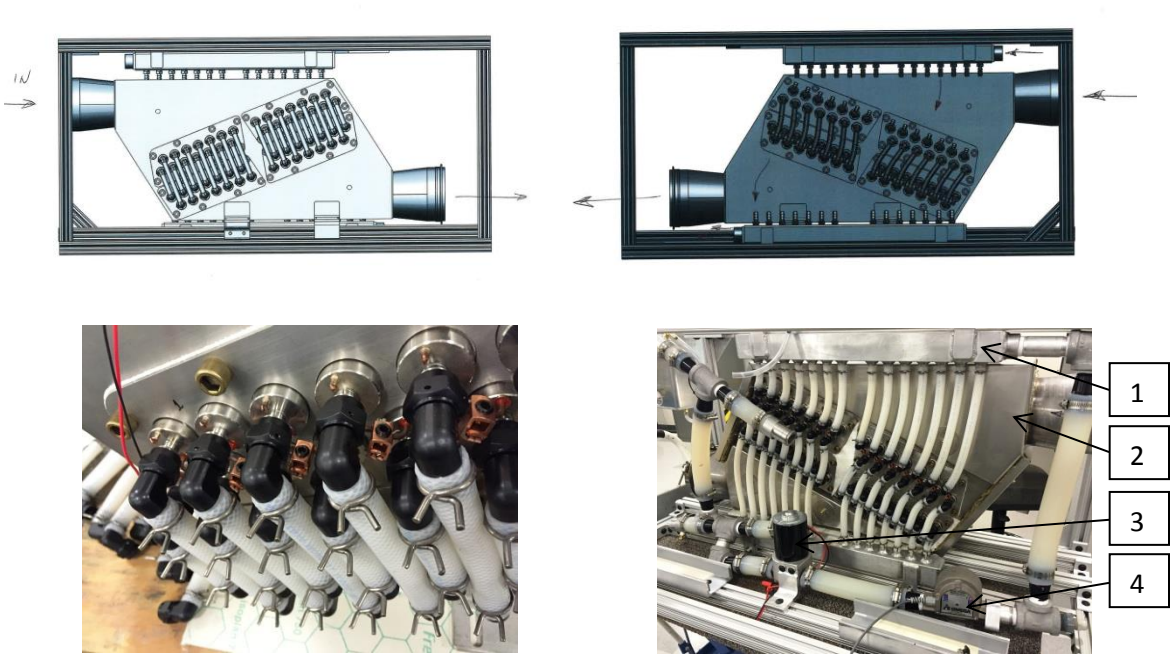

Figure 69 Water connection diagram: TARDEC TEG system. Top left: design of the front plumbing system. Bottom left detail of assembly execution. Top right: design of the back plumbing system. Bottom right: detail of the assembly execution. Bottom right: 1) manifold, 2) TEG, 3) water pump and 4) flow meter.

Testing of HDV TEG System

Initial tests were performed at Gentherm facilities in Azusa, California, using a low flow bench system providing hot gas at 600°C and 140kg/hr. These tests were used to verify assembly and cartridge polarity and to test the cooling system.

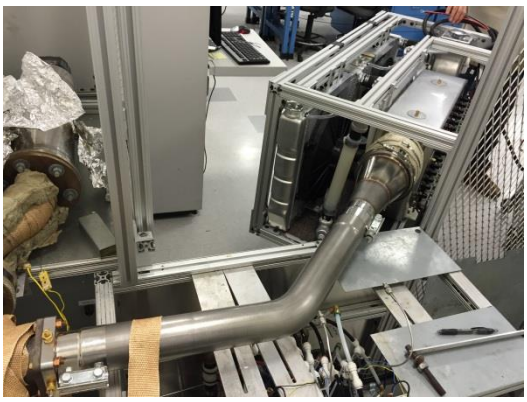

Figure 70 TEG testing at Gentherm facility.

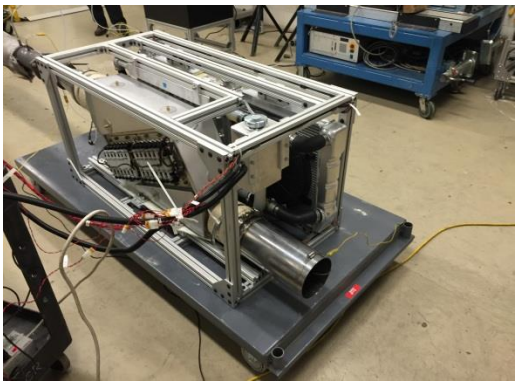


Figure 71 Left: TEG system installed at Tenneco test facility in Grass Lake, MI. Right: heat source is high capacity gas burner.

System level performance testing was conducted at the Tenneco test facility in Grass Lake, Michigan. The heat source was a gas burner simulating expected exhaust gas conditions. The flow rates and temperatures of the hot gas were 250-2550 kg/hr and 250-650^{o}C respectively. Cooling was provided by the TEG integrated cooling system. During all tests, ambient temperatures were between 15 and 40^{o}C and were not controlled. The highest ambient temperatures were at the highest thermal loads on the TEG. The maximum observed temperature difference between ambient and coolant was 35^{o}C – common in automotive air cooled systems.

A summary of test data is provided in Table 9. Power output is directly measured at all data points and reported as a peak power point. To validate accuracy of data, power is also calculated from open circuit voltage and resistance of the TEG system, both values match within 2% and only calculated value is reported here. Resistance was measured by recording the system voltage change as the electrical load to the system was varied. Peak recorded system power output was greater than 1.7kW (point 12-4 in Table 1). As shown in Figure 72, peak TEG performance is at the highest exhaust gas flow rates and temperatures. High temperature gas leads to high temperature at the TE elements and increases power output by simultaneously increasing heat flux through the TEG and thermodynamic heat-to-power conversion efficiency. Lower flow-rate gas is not as effective. At low flow rates, heat transfer between the gas and the high temperature heat exchanger is not very efficient. Cartridge-level efficiency is defined as the ratio of TEG power output and heat flux to the cooling system. Peak cartridge-level or thermoelectric efficiency is 10.2%. This is achieved at the highest temperatures and flow rates. At these conditions, all cartridges are exposed to the same temperature and perform equally well. A cartridge-level efficiency map would roughly follow the power output map so it is not shown here. In addition to cartridge-level efficiency, we report the system-level efficiency, defined as a ratio of TEG power output to total heat flux input from exhaust gas. Unlike the cartridge-level power output map, this system-level efficiency map indicates that maximum system-level efficiency is at the highest temperature and lowest flow rate conditions. Here, maximum system-level efficiency reaches 1.5%. This system was designed to provide power output on the order of 1.5kW and it was not optimized for maximum efficiency. If the system were designed with efficiency in mind, it would have more active components (cartridges). In

this case, the system efficiency map would have similar contours but peak values would be higher, reaching 4-5% with inevitably higher power outputs reaching 3-4kW.

Table 9 TEG test results

Test point	Temp	Coolant temp	Gas Flow	OCV	Resistance	Power	Cartridge efficiency	System efficiency
	°C	°C	kg/hr	V	Ohm	W		
2-1	441.1	37.5	250	31.7	0.69370	22	3.1%	0.6%
2-2	437.8	39.7	500	31.7	0.71300	353	5.2%	0.6%
2-3	440.1	47.2	1000	41.8	0.73780	591	6.4%	0.5%
2-4	435.2	54.5	1750	44.8	0.67870	740	7.2%	0.4%
2-5	435.4	59.9	2500	51.5	0.79410	834		0.3%
3-1	606.0	45.6	500	36.4	0.73180	453	5.8%	0.6%
3-2	616.2	52.8	1000	51.0	0.73260	887	7.2%	0.6%
3-3	616.5	61.3	1750	64.1	0.79380	1294	10.2%	0.5%
3-4	613.4	62.8	2100	70.5	0.79890	1554		0.4%
6-1	330.0	44.4	1200	29.8	0.70390	314	3.8%	0.3%
7-1	445.5	52.0	1350	45.7	0.78320	667	6.0%	0.4%
8-1	493.2	62.4	2500	55.8	0.72030	1079	7.6%	0.3%
9-1	512.1	70.5	2550	62.1	0.81300	1186		0.4%
11-1	508.9	36.7	250	24.9	0.67590	230	3.4%	0.7%
11-2	518.5	40.2	500	38.1	0.69960	519	5.8%	0.7%
11-3	511.3	49.8	1000	51.8	0.76960	873	6.7%	0.6%
11-4	522.0	55.1	1750	58.1	0.78190	1080	7.6%	0.5%
11-5	516.4	59.2	2500	62.1	0.77600	1243	6.6%	0.3%
12-1	628.1	56.2	250	46.5	0.76240	708	5.3%	1.6%
12-2	633.5	56.1	500	51.1	0.75930	859	6.3%	1.0%
12-3	644.0	60.2	1000	65.7	0.79350	1361		0.8%
12-4	644.8	68.7	1750	76.0	0.84070	1719		0.6%
1-1	251.3	30.2	250	8.8	0.52010	37	0.5%	0.1%
1-2	261.6	30.1	500	15.4	0.61790	96	2.6%	0.4%
1-3	260.2	31.9	1000	17.0	0.67020	108	2.9%	0.2%
1-4	255.3	35.6	1750	22.8	0.74740	174	3.3%	0.2%
1-5	259.6	37.3	2500	24.4	0.70370	212	3.7%	0.1%

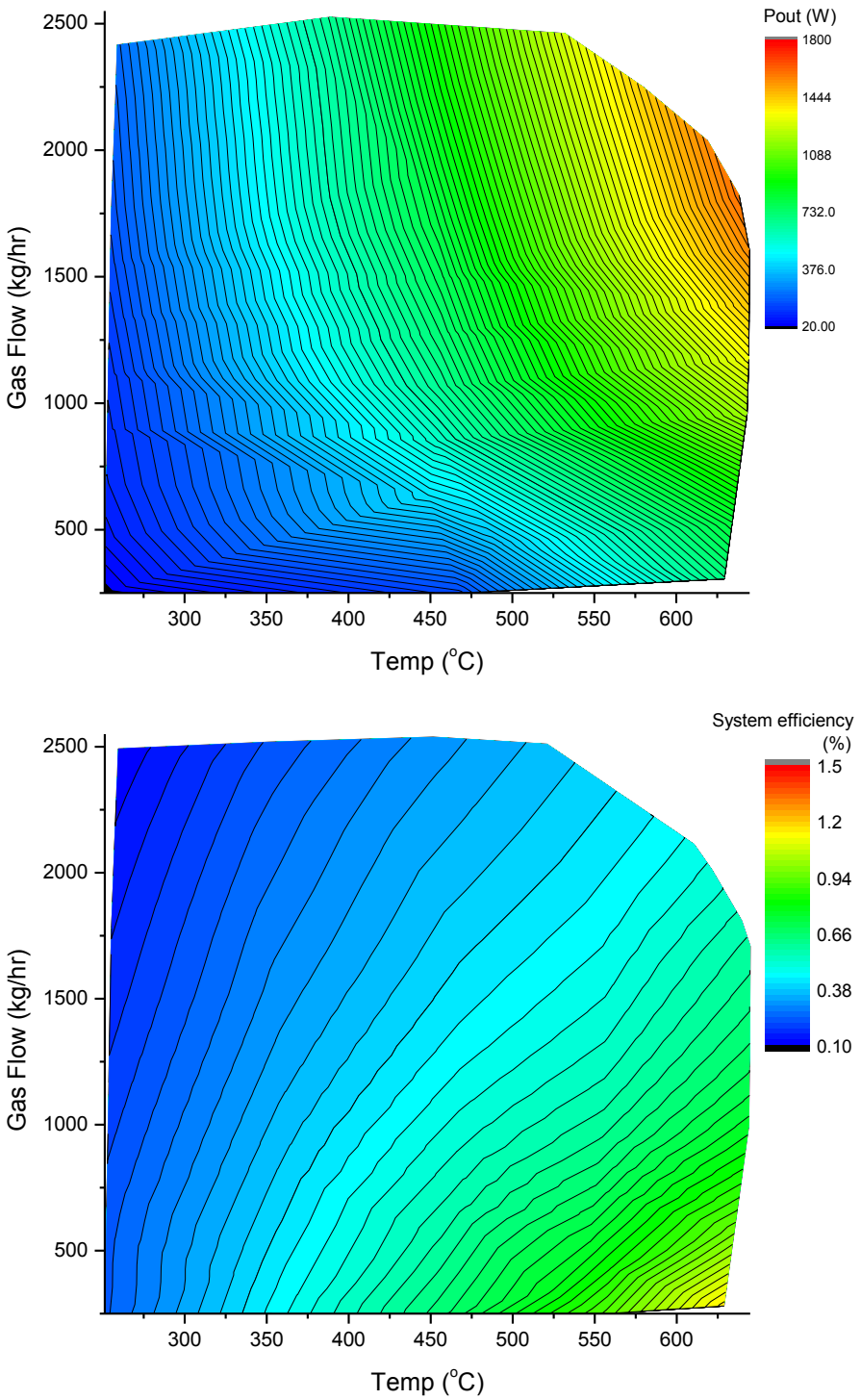

Figure 72 Top: Performance map showing TEG power output as a function of gas flow rate and temperature. Bottom: System-level efficiency map.

Thermoelectric materials research and development

Development of TE element manufacturing process

The objective of this part of program is to address the barriers to widespread market adoption, including the production readiness of TE materials Intention of this task was to

- Develop methods of manufacturing TE materials in quantities that are sufficient to satisfy the requirements of this program,
- Develop methods of controlling materials properties,
- Control material and metallization properties.

In order to fulfill the requirements of this program, Gentherm has developed methods of manufacturing TE elements. Process stability is monitored by measuring basic material properties such as ZT, Seebeck, electrical conductivity and thermal conductivity. Additionally, material properties such as interface electrical resistance between diffusion barrier and thermoelectric materials are measured. Characterizing interface resistance provides for a non-destructive method of monitoring interface properties.

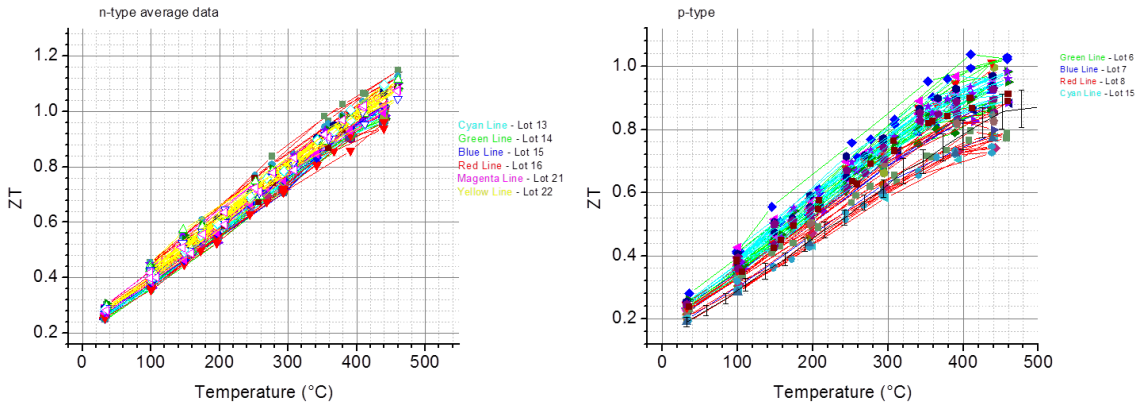

Figure 73 ZT values of materials produced at Gentherm.

The general intention of this task is to develop low cost manufacturing methods. Our analysis of conventional TE manufacturing methods shows that majority of cost of TE elements is not in the cost of raw TE elements. Cost of TE elements is driven by low material utilization and high costs of processes such as cutting, polishing and methods of manufacturing TE materials that will result in reliable performance and a low cost of manufacturing. Traditional process of manufacturing TE elements would consist of sintering large ingots of TE materials either as long rods or tin disks, cutting, polishing, metallization bonding and then final TE element cutting. In this case cost of raw TE elements (in case of skutterudites) would be only 10% of final TE element cost. Material utilization would be less than 60%. For this reason we have focused on process of manufacturing net shaped TE elements followed with application of metallization – completely skipping polishing and cutting steps. Our process cost models

show that in this case cost of finished elements can be 60-70% lower ant that material utilization can reach over 95%.

In this program, we were addressing the reduction of TE material manufacturing cost as a parallel activity to working with current production materials required to build TE devices. Low cost TE materials were not be used to build the devices that were previously described due to timing constraints. Our cost studies indicate a significant reduction of the manufacturing cost as shown in Figure 74. By normalizing to cost per kg of TE materials, we see that our process results in about a 30% reduction of the overall cost. In this case we are comparing our results with the process in which disks of TE materials are metalized and cut to size.

Figure 74 Comparison of manufacturing cost breakdown for traditional TE manufacturing process as compared to new Gentherm process. Significant cost reduction is achieved by reducing material waste and increasing yield through manufacturing net shaped thermoelectric materials.

In collaboration with Caltech, we are working on an analysis of material properties as a function of the starting materials purity, chemical composition, processing temperatures and etc. In summary: The Caltech group has developed a methodology which is required to better understand n type $CoSb_3$ based materials. By relying on systematic analysis of material structure and measured properties, they were able to develop material phase diagrams and characterize the electronic structure of these materials. The end result is better control of the materials ZT as shown in the attached diagram. In addition, the ZT values demonstrated by Caltech team are 10-20% higher than those produced by materials manufactured at Gentherm.

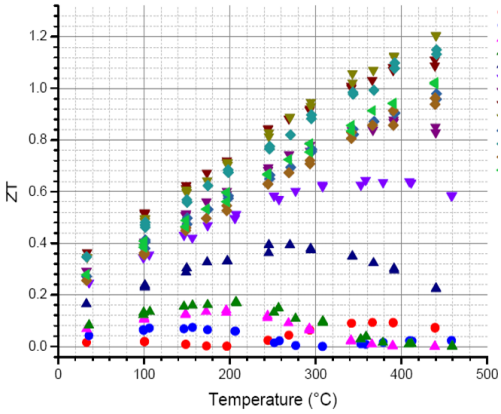

Figure 75 ZT values of n-type Skutterudite materials prepared at Caltech. Variations in ZT values demonstrate ability to control dopant and impurity levels and by doing so vary ZT.

In this program, we have investigated the ability to protect Skutterudite materials using an oxidation resistant coating. The goal was to use coatings in conjunction with aerogel encapsulation to both prevent sublimation and oxidation. Screening tests were conducted in air on coated coupons to identify the most promising coating candidates/techniques. We have demonstrated the ability to seal Skutterudite materials and protect them at temperatures exceeding 750K. As a part of this program, Gentherm worked on the development of coatings. The intention is to develop dielectric coatings that can be applied directly to the TE materials that provide two functions:

1) The hermetic sealing to protect the SKU from oxidation, which would enable lower cost manufacturing of cartridges with simplified geometry,

2) The suppression of antimony sublimation from the SKU material, which would enable higher operating temperatures and improve durability of TE elements.

Both functions require coating which would have good adhesion at the interface between TE materials and the coating. We have selected to pursue a dip coating approach and a plasma spraying approach. The plasma sprayed coatings showed high levels of porosity and were not able to provide a full hermetic sealing of the parts. The dip coating, in particular coating with enamels, showed great promise. However, after exposure to high temperature, the coatings tend to delaminate from the Skutterudite material. Figure 76 shows an example of n-type material where coatings fail after exposure to high temperature.

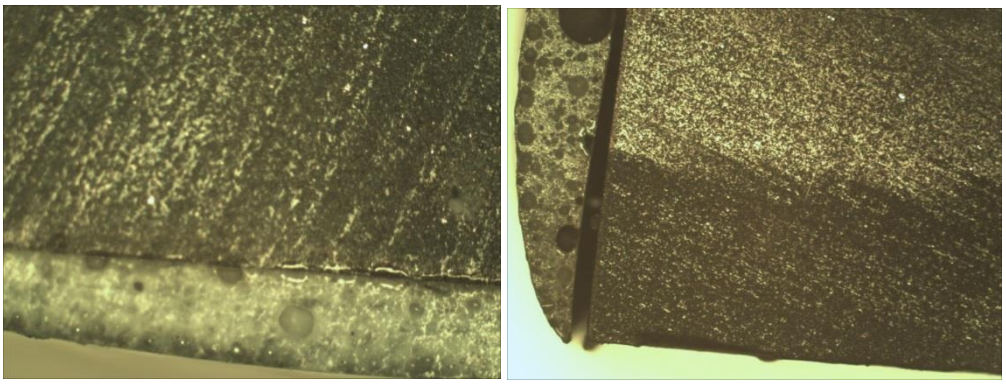

Figure 76 Left: Interface between enamel coating and Skutterudite material after dip coating and firing. Right: Interface after exposure to elevated temperature.

Some of the promising techniques were then applied to the assemblies of TE materials and shunts. In these tests we have observed delamination of the coatings at the metal/semiconductor interface and a reduction of the device efficiency due to thermal shorts through the coatings. In conclusion, we have identified hermetic sealing at the device level as a best method of protecting TE materials and other components from oxidation and reaction with ambient fluids. We did not observe the need for sublimation suppression in our devices.

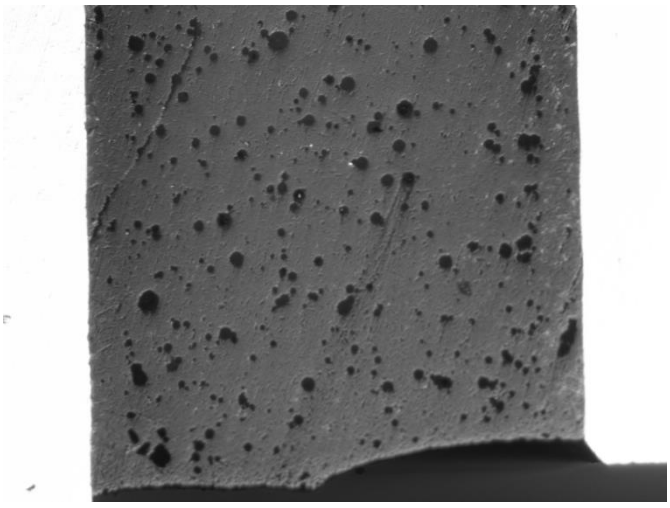

Figure 77 Glass ceramic seal at the electric feedthrough. Crack is visible in the upper right corner of this ceramic glass seal.

Process of manufacturing low cost TE elements

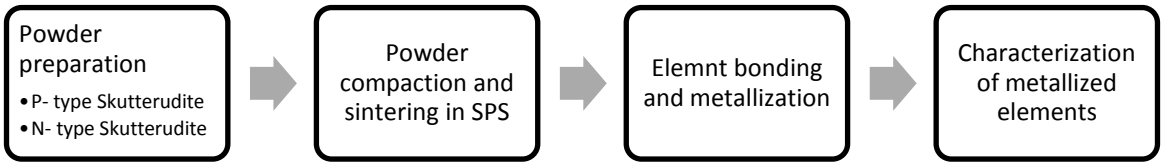

Figure 78 TE element manufacturing flow diagram.

Preparation and testing of TE elements is a process which can be divided in 4 steps as shown in the flow diagram.

Powder preparation:

Process developed by material suppliers. At Gentherm, powders are tested to verify quality of incoming materials for powder size distribution and for quality of thermoelectric properties of materials. Material properties are tested on coupons ½" DIA and 1/8" thick. Coupons are sintered in SPS following same general procedures used to prepare thermoelectric elements. The sintering process includes pressing at pressures reaching 60MPa and temperatures not exceeding 800C. For quality control purposes, material's Seebeck coefficient, thermal conductivity and electrical resistivity are measured. For clarity, when we evaluate material quality we evaluate only ZT which is non-dimensional figure of merit ZT. In general we use pass/fail criteria where peak ZT values of n type materials are expected to fall in the range 0.9-1.1 and for p type materials 0.7-0.9.

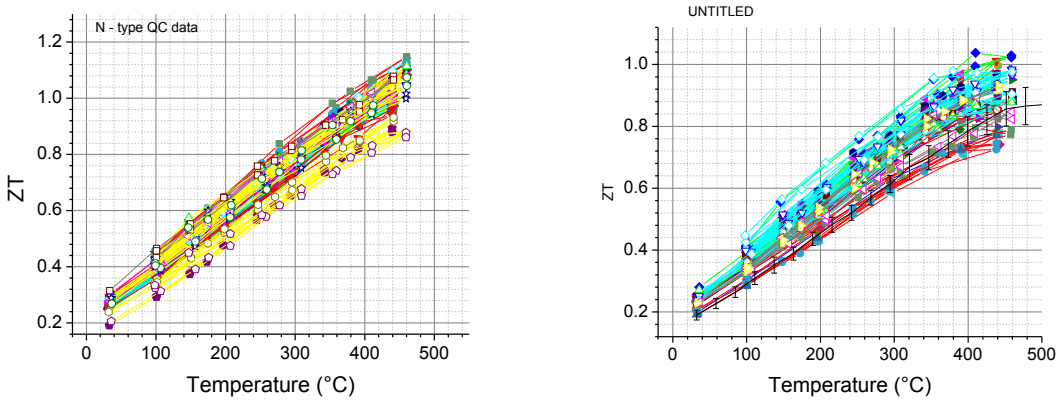

Figure 79 N type and p type materials ZT - QC data.

Powder compaction and sintering

Group of processes defined as powder compaction and sintering includes handling of powders and loading of tools in preparation for sintering and sintering process itself. Process developed at Gentherm includes loading of thermoelectric materials and one or more compliant layers. All materials are loaded in powder form into die set and simultaneously sintered in Spark Plasma Sintering system. Compliant material is used to reduce interface stress between thermoelectric material and metal to which TE materials are bonded. Gentherm has patented use of metal coated inorganic composites as ideal compliance materials. Inorganic filler improves thermal and electric conductivity and metal coating or metal matrix improves mechanical properties of TE elements.

The sintering process occurs in graphite tooling at the temperatures not exceeding 800C and pressures of 60MPa. Sintering of multilayer structures or sintering of finished TE elements is in our opinion most important segment of development of low cost TE devices. Cost of sintered TE elements dominates cost of manufacturing TE devices.

The cycle time is estimated to take 50 seconds with a 50% safety factor making the cycle rate 75 seconds. This is highly dependent on the flow ability of the powders and the timing necessary to ensure a quality product within process. In addition to design of tooling for powder handling we investigated flowability of powders. Powder flow is improved by milling and selecting fraction of powders with the best flow characteristics. Quality of powder is characterized using flow rate and CARR's index. CARR index is defined as a ratio of tap and bulk densities. As shown in Table 10 improved powders have significantly better flow characteristics as indicated with measured 10% compressibility. Micrographs shown in Figure 80 are used to illustrate difference in morphology between different fractions of powders. Particles larger than 50 mesh are too big to be used in this process. Particles smaller than 230 mesh do not flow and they could not be used with fill shoes. Optimal particle size is in the range of 50-230 mesh size. Same figure shows distribution of particle sizes in milled powders. As shown, 72% of powder is of satisfactory quality and 28% of powder must be recycled. Recycling process has not been developed yet.

Table 10 CARR index for Skutterudite powders.

Powder Flow Description

% Compressibility (CARR'S INDEX)=	$\frac{\textit{Tapped density-Bulk density}}{\textit{Tapped density}}$
% Compressibility	Flow Description
5-15	Exellent
12-16	Good
18-21	Fair
23-35	Poor
35-38	Very Poor
>43	Extrmely Poor

Powder Type	**Compressibility, CAR'S INDEX**	
SKU-P	**33**	**Poor**
SKU-n	**30**	
Improved P & N type SKU	**10**	**Exellent**

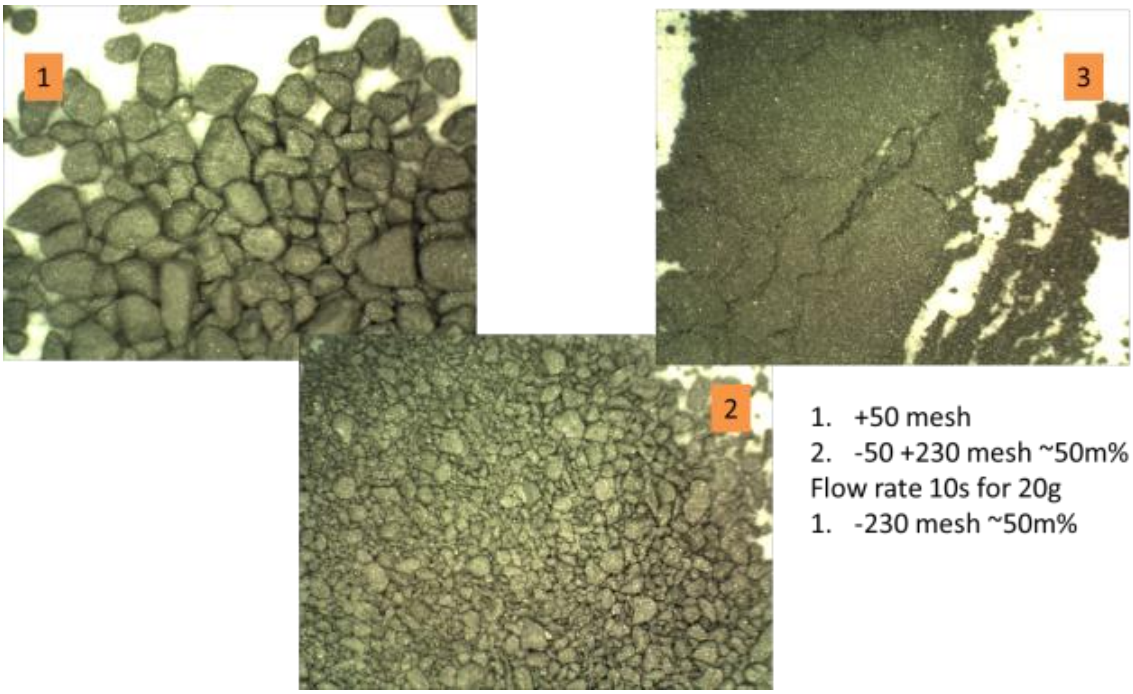

Figure 80 Observed structure of milled Skutterudite powders and their flow rate.

Element bonding and metallization

TE elements have metallization layers which act as diffusion barriers. Metallization layers are diffusion bonded to TE materials at the temperatures not exceeding 800C. Function of this layer is to prevent infiltration of metals into Skutterudite thermoelectric materials. In our process we bond shunts to metal contacts which are deposited to thermoelectric elements. Various bonding methods are explored. Both, diffusion bonding of metal to metal and bonding through liquid phase work for this class of TE elements. Type of bonding is truly a function of device design and various Ni, Ag, Au or Cu based braze materials are successfully used. Our observation is that bonding must occur at the temperatures less than 650 C in order to prevent phase separation in Skutterudite materials.

Characterization of metallized elements

Thermoelectric elements bonded to metal shunts are tested using destructive and nondestructive processes to determine their quality. Longitudinal spatially resolved measurement of resistivity of TE laments is used as our only nondestructive method. This method enables measurement of electrical interface contact resistance between metal shunt and metal, metallization and compliance layer and between TE material and other layers. In addition, using this measurement it is possible to identify cracks between layers of mentioned materials or identify cracks in TE materials. For example, Figure 3 field (a) shows element with crack in TE element, Figures 3 (c), (e) and (f) show cracks at the various

interfaces between TE material, metallization, compliance layer and metal bond. This nondestructive method does not allow us to determine exact interface where cracks appear.

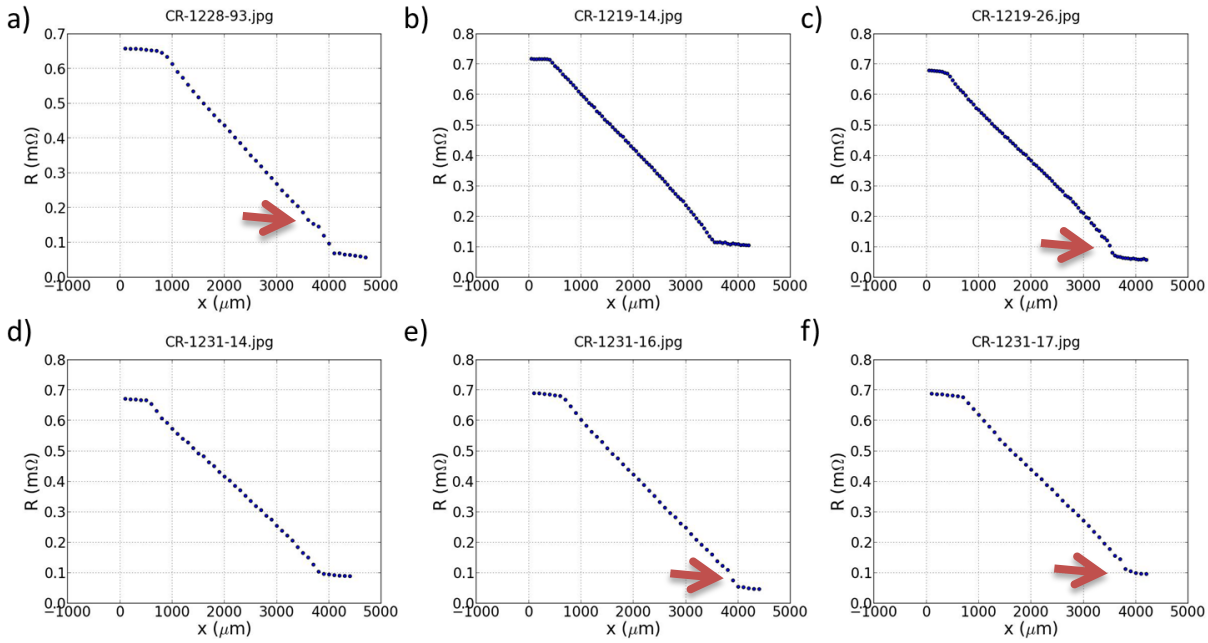

Figure 81 Longitudinal resistance scans.

Destructive methods can give us a bit more insight into observed discontinuities in longitudinal resistance. Best observations are made on the polished cross sections of bonded TE elements. One showed in Figure 4 would correspond to observation in Figure 3 (a) – discontinuity in resistance in bulk TE material corresponding to a hairline crack.

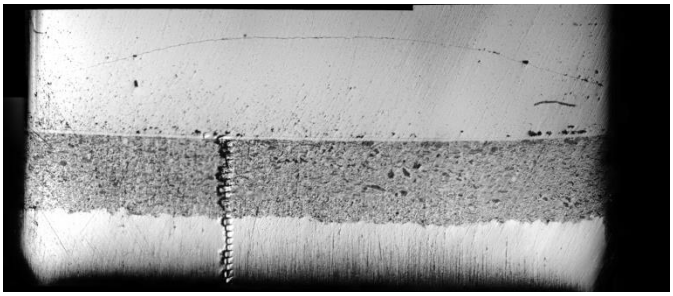

Figure 82 Hairline crack observed in TE material

We used nondestructive method to determine yield in manufacturing of TE elements based on selected process parameters. Sintering at 600C and 60MPa for 12min. Yield in manufacturing of p type materials is 85% and in manufacturing of n-type materials is 45%. Results were averaged over batch of ~600

elements. This means that with n-type materials 55% of samples have observed discontinuities in longitudinal resistance measurements as shown in Figure 3. As shown in Figure 5 n-type material yield varies as a function of tool batch. Every tool consists of Die and set of plungers with different gap between these 2 components. Based on this analysis we can deduce that yield or the quality of pressed part depends on the quality of fit between plungers and dies.

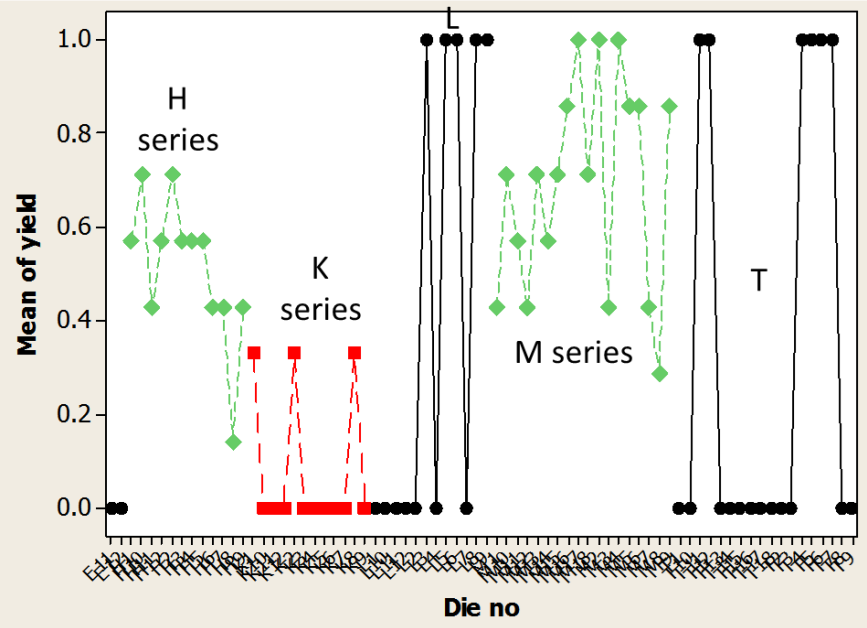

Figure 83 Yield as a function of tool batch.

Optimization of synthesis and thermoelectric properties of CoSb3-based skutterudites

Part of this program was dedicated to development of better performing skutterudite materials and in particular better performing n –type materials. Work was performed in collaboration with researchers at California Institute of technology in Pasadena. Among the best thermoelectric materials are *n*-type filled skutterudites based on $CoSb_3$. The addition of filler atoms, for example Yb, into a void site ($Yb_xCo_4Sb_{12}$) can lead to high *zT* by reducing the thermal conductivity while simultaneously doping the material (adding electrons as charge carriers) [1,2]. High *zT* values (greater than 1) have been reported for both single-element filling (Na[3], Ba[4], In[5], Ce[6], and so on) and multiple filling (In+Ce[7], Sr+Ba+Yb[8], Ba+La+Yb[9]). High *zT* in skutterudites is most often attributed to the addition of the filler atoms and subsequent reduction in thermal conductivity due to alloying disorder and the complex phonon modes of the filler atom[10-12]. Although low thermal conductivity is essential to high *zT*, the importance of the intrinsic electronic structure in skutterudites is often understated or ignored completely, especially given that the optimum doping carrier concentration is independent on the filler type.

High thermopower at high doping is essential for achieving the high *zT* in all *n*-type skutterudites. Here we investigate where this essential feature of the electronic structure comes from through a combination of experiments (doping study, optical band gap measurements) and calculations (DFT band structure calculation and Fermi surface plot).

The favorable electronic band structure in *n*-type $CoSb_3$ is typically attributed to three-fold degeneracy at the conduction band minimum accompanied by linear band behavior at higher carrier concentrations, which is thought to be related to the increase in effective mass as the doping level increases. Here, using combined experimental and computational studies; we show instead that a secondary conduction band with 12 conducting carrier pockets (that probably converges with the primary band at high temperatures shown in Figure 84) is responsible for the extraordinary thermoelectric performance of *n*-type $CoSb_3$ skutterudites. A theoretical explanation is also provided as to why the linear (or Kane-type) band feature is not beneficial for thermoelectrics. Results of theoretical modeling are summarized in graphs on Figure 85 and Figure 86. This work is recently published on Nature Materials [CLT2016].

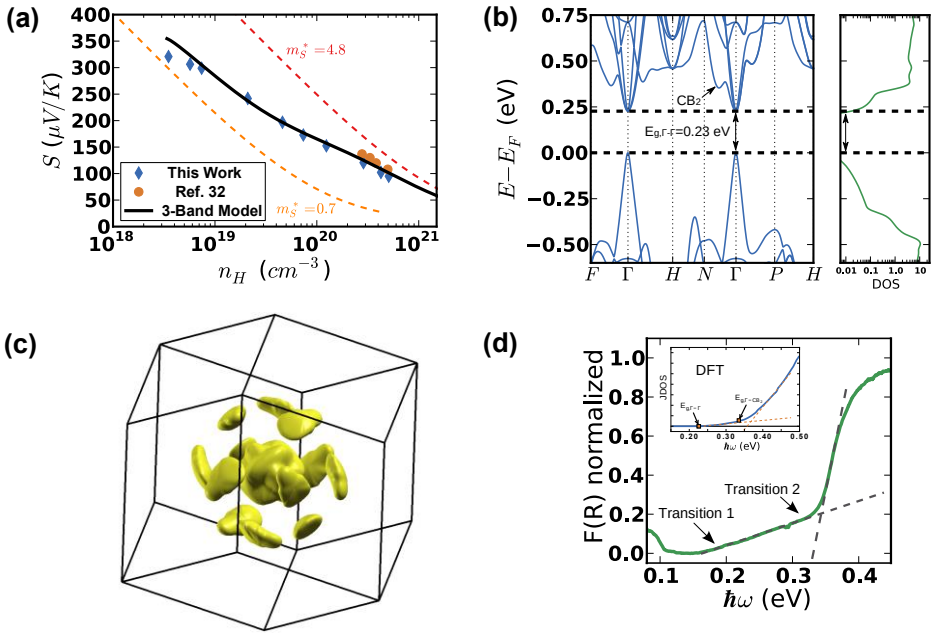

Figure 84: Experimental and theoretical evidence showing multiple conduction bands in n-type $CoSb_3$. (a) Pisarenko plot of Seebeck coefficient (S) vs. Hall carrier concentration (n_H) at 300K. (b) DFT calculated electronic band structure and density of states (DOS) for $CoSb_3$. (c) Fermi surface calculation for Fermi level 0.11 eV above the conduction band minimum showing the 12 pockets of the second conduction band CB_2 observed as a valley between $\Gamma - N$. (d) Room temperature optical absorption measurement with estimated joint density of states from DFT showing two distinct transitions.

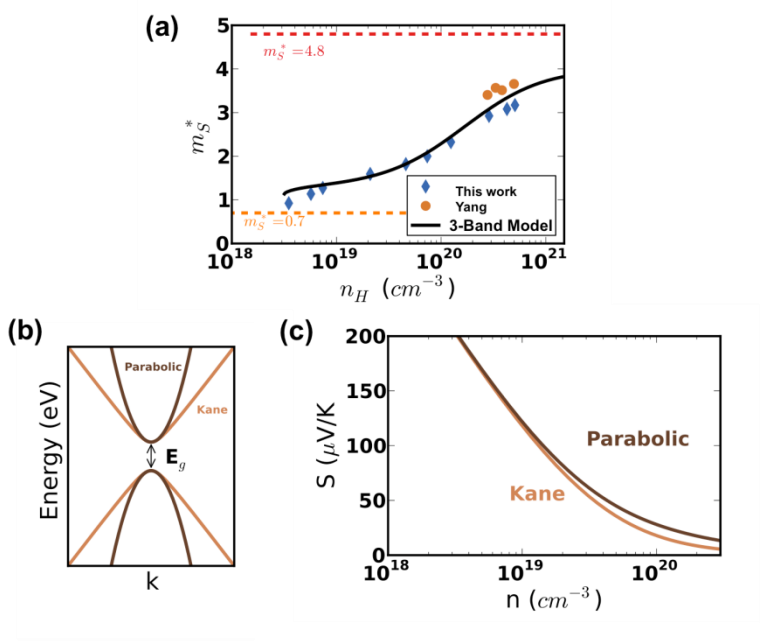

Figure 85 Band non-parabolicity and its effect on the Seebeck coefficient and energy-dependent Seebeck effective mass $\boldsymbol{m_S^*(E)}$. a) Effective mass $\boldsymbol{m_S^*(E)}$ derived from Seebeck coefficient and Hall effect measurements. The solid black line (three-band model) represents the prediction of a semi-empirical model with two conduction bands plus one valence band. Orange and red dashed lines indicate the band masses of the two individual conduction bands. The data of Yang *et al.* is included for comparison. b) Parabolic and Kane band dispersions with the same band-edge effective mass ($\boldsymbol{m_S^*(E=0)}$). c) Seebeck Pisarenko plot for both Kane and Parabolic bands, illustrating that $\boldsymbol{m_S^*(E)}$ actually decreases for Kane bands at a high carrier concentration.

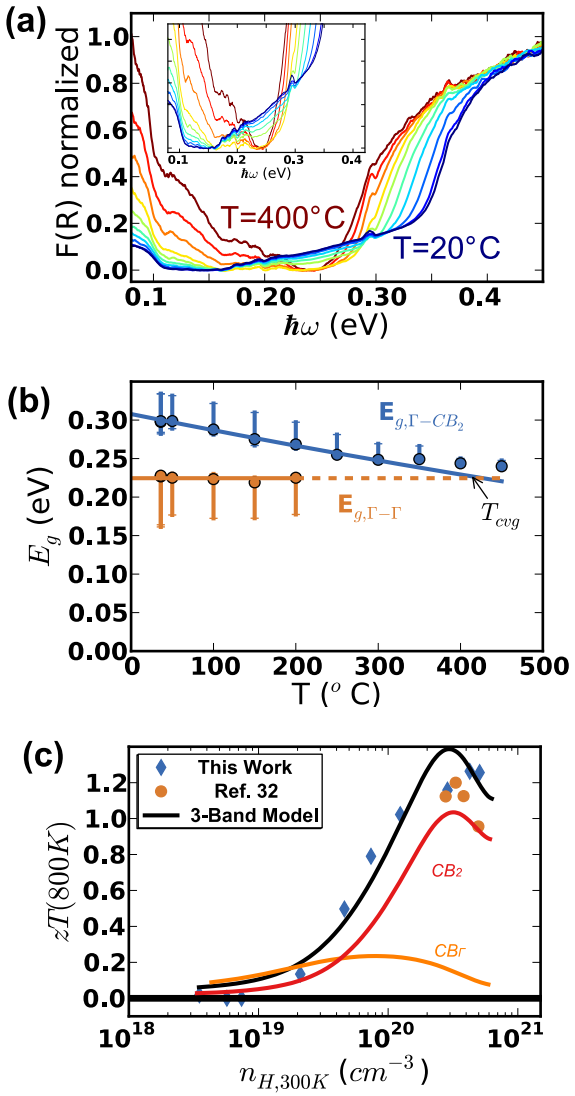

Figure 86: Band convergence at high temperatures in $CoSb_3$ as shown from optical absorption and thermoelectric figure of merit. (a) Temperature dependent optical absorption for $CoSb_3$ from 20 to 400°C. (b) Temperature dependent band gap for the direct ($E_{g,\Gamma-\Gamma}$) and indirect ($E_{g,\Gamma-CB_2}$) transitions indicating band convergence at $800 \pm 100\ K$. (c) zT at 800K vs carrier concentration n_H measured at 300K compared with that predicted with the model (solid black line).

Materials development summary

Main path toward reduction of overall TEG system cost is reduction of component cost and in particular cost of TE elements. At the device level, cost of TE elements can be as high as 30% of overall device cost. In this program we have demonstrated possibility of manufacturing net shaped TE elements for power generation applications. Applying methods described here, it is possible to reduce cost of manufacturing

TE elements by the factor of 3. Further reduction by similar factor is necessary. This cost saving can be achieved by further industrialization and automation of process. That investigation was beyond the scope of this program.

Skutterudites are excellent materials for power generation applications. When protected by pressurized inert gas they have low and hardly measurable rate of sublimation or loss of Sb. Materials are robust and show chemical stability t the temperatures of 600^{o}C and less. This is practical limit of use of these materials in automotive applications. Even at gas temperature reaching 800C it is virtually impossible to design TEG which would have TE element temperatures higher than 550^{o}C.

In this program we have quickly abandoned approach of developing coatings for TE elements. Our focus was to develop TEG which can work at TE material temperatures 550-600^{o}C. One of great challenges at these temperatures is to seal not only TE elements but also electrodes. Cheapest solution in this case is hermetic sealing. We acknowledge that it is possible to develop practical coatings which can operate at temperatures of 300^{-}C or less.

Products developed under the award

Publications, conference papers, or other public releases of results

“Thermoelectric Generator Performance for Passenger Vehicles”, Doug Crane and John LaGrandeur, March 20, 2012. TE Applications Conference in Baltimore

“TEG On-Vehicle Performance & Model Validation & What It Means For Further TEG Development”, Doug Crane, John LaGrandeur, Vladimir Jovovic, Marco Ranalli, Martin Adldinger, Eric Poliquin, Joe Dean, Dmitri Kossakovski, Boris Mazar, Clay Maranville, July 11, 2012 presented at the International Conference on Thermoelectrics in Aalborg, Denmark.

“Solid State Heat to Power in Marine Vessels”, John LaGrandeur, March 13, 2013, Navy Energy Recovery Workshop (ONR)

“Thermoelectric Waste Heat Recovery Program for Passenger Vehicles”, Doug Crane, May 17, 2013, DOE Annual Merit Review

“Waste heat recovery in passenger cars” Michael Mirsch, March 31, 2014, presentation at the VDI conference, Dusseldorf Germany

“Thermoelectric Waste heat recovery program for passenger vehicles”, Vladimir Jovovic, 2014 Annual Merit Review and Peer Evaluation Meetings (AMR) for the Hydrogen and Fuel Cells Program and the Vehicle Technologies Office, June 16–20, 2014, Washington, D.C.

"Convergence of multi-valley bands as the electronic origin of high thermoelectric performance in $CoSb_3$ skutterudites", Yinglu Tang et al. *Nature Materials* **14**, 1223–1228 (2015)

Yinglu Tang, at The California Institute of Technology PhD thesis,

Web site or other Internet sites that reflect the results of this project

http://www.gentherm.com/page/automotive-0

Networks or collaborations fostered

Program partners included BMW, Ford, Tenneco, NREL and Caltech and government agencies DOE and TARDEC

Technologies/Techniques

"THERMOELECTRIC DEVICES WITH INTERFACE MATERIALS AND METHODS OF MANUFACTURING THE SAME" Granted patent US 9178128 B2 11/3/2015

Inventions/Patent Applications, licensing agreements

Ref. no.	Patent/ Patent Application Title	Country	Inventors	Application No.	Filing Date
BSST.058A	THERMOELECTRIC SYSTEM WITH MECHANICALLY COMPLIANT ELEMENT	US	Jovoic Vladimir, Poliquin Eric	13/912007	6/6/2013
BSST.062A	CROSSMEMBER THERMOELECTRIC GENERATOR WITH IMPROVED THERMAL EXPANSION PROTECTION	US	CRANE, Douglas, T.;	13/912001	6/6/2013
BSST.062WO	CROSSMEMBER THERMOELECTRIC GENERATOR WITH IMPROVED THERMAL EXPANSION PROTECTION	WO	CRANE, Douglas, T.;	PCT/US2013/044608	6/6/2013
BSST.070PR	FUEL BURNER WITH THERMOELECTRIC GENERATOR FOR ELECTRIC VEHICLES	US	Kossakovski, Dmitri	61/589099	1/20/2012
BSST.070PR2	FUEL BURNER WITH THERMOELECTRIC GENERATOR FOR ELECTRIC VEHICLES	US	Kossakovski, Dmitri	61/755331	1/22/2013
BSST.071A	CATALYST-THERMOELECTRIC GENERATOR INTEGRATION	US	Ranalli, Marco; LaGrandeur, John;	13/745644	1/18/2013
BSST.071PR	CATALYST-THERMOELECTRIC GENERATOR INTEGRATION	US	Ranalli, Marco; LaGrandeur, John;	61/589088	1/20/2012
BSST.071WO	CATALYST-THERMOELECTRIC GENERATOR INTEGRATION	WO	Ranalli, Marco; LaGrandeur, John;	PCT/US2013/022299	1/18/2013
BSST.074A	THERMOELECTRIC DEVICES WITH INTERFACE MATERIALS AND METHODS OF MANUFACTURING THE SAME	US	Jovovic, Vladimir; Kossakovski, Dmitri; Heian, Ellen M.;	13/679473	11/16/2012
BSST.074PR	METHOD OF MANUFACTURING THERMOELECTRIC MATERIALS WITH INTEGRATED HOT AND COLD SHUNTS	US	Jovovic, Vladimir; Kossakovski, Dmitri; Heian, Ellen M.;	61/650385	5/22/2012
BSST.074WO	THERMOELECTRIC DEVICES WITH INTERFACE MATERIALS AND METHODS OF MANUFACTURING THE SAME	WO	Jovovic, Vladimir; Kossakovski, Dmitri; Heian, Ellen M.;	PCT/US2012/065588	11/16/2012

Other products

Seven light duty vehicle thermoelectric generators.

BMW X3 – installation of TEG system

Ford F350 – installation of TEG system

BFV – 2kW TEG system

Graphical content

References

[DSP2015] URL: http://www.dspace.com/en/pub/home/products/hw/micautob.cfm (Nov 3rd, 2015)

[GPO2015] URL: http://www.gpo.gov/fdsys/pkg/CFR-2013-title40-vol20/pdf/CFR-2013-title40-vol20-sec86-1869-12.pdf (Dec 4th, 2015)

[EPA2016] URL:https://www.epa.gov/sites/production/files/2016-02/documents/420f14040a.pdf

[FAU2016] URL: http://www.faurecia.com/en/innovation/discover-our-innovations/energy-heat-recovery-system-ehrs

[HRC2014] URL: http://cordis.europa.eu/result/rcn/58791_en.html

[FHWA2016] URL: https://www.fhwa.dot.gov/ohim/onh00/bar8.htm

[CLT 2016] Yinglu Tang, Zachary M. Gibbs, Luis Agapito, Guodong Li, Hyun-Sik Kim, Marco Buongiorno-Nardelli, Stefano Curtarolo, G. Jeffrey Snyder, " Convergence of the Multivalley Bands as the Electronic Origin of High Thermoelectric Performance in $CoSb_3$ Skutterudites" *Nature Materials* ***DOI:10.1038/NMAT4430***

[CRN2011] Crane, D.T., *An Introduction to System Level Steady-State and Transient Modeling and Optimization of High Power Density Thermoelectric Generator Devices Made of Segmented Thermoelectric Elements.* Journal of Electronic Materials, 2011. **40**(5): p. 561-569.

List of Acronyms

TE	Thermoelectric
DC	direct current
g/s	grams per second
kPa	kilopascal
A	area (m^2)
Cp	specific heat (J/kgK)
h	heat transfer coefficient (W/m^2K)
I	electrical current (A)

K	thermal conductance (W/K)
m	mass (kg)
Q	heat flow (W)
R	electrical resistance (ohm)
t	time (s)
T	temperature (K)
PID	proportional integral derivative
psid	pounds per square inch differential
RH	relative humidity
TEG	thermoelectric generator, thermoelectric power generator
VFR	volumetric flow rate
WEG	water/ethylene glycol
LDV	light duty vehicle, passenger vehicle
MDV	medium duty vehicle
HDV	heavy duty vehicle
TARDEC	United States Army Tank Automotive Research, Development and Engineering Center
DOE	United States Department of Energy
BFV	Bradley Fighting Vehicle

Supplemental guidelines

NETL cannot release technical reports that include Limited Rights Data (such as trade secret, proprietary or business sensitive information). Thus, if such information is important to technical reporting requirements, it **must** be submitted in a separate appendix to the electronic technical report. This appendix **MUST NOT** be submitted in an electronic format but rather submitted separately in **TWO GOOD QUALITY PAPER COPIES** when the electronic version of the sanitized technical report is submitted. The appendix must not be referenced in or incorporated into the sanitized technical report deliverable under the award. The appendix must be appropriately marked and identified. Only the legend provided in the Rights in Data clause in this award may be placed on

the appendix. The appendix must be sent to:

NETL AAD DOCUMENT CONTROL

BUILDING 921

U.S. DEPARTMENT OF ENERGY

NATIONAL ENERGY TECHNOLOGY LABORATORY

P.O. BOX 10940

PITTSBURGH, PA 15236-0940

Further, if this award authorizes the recipient under the provisions of The Energy Policy Act of 1992 (EPAct) to request protection from public disclosure for a limited period of time of certain information developed under this award, the main body of electronic technical reports **MUST NOT** contain such Protected Information. **TWO GOOD QUALITY PAPER COPIES** of such information must be submitted to the address above in a separate appendix to the sanitized electronic version of the technical report. The appendix must not be referenced in or incorporated into, the sanitized technical report deliverable under the award. In accordance with the clause titled "Rights in Data-Programs Covered Under Special Data Statutes," the appendix must be appropriately marked, including the date when the period of protection for the data ends. The EPAct appendix must be appropriately identified with the recipient's name, award number, type of report (final or topical), and reporting period start and end dates.

Company Names and Logos -- Except as indicated above, company names, logos, or similar material should not be incorporated into reports.

Copyrighted Material -- Copyrighted material should not be submitted as part of a report unless written authorization to use such material is received from the copyright owner and is submitted to DOE with the report.

Measurement Units -- All reports to be delivered under this instrument must use the SI Metric System of Units as the primary units of measure. When reporting units in all reports, primary SI units must be followed by their U.S. Customary Equivalents in parentheses ( ). **The Recipient must insert the text of this clause, including this paragraph, in all subcontracts under this award.** Note: SI is an abbreviation for "Le

Systeme International d'Unites."